MINISTÉRIO DA EDUCAÇÃO
UNIVERSIDADE FEDERAL RURAL DA AMAZÔNIA- UFRA
PROGRAMA DE PÓS-GRADUAÇÃO EM AGRONOMIA

YAN NUNES DIAS

Uso de biochars amazonicos na remediação de resíduos de mineração ricos em arsênio oriundo de mineração de ouro na Amazônia

Use of Amazonian biochars in the remediation of arsenic-rich mining residues from gold mining in the Amazon

Belém
2022

MINISTÉRIO DA EDUCAÇÃO
UNIVERSIDADE FEDERAL RURAL DA AMAZÔNIA- UFRA
PROGRAMA DE PÓS-GRADUAÇÃO EM AGRONOMIA

YAN NUNES DIAS

Uso de biochars amazônicos na remediação de resíduos de mineração ricos em arsênio oriundo de mineração de ouro na Amazônia

Use of Amazonian biochars in the remediation of arsenic-rich mining residues from gold mining in the Amazon

Tese apresentada à Universidade Federal Rural da Amazônia, Programa de Pós-Graduação em Agronomia, como parte das exigências para obtenção do título de Doutor em Agronomia.

Orientador: Prof. Dr. Antonio Rodrigues Fernandes

Belém
2022

Dados Internacionais de Catalogação na Publicação (CIP)
Bibliotecas da Universidade Federal Rural da Amazônia
Gerada automaticamente mediante os dados fornecidos pelo(a) autor(a)

D541u Dias, Yan Nunes
Uso de biochars amazonicos na remediação de resíduos de mineração ricos em arsênio oriundo de mineração de ouro na Amazônia / Yan Nunes Dias. - 2023.
104 f. : il. color.

Tese (Doutorado) - Programa de Pós-Graduação em Agronomia (PPGA), Campus Universitário de Belém, Universidade Federal Rural Da Amazônia, Belém, 2023.
Orientador: Prof. Dr. Antonio Rodrigues Fernandes

1. Biocarvão. 2. Gestão de resíduos. 3. Resíduo de mineração. 4. Cachoeira do Piriá. 5. Biochar. I. Fernandes, Antonio Rodrigues, *orient.* II. Título

CDD 378.8115

Sumário

RESUMO

O processo mineração gera grandes quantidades de resíduos sólidos, os quais possuem grandes quantidades de elementos potencialmente tóxicos (EPTs), que são extremamente nocivos ao ambiente e a saude humana (por exemplo o arsênio). Um exemplo é a MAPE (mineração artesanal e de pequena escala) no município de Cachoeira do Piriá, estado do Pará, na localidade é realizada a exploração de ouro. Nesse contexto, esta pesquisa relaciona o uso de biocarvão para redução da biodisponibilidade e sua integração na avaliação do risco causado por arsênio (As) oriundo de residuos de mineração de ouro, com a finalidade de uso em programas de remediação ambiental. No capitulo 1, foi avaliada ainfluencia de 3 biocarvões (caroço de açaí, tegumento de castanha do Pará e torta de palmiste) em dois tipos de resíduos de mineração, aplicados a uma taxa de 5%. A adição dos 3 biocarvões proporcionaram o acumolo de As em frações mais estáveis e por consequência diminuíram a biodisponibilidade de As nos dois resíduos, o que pode auxiliar em programas de remediação ambiental. No capitulo 2, foi avaliada a influencia do enriquecimento do biocavão com fósforo (P) com uso de superfosfato simples e triplo (SFS e SFT) na bioacessibilidade, no acumulo de As em alface (*Lactuca Sativa*) e a interação do biochar na avaliação de risco a saúde humana com a ingetão de solo e material vegetal contaminado. Todos os biochars elevaram a bioacessibilidade de As, devido ao aumento dos teores de P no resíduo. A adição dos biochars proporcionaram a diminuição da translocação e acumulo de As nas folhas de alface, com excessão na condição de excesso de P (SFT). A adição dos biochars enriquecidos proporcionaram a diminuição dos níveis de avaliação de risco (HI), relacionado principalmente a diminuição do acumulo de As na folhas de alface. O enriqueciemento com SFS obteve os melhores resultados principalmente na disponibilização de nutrientes, diminuição do acumulo de As nas folhas de alface e por isso pode ser indicado como remediador ambiental, principalmente com o auxilio de espécies fitorremediadoras.

Palavras-chave: Pirolise; Gestão de resíduos; Resíduo de mineração; Cachoeira do Piriá

ABSTRACT

The mining process generates large amounts of solid waste, which have large amounts of potentially toxic elements (PTE's), which are extremely harmful to the environment and human health (eg arsenic). An example is MAPE (artisanal and small-scale mining) in the municipality of Cachoeira do Piriá, state of Pará, where gold exploration is carried out. In this context, this research relates the use of biochar to reduce bioavailability and its integration in the assessment of the risk caused by arsenic (As) from gold mining residues, with the purpose of use in environmental remediation programs. In chapter 1, the influence of 3 biochars (açaí kernel, Brazil nut husk and palm kernel cake) on two types of mining residues was evaluated, applied at a rate of 5%. The addition of the 3 biochars provided the accumulation of As in more stable fractions and consequently decreased the bioavailability of As in the two residues. In chapter 2, the influence of enrichment of biocavion with phosphorus (P) using single and triple superphosphate (SFS and SFT) on bioaccessibility, As accumulation in lettuce (Lactuca Sativa) and the interaction of biochar in the evaluation of risk to human health through ingestion of contaminated soil and plant material. All biochars increased the bioaccessibility of As, due to the increase of P contents in the residue. The addition of biochars provided a decrease in the translocation and accumulation of As in lettuce leaves, with the exception of the excess P condition (SFT). The addition of enriched biochars provided a decrease in risk assessment (HI) levels, mainly related to a decrease in As accumulation in lettuce leaves. The enrichment with SFS obtained the best results mainly in the availability of nutrients, reduction of the accumulation of As in the lettuce leaves and therefore it can be indicated as an environmental remedy, mainly with the help of phytoremediation species.

Key words: Pyrolysis; Mining waste; Cachoeira do Piriá

CONTEXTUALIZAÇÃO

A problemática da gestão de resíduos sólidos tem grande repercusão devido aos seus efeitos diretos relacionado aos meio-ambiente e por consequência ao ser humano. No contexto urbano, os principais relacionados aos resíduos sólidos são provocados pela sua deposição ou descarte inadequado, o que provoca a problemas relacionados a: poluição visual; proliferação de vetores de doenças; prejudica o sistema de drenanegem urbana etc. Na área agrícola, uma das problemáticas é a grande geração de resíduos sólidos orgânicos o qual é aproveitado, mas dependendo da sua origem a produção é tão elevada que não é possível o seu total reaproveitamento.

Em relação aos problemas ambientais em grande escala, a questão da gestão de resíduos sólidos (estéril e rejeitos) é ligada a grandes empreendimentos, como por exemplo a exploração mineral não legalizada (garimpos), por isso não se preocupam com estudos de impactos ambientais prévios que tem a finalidade de prever e tentar buscar alternativas que busquem minimizar os problemas ambientais gerados (antes, durante e depois) do processo de mineração.

Esse resíduo sólido oriundo de garimpos devidos aos processos utilizados para a exploração tem normalmente inúmeros elementos potencialmente tóxicos (EPT ou PTE), os quais dependendo da forma, tipo e quantidade propiciam inúmeros malefícios caso não ocorra nenhum tipo de cuidado com seu manuseio e deposição. Os resíduos comumente são depositados de forma inadequada o que trás maleficio para o solo, água, plantas e organismos encontrados em regiões próximas a deposição. O principal problema relacionado aos EPTs oriundo do estéril/rejeito é a sua inserção na cadeia trófica visto que esses elementos não são degradados.

A biodisponibilidade se refere à capacidade de um metal de interagir com as matrizes ambientais (por exemplo o solo), que sofre vários processos de destino/transporte, representando uma parte do reservatório total do metal (considerado como um sistema potencialmente biodisponível). Assim, o elemento biodisponivel é aquele que em determinado momento seja capaz de entrar em contato ou penetrar em um organismo, dependendo das condições ambientais (USEPA 2007: RYU et al., 2010; CAPORALE-VIOLANTE. 2016; KIM et al., 2015; TANG et al., 2018; CHEN et al., 2020; LOUZON et al., 2020; ZHAO et al., 2020; ZHENG et al., 2020).

No solo, a biodisponibilidade tem relação direta com a absorção de nutrientes por plantas. Especies vegetais necessitam de vários elementos quimicos (macro e micronutrientes) os quais auxiliam no seu desenvolvimento, a maioria dos nutrientes são absorvidos pelas raizes da planta, por isso a disponibilidade de contaminantes no solo pode proporcionar seu acumulo nos compartimentos vegetais. Existe uma grande problemática relacionado ao acumulo de contaminantes em vegetais, principalmente quando existe a possibilidade deles serem comestiveis.

O biochar tem influência direta na biodisponibilidade dos compostos devido a processos de complexação, adsorção e precipitação, proporcionados por suas características físico-químicas (pH, cinzas, componentes orgânicos e de sua estrutura porosa) que auxiliam na indisponibilidade de contaminantes (MUNIR et al., 2020; NEJAD et al., 2021; YUAN et al., 2021). Um fator relavante para a biodisponibilidade de EPT’s é a presença de ions metalicos no biocarvão (Fe, Mn, Ca, Mg e P) (YIN et al., 2021; XIAO et al., 2020; ZOU et al., 2021; XIANG et al., 2020), por exemplo o fosforo (P) possuiu importancia variável dependendo da caracteristica do EPT, para elementos aniônicos ocorre a competição por sitios superficiais de adsorção (estimulo a solubilização de ânions) e ja para catiônicos devido as cargas opostas não há a competição

por sitios de adsorção (estimulando a adsorção eletrostática e a formação de compostos insoluveis de fosfato) (ZHANG et al., 2020).

A biodisponibilidade humana é associada a quantidade em que o componente é absorvido (via ingestão, respiração, contato direto) e após os processos de absorção/digestão são metabolizados no trato-gastrointestinal e atinge a circulação sistêmica (DEAN, 2007; EL-KATTAN, 2017; HU & LI, 2011). Assim como esses processos estão relacionados a absorção de nutrientes/remédios por seres humanos, os mesmos conceitos podem ser considerados em relação as atividades de contaminação com elementos potencialmente tóxicos (EPTs). Para avaliar os riscos relacionados ao contato com os EPTs, faz-se necessário o uso de métodos de avaliação de risco a saúde humana.

A avaliação de risco a saúde humana é uma metodologia utilizada com a finalidade de estimar os efeitos tóxicos associados a exposição de substancias químicas tóxicas, como os EPTs, a qual consiste nas etapas a seguir: (1) identificação do perigo, ou seja, realização da caracterização inicial do local possivelmente contaminado e dos níveis de contaminante; (2) avaliação da exposição, determinada pela intensidade, frequência e duração da exposição ao contaminantes (usualmente determinado através do cálculo de ingestão média diária por 3 vias de exposição: ingestão, inalação e contato dérmico); (3) avaliação da toxidade e dose-resposta, a paritr de valores padronizados de fator sloop (SF), o qual considera o potencial risco associado a ocorrência de efeitos cancerígenos devido a exposição prolongada e a dose de referência diária (Rfd), considerando valores máximos de interação com o contaminante por 3 vias de exposição: ingestão, inalação e contato dérmico; e (4) caracterização que se utiliza das etapas anteriores para apresentar um valor fixo, determinando o grau de probabilidade para o desenvolvimento de

problemas de saúde, cancerígenos e não-cancerígeno (USEPA, 2001; 2007; OROSUN, 2021).

Comumente, os valores utilizados para os cálculos de avaliação de risco são os teores dos contaminantes extraídos utilizando a metodologia EPA 3051A ou EPA 3050B. Esses métodos utilizam-se de ácidos concentrados e que com o auxílio de micro-ondas, potencializa seu poder de dissolução, sendo considerados teores totais (excluindo a fração silicatada e ligada ao titânio) (USEPA, 1996; 2007; RODRIGUES et al., 2018). Altas concentrações de metais no ambiente, não necessariamente significam a possibilidade de transferência e consequentemente causar efeitos adversos aos organismos. Os principais riscos estão associados a biodisponibilidade, que está relacionada à interação do contaminante com o ambiente/organismos (USEPA, 2007; SUM et al., 2017; HAMID et al., 2018; ZHANG et al., 2018; LIU-HAN, 2020).

Uma grande variedade de pesquisas comprovam a diminuição da biodisponibilidade de contaminantes no solo após a adição de biochars, provocando a diminuição dos teores nas frações biodisponíveis F1 (solúvel/trocável/carbonatos) relacionados ao método BCR e F1+F2 (solúvel/trocável + carbonatos) do método de Tissier (1979), por consequência dessa menor biodisponibilidade ocorre menor absorção pelos vegetais e menor risco de lixiviação (ZHANG et al., 2016; ZHANG et al., 2017; MENG et al., 2018; HAO et al., 2019; HUANG et al., 2020), por conseguinte menor risco aos ecosistemas e a saúde. Recentemente, Huang et al (2016) e Jayarathne et al (2018) buscaram fazer a integração do fracionamento (bio)geoquimico, mais especificamente a fração biodisponível (fração soluvel+ trocável+ carbonatos), com a avaliação de risco à saúde humana e confirmaram que essa integração é extremamente necessária, devido ao fato de que a interação eletroquimica de esfera externa ou interna (JAYARATHNE et al., 2017) dos EPT’s com as diferentes particulas do material sólido é um fator chave para a

uma avaliação mais precisa dos possiveis impactos ambientais proporcionados pelos contaminantes.

Portanto, a integração da biodisponibilidade a avaliação de risco é um passo fundamental para um protocolo de controle mais realista da possível contaminação humana, devido a exposição aos possíveis contaminantes. O que torna a integração mais realista é o fato de que a biodisponibilidade do contaminante pode ser alterada em curtos períodos e/ou devido as alterações físico-química-biológicas, proporcionada pela adição de amenizantes (materiais orgânicos e biochars). Por conta dessa variação em curto período (diferentemente dos teores totais que sofrem variações em longos períodos), o monitoramento do risco ambiental de empreendimentos minerais torna-se mais eficiente apartir da definição da biodisponibilidade como valor norteador para tomada de decisão de quais materiais são mais apropriados para remediação de áreas degradadas.

REFERÊNCIAS

Caporale, A.G., Violante, A., 2016. Chemical Processes Affecting the Mobility of Heavy Metals and Metalloids in Soil Environments. Current Pollution Reports 2, 15–27. doi:10.1007/s40726-015-0024-y

Chen, X., Singh, A., Kitts, D.D., 2020. In-vitro bioaccessibility and bioavailability of heavy metals in mineral clay complex used in natural health products. Scientific Reports 10, 1–10. doi:10.1038/s41598-020-65449-4

Dean, J.R., 2007. BIOAVAILABILITY, BIOACCESSIBILITY AND MOBILITY OF ENVIRONMENTAL CONTAMINANTS, John Wiley & Sons. ISBN 978-0-470-02577-2.

El-Kattan, A.F., 2016. Oral Bioavailability Assessment: Basics and Strategies for Drug Discovery and Development, Oral Bioavailability Assessment: Basics and Strategies for Drug Discovery and Development. doi:10.1002/9781118916926

Hamid, Y., Tang, L., Wang, X., Hussain, B., Yaseen, M., Aziz, M.Z., Yang, X., 2018. Immobilization of cadmium and lead in contaminated paddy field using inorganic and organic additives. Scientific Reports 8, 1–10. doi:10.1038/s41598-018-35881-8

Hao, J., Wei, Z., Wei, D., Ahmed Mohamed, T., Yu, H., Xie, X., Zhu, L., Zhao, Y., 2019. Roles of adding biochar and montmorillonite alone on reducing the bioavailability

of heavy metals during chicken manure composting. Bioresource Technology 294, 122199. doi:10.1016/j.biortech.2019.122199

Hu, M., Li, X., 2011. Oral Bioavailability: Basic Principles, Advanced Concepts, and Applications, Oral Bioavailability: Basic Principles, Advanced Concepts, and Applications. doi:10.1002/9781118067598

Huang, C., Wang, W., Yue, S., Adeel, M., Qiao, Y., 2020. Role of biochar and Eisenia fetida on metal bioavailability and biochar effects on earthworm fitness. Environmental Pollution 263, 114586. doi:10.1016/j.envpol.2020.114586

Huang, J., Li, F., Zeng, G., Liu, W., Huang, X., Xiao, Z., Wu, H., Gu, Y., Li, X., He, X., He, Y., 2016. Integrating hierarchical bioavailability and population distribution into potential eco-risk assessment of heavy metals in road dust: A case study in Xiandao District, Changsha city, China. Science of the Total Environment 541, 969–976. doi:10.1016/j.scitotenv.2015.09.139

Jayarathne, A., Egodawatta, P., Ayoko, G.A., Goonetilleke, A., 2017. Geochemical phase and particle size relationships of metals in urban road dust. Environmental Pollution 230, 218–226. doi:10.1016/j.envpol.2017.06.059

Jayarathne, A., Egodawatta, P., Ayoko, G.A., Goonetilleke, A., 2018. Assessment of ecological and human health risks of metals in urban road dust based on geochemical fractionation and potential bioavailability. Science of the Total Environment 635, 1609–1619. doi:10.1016/j.scitotenv.2018.04.098

Kim, R.Y., Yoon, J.K., Kim, T.S., Yang, J.E., Owens, G., Kim, K.R., 2015. Bioavailability of heavy metals in soils: definitions and practical implementation—a critical review. Environmental Geochemistry and Health 37, 1041–1061. doi:10.1007/s10653-015-9695-y

Liu, M., Han, Z., 2020. Distribution and Bioavailability of Heavy Metals in Soil Aggregates from the Fenhe River Basin, China. Bulletin of Environmental Contamination and Toxicology 104, 532–537. doi:10.1007/s00128-020-02810-3

Louzon, M., Pelfrêne, A., Pauget, B., Gimbert, F., Morin-Crini, N., Douay, F., de Vaufleury, A., 2020. Bioaccessibility of metal(loid)s in soils to humans and their bioavailability to snails: A way to associate human health and ecotoxicological risk assessment? Journal of Hazardous Materials 384, 121432. doi:10.1016/j.jhazmat.2019.121432

Meng, J., Tao, M., Wang, L., Liu, X., Xu, J., 2018. Changes in heavy metal bioavailability and speciation from a Pb-Zn mining soil amended with biochars from co-pyrolysis of rice straw and swine manure. Science of the Total Environment 633, 300–307. doi:10.1016/j.scitotenv.2018.03.199

Munir, M.A. M., Liu, G., Yousaf, B., Ali, M.U., Abbas, Q., Ullah, H., 2020. Synergistic effects of biochar and processed fly ash on bioavailability, transformation and accumulation of heavy metals by maize (Zea mays L.) in coal-mining contaminated soil. Chemosphere 240, 124845. doi:10.1016/j.chemosphere.2019.124845

Nejad, Z. D., Rezania, S., Jung, M.C., Al-Ghamdi, A.A., Mustafa, A.E.Z.M.A., Elshikh, M.S., 2021. Effects of fine fractions of soil organic, semi-organic, and inorganic amendments on the mitigation of heavy metal(loid)s leaching and bioavailability in a post-mining area. Chemosphere 271, 129538. doi:10.1016/j.chemosphere.2021.129538

OROSUN, M.M., 2021. Assessment of Arsenic and its Associated Health Risks due to Mining Activities in parts of North-Central Nigeria: Probabilistic Approach Using Monte Carlo. Journal of Hazardous Materials 412, 125262. doi:10.1016/j.jhazmat.2021.125262

Rodrigues, S.M., Cruz, N., Carvalho, L., Duarte, A.C., Pereira, E., Boim, A.G.F., Alleoni, L.R.F., Römkens, P.F.A.M., 2018. Evaluation of a single extraction test to estimate the human oral bioaccessibility of potentially toxic elements in soils: Towards more robust risk assessment. Science of the Total Environment 635, 188–202. doi:10.1016/j.scitotenv.2018.04.063

Ryu, H., Chung, J.S., Nam, T., Moon, H.S., Nam, K., 2010. Incorporation of heavy metals bioavailability into risk characterization. Clean - Soil, Air, Water 38, 812–815. doi:10.1002/clen.201000070

Sun, J., Yu, R., Hu, G., Jiang, S., Zhang, Y., Wang, X., 2017. Bioavailability of heavy metals in soil of the Tieguanyin tea garden, southeastern China. Acta Geochimica 36, 519–524. doi:10.1007/s11631-017-0224-9

Tang, W., Xia, Q., Shan, B., Ng, J.C., 2018. Relationship of bioaccessibility and fractionation of cadmium in long-term spiked soils for health risk assessment based on four in vitro gastrointestinal simulation models. Science of the Total Environment 631–632, 1582–1589. doi:10.1016/j.scitotenv.2018.03.154

Xiang, W., Zhang, X., Chen, J., Zou, W., He, F., Hu, X., Tsang, D.C.W., Ok, Y.S., Gao, B., 2020. Biochar technology in wastewater treatment: A critical review. Chemosphere 252, 126539. doi:10.1016/j.chemosphere.2020.126539

Xiao, J., Hu, R., Chen, G., Xing, B., 2020. Facile synthesis of multifunctional bone biochar composites decorated with Fe/Mn oxide micro-nanoparticles: Physicochemical properties, heavy metals sorption behavior and mechanism. Journal of Hazardous Materials 399. doi:10.1016/j.jhazmat.2020.123067

Yin, Q., Liu, M., Li, Y., Li, H., Wen, Z., 2021. Computational study of phosphate adsorption on Mg/Ca modified biochar structure in aqueous solution. Chemosphere 269, 129374. doi:10.1016/j.chemosphere.2020.129374

Yuan, C., Gao, B., Peng, Y., Gao, X., Fan, B., Chen, Q., 2021. A meta-analysis of heavy metal bioavailability response to biochar aging: Importance of soil and biochar properties. Science of the Total Environment 756, 144058. doi:10.1016/j.scitotenv.2020.144058

Zhang, G., Guo, X., Zhao, Z., He, Q., Wang, S., Zhu, Y., Yan, Y., Liu, X., Sun, K., Zhao, Y., Qian, T., 2016. Effects of biochars on the availability of heavy metals to ryegrass

in an alkaline contaminated soil. Environmental Pollution 218, 513–522. doi:10.1016/j.envpol.2016.07.031

Zhang, H., Shao, J., Zhang, S., Zhang, X., Chen, H., 2020. Effect of phosphorus-modified biochars on immobilization of Cu (II), Cd (II), and As (V) in paddy soil. Journal of Hazardous Materials 390. doi:10.1016/j.jhazmat.2019.121349

Zhang, J., Li, H., Zhou, Y., Dou, L., Cai, L., Mo, L., You, J., 2018. Bioavailability and soil-to-crop transfer of heavy metals in farmland soils: A case study in the Pearl River Delta, South China. Environmental Pollution 235, 710–719. doi:10.1016/j.envpol.2017.12.106

Zhang, R.H., Li, Z.G., Liu, X.D., Wang, B. cai, Zhou, G.L., Huang, X.X., Lin, C.F., Wang, A. hua, Brooks, M., 2017. Immobilization and bioavailability of heavy metals in greenhouse soils amended with rice straw-derived biochar. Ecological Engineering 98, 183–188. doi:10.1016/j.ecoleng.2016.10.057

Zhao, L., Yan, Y., Yu, R., Hu, G., Cheng, Y., Huang, H., 2020. Source apportionment and health risks of the bioavailable and residual fractions of heavy metals in the park soils in a coastal city of China using a receptor model combined with Pb isotopes. Catena 194, 104736. doi:10.1016/j.catena.2020.104736

Zheng, S., Wang, Q., Yu, H., Huang, X., Li, F., 2020. Interactive effects of multiple heavy metal(loid)s on their bioavailability in cocontaminated paddy soils in a large region. Science of the Total Environment 708, 135126. doi:10.1016/j.scitotenv.2019.135126

Zou, H., Zhao, J., He, F., Zhong, Z., Huang, J., Zheng, Y., Zhang, Y., Yang, Y., Yu, F., Bashir, M.A., Gao, B., 2021. Ball milling biochar iron oxide composites for the removal of chromium (Cr(VI)) from water: Performance and mechanisms. Journal of Hazardous Materials 413, 125252. doi:10.1016/j.jhazmat.2021.125252

CAPITULO 1

Aprovado para a publicação na Journal of Environmental Management

BIOCHAR MITIGATES BIOAVAILABILITY AND ENVIRONMENTAL RISKS OF ARSENIC IN GOLD MINING TAILINGS FROM THE EASTERN AMAZON

Yan Nunes Dias[a*], Wendel Valter da Silveira Pereira[a], Marcela Vieira da Costa[a], Edna Santos de Souza[b], Silvio Junio Ramos[c], Cristine Bastos do Amarante[d], Willison Eduardo Oliveira Campos[e], Antonio Rodrigues Fernandes[a]

[a]Institute of Agricultural Sciences, Federal Rural University of the Amazon, 66077-830, Belém, Pará, Brazil.

[b]Xingu Institute of Studies, Federal University of Southern and Southeastern Pará, 68380-000, São Félix do Xingu, Pará, Brazil.

[c]Vale Institute of Technology – Sustainable Development, 66055-090, Belém, Pará, Brazil.

[d]Chemical Analysis Laboratory, Emílio Goeldi Museum of Pará, 66077-830, Belém, Pará, Brazil.

[e]Department of Teaching, Research and Extension, Federal Institute of Amazonas, 69552-555, Tefé, Amazonas, Brazil.

[*]Author by correspondence. E-mail: yan.dias@ufra.edu.br

GRAPHICAL ABSTRACT

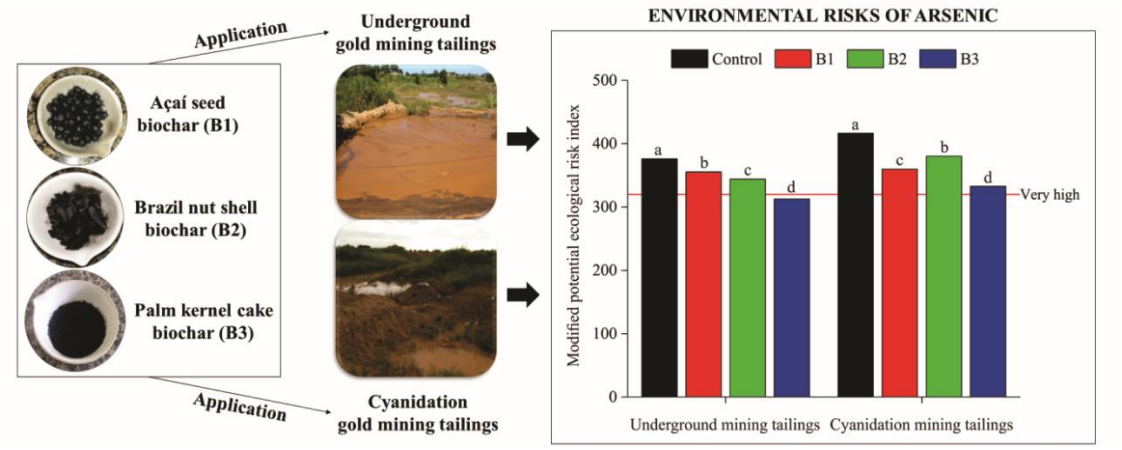

HIGHLIGHTS

- Three different biochars never studied before in As remediation were tested

- Bioavailable concentrations of As were reduced (4-17 mg kg^{-1}) after biochar addition

- Biochar addition statistically reduced the environmental risks of As (6-20%)

- Biochar efficiency showed the order palm kernel cake > Brazil nut shell > açaí seed

ABSTRACT

Artisanal gold mining has generated tailings highly contaminated by arsenic (As) in Cachoeira do Piriá, eastern Amazon, leading to severe risks to the environment. Such risks should be mitigated considering the bioavailable concentration of the element, since it implies immediate damage to the ecosystem. The objective of this study was to evaluate the potential of biochars in mitigating the environmental risks of bioavailable As concentrations in gold mining tailings from underground and cyanidation exploration. The biochar addition increased mineral components, cation retention, phosphorus in all fractions, and organic and inorganic carbon. The bioavailability of As was reduced after adding the biochars, following the order palm kernel cake biochar > Brazil nut shell biochar > açaí seed biochar, with reductions of up to 13 mg kg^{-1} in the underground mining tailings and 17 mg kg^{-1} in the cyanidation mining tailings. These results contributed to the statistically significant reduction of the environmental risks in both mining tailings (6 to 17% in the underground mining tailings and 9 to 20% in the cyanidation mining tailings), which was emphasized by Pearson's correlation and multivariate analyzes. The incorporation of the bioavailable fractions of As (from sequential extraction) in the environmental risk assessment was a promising method for evaluating the efficiency of biochars in mitigating the damage caused by this metalloid in gold mining tailings.

Keywords: arsenic contamination; arsenic bioavailability; arsenic exposure; environmental risks.

1. INTRODUCTION

Arsenic (As) is the most toxic element according to the Agency for Toxic Substances and Disease Registry (ATSDR, 2017), strongly associated with carcinogenesis in humans (Jaishankar et al., 2014; Singh et al., 2007). The main anthropic source of this metalloid in the environment is mining, due to the exposure of As-rich minerals to weathering (Drahota et al., 2014; Ono et al., 2012; Souza Neto et al., 2020), which can cause heavy environmental contamination, including soils in areas far from the exploration sites, as well as water bodies that could provide water for human consumption and industrial activities (Panagopoulos, 2021a, 2021b, 2021c). This problem is more pronounced in artisanal mining areas, where low mineral recovery techniques are used and the residues are improperly deposited in the environment (Souza Neto et al., 2020).

Total concentrations of potentially toxic elements (PTEs), including As, are usually adopted to assess the risks associated with these elements in contaminated areas. However, this information is not a proper predictor when evaluated individually, due to the fact that it does not reveal the mobility and bioavailability of these contaminants (Adamo et al., 2018; Alan and Kara, 2019; Gope et al., 2017; Nkinahamira et al., 2019). On the other hand, sequential extractions indicate the main fractions in which the PTEs are linked (Gabarrón et al., 2019), allowing to understand the actual risks caused by these elements in contaminated materials (Huang et al., 2016; Jayarathne et al., 2018).

Biochar is a carbonaceous material resulting from the pyrolysis of biomass under low oxygenation, suitable for controlling contamination (Lehmann et al., 2011, 2006; Penido et al., 2019; Uchimiya et al., 2011) and improving soil fertility and biological properties (Bashir et al., 2018; Chen et al., 2020; Liu et al., 2016; Penido et al., 2019; Sun et al., 2020; Wang et al., 2021). Some studies have evaluated the potential of biochar for environmental remediation using sequential extractions, showing how this material

affects chemical fractionation, mobility and bioavailability of PTEs (Chen et al., 2020; Huang et al., 2020; Lin et al., 2019; Wan et al., 2020; Wang et al., 2020a).

The effects of biochar on the bioavailability of PTEs are related to complexation, adsorption, and precipitation processes promoted by its physicochemical properties (Derakhshan Nejad et al., 2021; Mujtaba Munir et al., 2020; Yuan et al., 2021) and concentrations of metallic ions, such as iron (Fe), manganese (Mn), calcium (Ca) and magnesium (Mg), as well as non-metallic ions, such as phosphorus (P) (Xiang et al., 2020; Xiao et al., 2020; Yin et al., 2021). The application of biochar does not change the total concentrations of PTEs, but rather the bioavailable fraction, which most interacts with the environment (O'Connor et al., 2018; Wang et al., 2021) and threatens the food chain, due to the greater potential for absorption by plants (O'Connor et al., 2018; Peijnenburg, 2020). Thus, our study is a pioneer in assessing the environmental risk of As based on the bioavailable concentrations of this element, in gold mining tailings treated with two biochars never tested before for this purpose.

In Cachoeira do Piriá, northeastern Amazon, different forms of artisanal gold mining have produced tailings highly contaminated by As, which are improperly deposited in the environment and require remediation to protect the ecosystem and local population (Souza Neto et al., 2020). The use of agro-industrial residues (largely produced in the Amazon), in the form of biochar, can be an interesting alternative for the remediation of these tailings, but this has not been studied so far. Therefore, the objectives of this study were: i) to evaluate the effect of biochars on the mobilization of As in two types of gold mining tailings, and ii) to characterize the efficiency of biochars in reducing the environmental risks of As based on the bioavailable concentrations of this metalloid.

2. MATERIAL AND METHODS

2.1. Collection of mining wastes

Mining wastes were collected in the municipality of Cachoeira do Piriá, state of Pará, northern Brazil. In this area, mining was carried out by both companies and artisanal workers until 2013, in sites where gold occurs at depths ranging from 40 to 150 m, in quartz veins, vein networks, and shear zones (Mosher, 2013; Santos, 2004). Currently, exploration is performed only by a cooperative through three main ways: i) underground mining, whose tailings have different deposition periods; ii) cyanidation mining, in which underground mining tailings are reprocessed using cyanide; and iii) colluvial mining (Souza Neto et al., 2020).

This study considered two tailings highly contaminated by As (Souza Neto et al., 2020), identified as: i) underground mining tailings, deposited seven years before the collection, from exploration at a depth of approximately 150 m, in which amalgamation is carried out with the conduction of the leachate (solid material and water) on copper plates containing mercury for gold retention, occupying an area greater than 12 ha (Fig. 1S); and ii) cyanidation mining tailings, from recent reprocessing of underground mining tailings with alkaline cyanide solution to complex the residual gold, deposited in area equivalent to 3 ha (Fig. 1S). Both tailings were collected in April 2018, at random to obtain a better representation of each deposition area.

2.2. Production of biochars

Açaí palm (*Euterpe oleracea* Mart.) seeds, Brazil nut (*Bertholletia excelsa* Bonpl.) shells, and palm kernel cake from the processing of oil palm (*Elaeis guineensis* Jacq.) were used in the production of biochars. Açaí seeds and Brazil nut shells were collected at fairs in the municipality of Belém, state of Pará, where the respective pulp

and nuts are processed and sold. Palm kernel cake was collected at a company located in the municipality of Santa Bárbara do Pará, also in the state of Pará. These materials were selected due to the high regional production, varied proportions of lignin, cellulose and hemicellulose, and the potential as adsorbent materials, which is indicated for the remediation of degraded areas (Dias et al., 2019).

These wastes were washed with deionized water and dried in an oven at 50 ºC for 24 h. After that, 100 g of each material were weighed, placed in porcelain crucibles, and pyrolyzed in a muffle oven at 700 ºC, under a heating rate of 3.33 ºC/min. This temperature was adopted due to the generation of biochars with better characteristics and greater adsorption capacity (Dias et al., 2019). The biochars were crushed, sieved (100 mesh), and identified as: B1 - açaí seed biochar; B2 - Brazil nut shell biochar; and B3 - palm kernel cake biochar.

2.3. Characterization of mining tailings and biochars

The concentrations of As in the tailings were extracted according to the EPA 3051A method (USEPA, 2007), in which 9 mL HNO_3 and 3 mL HCl were applied in 0.5 g of each sample, in triplicate, with digestion in a microwave oven (CEM corporation, model MARS 5®). The quantification was carried out using inductively coupled plasma mass spectrometry (ICP-MS, PerkinElmer), including the ERM® CC-141 certified reference material and blank samples to ensure analytical quality. The recovery rate of As was 95%.

The mineralogical characterization (0.15 mm fine fraction) was performed by PANalytical X'PERT PRO MPD (PW 3040/60) diffractometer powder method, with goniometer PW3050/60 (θ/θ), ceramic-ray tubes with Cu (Kα1 = 1.540598 Å), model PW3373/00, long fine focus (2200 W - 60 kV), Kβ nickel filter. The instrumental

scanning conditions were: 4° to 70°2θ, step size 0.02° 2θ and time/step of 10 s, divergent and automatic slit and anti-spreading of 4°; 10-mm mask; sample in circular motion with frequency of 1 rotation/s for all samples. The materials were identified using X-ray diffraction (Fig. 2S).

In the characterization of biochars, the pH in water was determined at a ratio of 1:10 (solid:solution) (Singh et al., 2017), and the point of zero charge (PZC) was found according to Uchimiya et al., (2011), when the initial and final pH values were equal. The total levels of C, H, N and S were determined using an elemental analyzer (PerkinElmer, model 2400) and the ash content was quantified by combustion of 1 g of biochar in a muffle oven, maintained at 500 ºC for 1 h and 700 ºC for 2 h (Melo et al., 2013).

The pseudo total concentrations of elements were extracted using the same method used in the characterization of tailings (EPA 3051A) (USEPA, 2007). The analyzes were performed in triplicate, including the ERM® CC-141 certified reference material and blank samples, in order to ensure analytical quality. The recovery rates ranged from 85 to 97%.

2.4. Biochar application experiment

The two artisanal mining tailings were subjected to the application of 5% of biochar. Each treatment (Control, B1, B2 and B3) had five replications, totaling 20 experimental units per tailing, which were conducted in a completely randomized design and maintained at 50% of the total water holding capacity throughout the incubation period, with addition of ultrapure water (Milli-Q).

One year after the addition of biochars, the pseudo total concentrations of Al, Ca, Co, Cu, Fe, K, Mg, Mn, P, S and Zn were quantified by the method EPA 3051A (USEPA, 2007), with recovery rates varying from 87 to 93%. The pH was obtained with a

potentiometer in water (1:10 ratio) (Souza et al., 2019) and the cation exchange capacity (CEC) was quantified by the modified method of NH_4-acetate displacement (Yuan et al., 2011). Contents of organic carbon (OC) and inorganic carbon (IC) were determined by loss of mass via dry combustion in a muffle oven, under temperatures of 450 and 950 °C, respectively. Total carbon (TC) was obtained by the sum of OC and IC (Hussain et al., 2019).

The fractionation of P was performed due to the role that this element plays on the dynamics of As (Xiang et al., 2020; Xiao et al., 2020; Yin et al., 2021). This analysis followed the methodology proposed by He et al., (2014), which allowed to obtain the following fractions: i) soluble inorganic P (P_{sol}), extracted using ultrapure water; ii) labile inorganic P (P_{lab}), extracted using 0.5 M $NaHCO_3$; iii) adsorbed inorganic P (P_{ads}), extracted using 0.1 M NaOH; iv) P associated with minerals (P_{min}), extracted using 1 M HCl; and v) residual P (P_{res}), obtained with acid digestion (method EPA 3051A) of the solid material remaining from the previous extractions. The P_{sol}, P_{lab}, IP_{ads}, and P_{min} fractions were quantified by the colorimetric method described by Murphy and Riley (1962), while the P_{res} fraction was quantified using ICP-MS.

2.5. Chemical fractionation of As

The sequential extraction developed by Drahota et al., (2014) was used to study the chemical fractionation of As. This method can be adopted reliably for the partitioning of As in mining wastes, allowing to determine the association of this element with the following fractions: readily soluble (F1); adsorbed (F2); amorphous and poorly-crystalline arsenates, oxides and hydroxosulfates of Fe (F3); well-crystalline arsenates, oxides, and hydroxosulfates of Fe (F4); and sulfides and arsenides (F5).

The F1 fraction was extracted with ultrapure water (1:25 sample:water), stirred for 10 h; the F2 fraction was obtained with 0.01 M $NH_4H_2PO_4$ (1:100 sample:solution), stirred for 16 h; the F3 fraction was extracted with 0.2 M NH_4-oxalate/oxalic acid (1:100 sample:solution, in the dark, pH 3, stirred for 2 h; the F4 fraction was extracted with 0.2 M NH_4-oxalate/oxalic acid (1:100 sample:solution, pH 3, at 80 ºC), stirred for 4 h; and the F5 fraction was extracted with KCl/HCl/$KHNO_3$ solution (1:100 sample:solution). The concentrations were obtained by flame atomic absorption spectrometry (FAAS) (Thermo Scientific, model iCE3000) with a hydride generator (Thermo Scientific, model VP100). To guarantee the analytical quality, these analyzes were performed in triplicate and included a blank sample in each battery. The recovery rate of As was represented by the ratio between the sum of the concentrations found in the F1, F2, F3, F4 and F5 fractions and the total concentration, varying from 92.2 to 97.3%.

2.6. Environmental risk assessment

In this study, the bioavailable concentration (BAC) of As was represented by the soluble and adsorbed fractions (F1 + F2), due to the easier release of the metalloid from these fractions to the ecosystem (Dong et al., 2020; Jayarathne et al., 2018; Silva Júnior et al., 2019). In order to understand the role of biochars in mitigating the environmental risks associated with As in the studied mining tailings, the potential ecological risk index (PERI) was calculated.

The PERI was first proposed by Hakanson (1980), to assess the impact of PTEs on ecosystems considering pseudo total concentrations (Zhang et al., 2018). Although this index has been widely used to study the ecological risk in soils and mining wastes (Kowalska et al., 2018; Lin et al., 2019; Pereira et al., 2020; Tapia-Gatica et al., 2020; Xiao et al., 2019), it can overestimate the risks by not considering the bioavailable

fraction, which has immediate effect on the ecosystem (O'Connor et al., 2018; Peijnenburg, 2020). Therefore, the bioavailable concentrations were incorporated into the calculation of the modified ecological risk index ($PERI_m$) according to the methodology proposed by Jayarathne et al., (2018), following equation 1:

$$PERI_m = T_{As} \times \left(\frac{BAC_{As}}{NC_{As}}\right) \quad \text{Equation 1}$$

Where T_{As} is the toxic response factor of As (10) (Hakanson, 1980); BAC_{As} is the sum of the As concentrations (mg kg^{-1}) in the F1 and F2 fractions (bioavailable fraction); and NC_{As} is the concentration of As in the reference area (2.06 mg kg^{-1}) (Souza Neto et al., 2020). The results were interpreted according to Hakanson (1980), where PERI ≤ 40 indicates low risk, 40 < PERI ≤ 80 indicates moderate risk, 80 < PERI ≤ 160 indicates considerable risk, 160 < PERI ≤ 320 indicates high risk, and 320 < PERI indicates very high risk.

2.7. Statistical analyzes

The results were submitted to the Shapiro-Wilk normality test ($p < 0.05$). Given normality, an analysis of variance (ANOVA) was performed and the averages were compared using the Tukey test ($p < 0.05$). Relationships between the properties of the biochars and As fractions in the tailings were evaluated by principal component analysis (PCA). In addition, to corroborate the results obtained in the PCA, Pearson's correlation analysis (p <0.05) was carried out.

A multiple linear regression analysis was performed to generate a robust model for estimating the bioavailability of As. Variables for modeling were selected using Pearson's correlation ($p < 0.05$), while the most appropriate model was selected based on

the F test ($p < 0.05$) and AIC (Akaike Information Criterion) values. The equation of the multiple linear regression was obtained by the Stepwise method, eliminating the variables without statistical significance for the model. The precision and accuracy of the selected model were assessed using the coefficient of determination (R^2), adjusted coefficient of determination (R^2 adjusted), and normalized root mean square error (NRMSE) (Waterlot et al., 2016). All statistical analyzes were performed using R, version 4.1.1 (R Core Team, 2021).

3. RESULTS AND DISCUSSION

3.1. General characteristics of biochars and mining tailings

All biochars studied showed alkaline pH (Table 1), which is related to the accumulation of ash, common in the pyrolysis of organic materials under high temperatures (Adhikari et al., 2019). The ash content had an inverse behavior (B3 > B1 > B2) in relation to the carbon content (B2 > B1 > B3). Biochars with higher ash contents, such as B1 and B3, are rich in inorganic compounds (Domingues et al., 2017) and have lower carbon contents. On the other hand, the lower ash content in B2 is related to the higher carbon content, resulting from the high content of lignin in the source (Dias et al., 2019).

The biochars presented varied levels of P, Ca, Mg, Mn, Fe and S (Table 1). Such variations can be explained by the different chemical compositions of the materials used as sources (Wang et al., 2021). The fractions of P followed the same trend as the total contents of this element (B3 > B1 > B2). In the environment, P tends to be available after the mineralization of organic material (Wierzbowska et al., 2020), which occurs through pyrolysis in the case of biochars (Adhikari et al., 2019; He et al., 2014).

The pseudo total concentrations of elements were varied in the two gold mining tailings (Table 2), mainly due to the different exploration processes. In both materials, the concentrations of As were extremely higher than the quality reference value (1.4 mg kg^{-1}) established for soils from the state of Pará (Fernandes et al., 2018) and the investigation value (35 mg kg^{-1}) established by the National Environment Council for Brazilian soils (CONAMA, 2009), suggesting potential risks to human health due to As exposure.

The underground mining tailings showed a higher concentration of As when compared to the cyanidation mining tailings, which may be directly related to losses during the dissolution of minerals in cyanidation (Kyle et al., 2012). Such losses can harm the environment and human health due to the contamination of soil, water, and plants (Pereira et al., 2020; Souza Neto et al., 2020). The concentrations found in both tailings are higher than those found by Souza et al., (2017) in Serra Pelada, Brazil, and by Ding et al., (2016) in China.

3.2. Influence of biochars on tailings properties

The addition of biochars increased the concentrations of Co, K, Mn, P and S in the underground mining tailings, as well as Fe, Ca, Cu, K, Mg, Mn, P and S in the cyanidation mining tailings (Table 3). These findings indicate that biochars were relevant sources of inorganic components, which is commonly observed in studies assessing these materials. In a low fertility soil from Nepal, the addition of biochar improved the levels of Ca, Mg, K and P (Pandit et al., 2018). Biochars produced with residues from the southeastern Brazil increased the levels of K and Ca in the soil (Domingues et al., 2017).

The fractionation of P was modified by the application of biochar in both tailings (Table 4). B3 added higher levels of P in all fractions, which is related to the higher total concentrations in this material, followed by B1 and B2 (Table 1). P-rich biomasses, such

as palm kernel cake (used in the production of B3), tend to release high levels of this element during pyrolysis (Wang et al., 2021). After the application of biochar, the availability of P is controlled by the biological activity in the environment, in addition to reactions with inorganic colloids (Hosseini et al., 2019; Richardson and Simpson, 2011).

The addition of biochar increased the CEC in the tailings (Table 4), which is related to the negative charges from organic groups (with high reactivity) and alkaline components of ash, increasing the amount of cation sorption sites (Hailegnaw et al., 2019; Munera-Echeverri et al., 2018). In addition to CEC, the C content also increased with the addition of biochars to the tailings (Table 4), derived from the partial pyrolysis of biomass and carbonates in the ash, as well as the generation of pyrogenic C during the mineralization of OC to IC in pyrolysis (Amoakwah et al., 2020; Dong et al., 2019; Shi et al., 2021). Increase in C with the addition of biochar was also observed by Luo et al., (2020) in soils from China.

3.3. Effects of biochars on As fractionation

3.3.1. Underground mining tailings

All fractions of As were influenced by the biochars, with the exception of the F1 fraction after the addition of B2 (Fig. 1), whose low solubilization potential is related to the lower levels of OC and P (Table 4), resulting in less repulsion of As (Williams et al., 2011; Zheng et al., 2012). On the other hand, the greater solubilization of As with the addition of B1 and B3 is related to the higher contents of ash (Table 1), which is rich in carbonates, hydroxides and oxides, and mineral components (Beiyuan et al., 2017; Dias et al., 2019). Such conditions increased the pH of the tailings (Table 4), favoring the repulsion/solubilization of As oxianions that tend to be easily desorbed (Kim et al., 2018; Tian et al., 2021; Zhang et al., 2020) and replaced by basic components.

The greater solubility of As promoted by B3 in relation to B1 can be explained by the higher levels of P (total and fractions) and OC provided by this biochar (Table 4). In this process, the release of As is from the replacement of this metalloid by P (phosphate ions) on the surface of the tailings particles, due to the chemical similarity between these elements and greater solubilization provided by organic components (Beesley et al., 2014; Lin et al., 2017; Smith and Naidu, 2009; Yin et al., 2017).

The application of B1 and B3 promoted the mobilization of As from the F2, F3 and F4 fractions to the F1 fraction (Fig. 1). These two biochars present higher levels of P (Table 4), which has the potential to replace the electrostatically adsorbed As (Beesley et al., 2014; Lin et al., 2017). Moreover, the dissolved organic matter resulting from the application of these biochars may have caused the dissolution of Fe and Mn oxides (responsible for more stable bonds), releasing the precipitated and adsorbed As (Beiyuan et al., 2017; Kim et al., 2020, 2019, 2018). On the other hand, the dissolution of Fe and Mn oxides may have been lower with the application of B2 due to the lower levels of lignin, producing a lower content of dissolved organic matter (Dias et al., 2019; Kim et al., 2020).

With the addition of B2, the concentrations of As decreased in the F3 fraction and increased in the F5 fraction (Fig. 1), which is due to the dissolution of amorphous minerals (Kim et al., 2018), followed by readsorption in the crystalline fraction, in which As presents greater stability. The higher concentrations of Fe, Co and Mn after application of B2 (Table 3) suggest increased contents of crystalline oxides formed by these elements, causing higher adsorption and lower mobility of As, which has greater stability when bound to oxides (Yin et al., 2017; Yu et al., 2017, 2015). These bonds become stronger and more stable with the aging of the tailings, which decreases solubilization (Agrafioti et al., 2014; Beiyuan et al., 2017; Zhang et al., 2020). B1 was the only biochar that reduced

the concentrations of As in the most stable fraction (F5) (Fig. 1), possibly due to the lower levels of Fe in this biochar (Table 1), which may have favored the mobilization of As to less stable fractions.

3.3.3. Cyanidation mining tailings

The application of B1, B2 and B3 reduced the concentrations of As by 15.3, 10.3 and 20.6% in the F2 fraction; 25, 15.3 and 11.1% in the F3 fraction; and 61.6, 24.9 and 19.7% in the F4 fraction, respectively, in relation to the control treatment. Such reductions are directly related to the increment in CEC with the addition of these biochars (Table 4), which increased the electrostatic repulsion of As and favored the mobilization of this metalloid (Lomaglio et al., 2017; Tian et al., 2021; Zhang et al., 2020).

The decrease of As concentrations in the F3 and F4 fractions (Fig. 1) with the application of all biochars, especially B1, may be related to the reductive dissolution of Fe and Mn in oxides, caused by the increment in OC, which was more pronounced with the addition of B1 (Table 4) and may have led to the solubilization (Beiyuan et al., 2017; Kim et al., 2018; Wang et al., 2017) and mobilization of As for both less stable (F1 fraction) and more stable (F5 fraction) forms.

The concentrations of As increased in the F5 fraction, corresponding to 38.6, 12.6 and 4% after application of B1, B2 and B3, respectively (Fig. 1). The greater percentage with the addition of B1 is related to the higher concentrations of S, Fe, Ca, Cu and Mn (Table 3), suggesting that greater contents of sulfide compounds tend to favor more stable chemical bonds between As and sulfides (Drahota et al., 2014; Wang et al., 2015). The stabilization of As with the application of biochar was also observed by Luo et al., (2020) in soils from China, as well as by Zhang et al., (2020) in sediments from the same country.

3.4. Multivariate analyzes and Pearson's correlation

In the underground mining tailings, the PCA revealed that the first two principal components (PC) explained 97.2% of the total data variation, with 82.5% explained by PC1 and 14.7% by PC2 (Fig. 2). PC1 was positively dominated by the ash content, total P and fractions, and the F1 fraction of As, indicating that this metalloid is influenced by soluble components (ash) and that there is competition for adsorption sites with phosphate ions, in addition to the dominance of the properties of B3, which promoted greater solubilization of As. Moreover, PC1 was negatively related to CEC, pH, TC and S of B1 and B2, and the F2, F3 and F4 fractions of As. PC2, in turn, was positively dominated by the F5 fraction of As and the contents of S and Fe from biochars, as well as negatively dominated by the concentration of Mn in the biochars, demonstrating the effect of mineral components (Fe, Mn and S) on the retention of As in less available fractions.

Significant Pearson's correlations ($p < 0.05$) were found between the fractions of As and the properties of biochars in the underground mining tailings (Table 1S), which supports that the addition of these materials modified the bioavailability of the metalloid. The F1 fraction of As showed a positive correlation with ash, Ca, Al, Mn, Mg and P fractions of biochars; the F2, F3 and F4 fractions of As presented negative correlations with ash, Ca, Al, Mn, Mg and P fractions of the biochars; and the F5 fraction of As showed positive correlations with the levels of Fe and Ca in the biochars (Table 1S). Such results indicate that the biochar properties (ash, Ca, Al, Mn, Mg and fractions of P) were essential for the solubilization of As from the most stable fractions (Fig. 1).

The first two principal components accounted for 95.6% of the data variation in the cyanidation mining tailings (Fig. 2), with 77.4% explained by PC1 and 18.2% explained by PC2. PC1 was positively dominated by N, ash, total P and fractions, in addition to the properties of B3, and negatively dominated by CEC, pH, TC, S, and F1

and F2 fractions of As from B1 and B2, due to the greater solubilization caused by the addition of these biochars to the tailings (Fig. 1). PC2 was positively dominated by the F3 and F4 fractions of As and the content of Fe from biochars, and negatively dominated by the F5 fraction of As and the concentration of Mn in the biochars, indicating the influence of mineral components on the retention of As in less reactive fractions.

In the cyanidation mining tailings, the F1 and F2 fractions of As showed negative correlations with ash, Fe, Ca, Al, Mn, Mg and P fractions, as well as positive correlations with pH, CEC and TC of biochars; the F3 and F4 fractions of As showed positive correlations with O, Fe and Ca of biochars; and the F5 fraction of As had negative correlations with Fe, Ca and Al of biochars (Table 1S). These results demonstrate that the changes promoted by the biochar properties (pH, CEC and TC) contributed to the solubilization of As, and that the mineral content (Fe, Ca, Al, Mn and Mg) led to the accumulation of As in less reactive fractions in these materials (Fig. 1).

The models proposed to estimate the bioavailability of As were: i) properties of biochars; ii) properties of mining tailings; and iii) interaction between properties of biochars and mining tailings. The ANOVA revealed that there are no significant differences between the models (Table 2S). The model represented by the interaction between materials showed higher adjustment values (adjusted R^2) and lower AIC (Table 3S). Therefore, this model was selected as the most representative for multiple linear regression.

The multiple linear regression (Table 4S) revealed that the properties most related to the bioavailability of As were: adsorbed As, total P and fractions (soluble, adsorbed and mineral), and organic carbon in the mining tailings; and ash, CEC, N and P fractions (soluble, adsorbed and mineral) in the biochars. Based on the values of NRMSE and R^2 (Fig. 3S), it is possible to state that the selected model was appropriate for predicting the

As bioavailability. All characteristics included in the model ($p < 0.05$) indicate the direct influence of ash (rich in P) and organic compounds (OC and N) in the solubilization of As from stable fractions (Kim et al., 2020, 2018) and, consequently, greater bioavailability. These results suggest that the multiple linear regression can be an important tool, due to the direct influence of the materials on the bioavailability of contaminants (O'Connor et al., 2018; Peijnenburg, 2020).

3.5. Bioavailability and environmental risks of As

The application of biochar decreased the bioavailable concentrations of As in both mining tailings, with results ranging from 64.4 to 77.48 mg kg^{-1} in the underground mining tailings, and from 68.55 to 85.78 mg kg^{-1} in the cyanidation mining tailings (Fig. 4S). These reductions are related to the increase in IC and metal ions such as Al, Fe and Mn (Tables 3 and 4), which contributed to a greater retention of anions in more stable fractions (Wu et al., 2020). The greater bioavailability of As in the cyanidation mining tailings may be related to the use of Na cyanide solution during gold extraction (Kuyucak and Akcil, 2013), which promotes partial dissolution of Fe, Al and Mn minerals (Rubinos et al., 2011), releasing As. After dissolution, the metalloid tends to be even more desorbed with increasing pH, due to competition with OH^- ions (Li et al., 2017; Vodyanitskii, 2006; Xue et al., 2019; Yin et al., 2015).

The bioavailable concentrations of As were incorporated into the assessment of environmental risks to reveal the actual damage of the metalloid. In the control treatment, which indicates the conditions in which tailings are deposited, the $PERI_m$ values were 376.12 in the underground mining tailings and 416.39 in the cyanidation mining tailings (Fig. 3). These results were lower than those obtained by Souza Neto et al., (2020), who studied the environmental risk of As in the same locality, based on pseudo total

concentrations, and observed PERI values of 14131 in the underground mining tailings and 8951 in the cyanidation mining tailings, indicating possible overestimation of risks.

The application of B3 in the underground mining tailings was the only treatment that promoted a change in the class of risk according to the classification proposed by Hakanson (1980) for PERI values, modifying the ecological risk from very high to high (Fig. 3). However, the ecological risk was significantly reduced in all treatments after the application of biochars ($p < 0.05$), with reductions of 5.51, 8.53 and 16.88% in the underground mining tailings, and 13.60, 8.69 and 20.08% in the cyanidation mining tailings, in response to the application of B1, B2 and B3, respectively.

The adoption of bioavailability can be an important tool for the proper assessment of As risk, considering that high bioavailable levels indicate higher mobility and, consequently, greater risk to the environment (Dong et al., 2020; Silva Júnior et al., 2019). In this study, the application of biochars increased the concentrations of As in more stable fractions and decreased the bioavailable level, which is a highly beneficial process for the environment. Moreover, the reduction of the bioavailable fraction and the ecological risk may also imply a reduction in the risk to human health, due to lower As entry into the food chain.

The application of biochar can reduce soil density (Cao et al., 2014) and increase water infiltration into the soil (with increasing porosity), which is fundamental to reduce the dispersion of PTEs (Cao et al., 2014; Chen et al., 2016). On the other hand, biochar can confer less resistance to the soil in relation to external agents, especially in areas of accentuated relief, which are more susceptible to losses by erosion. In these cases, an interesting alternative is the application of biochar together with limestone, which has the potential to improve soil resistance and stability and, consequently, reduce losses by erosive agents (Wang et al., 2020b), protecting water resources for human consumption

(Koley, 2021). The adoption of these practices can also promote improvements in soil conditions for plant growth, contributing to increased plant cover and slope stability (Chen et al., 2016).

To better assess the effects of biochars on the environment, it is essential to conduct the new studies involving the bioavailability of As. The application of different rates of biochars under field conditions, including an expressive number of samples and areas, and in different positions in the relief, aiming to have a greater representation of the bioavailable concentrations, to estimate models that can accurately predict the environmental risks of the element (Jia et al., 2021). It would also be interesting to collect organisms (such as plants and fish) to analyze the As content in the issue, aiming to know the content absorbed and bioaccumulated from the environment (Lima et al., 2022; Ray et al., 2021), which could reinforce the role of biochar in reducing the risks to the environment and human health from As exposure.

4. CONCLUSIONS

The chemical properties of biochars have a direct influence on the solubility of As in the mining tailings, with emphasis on the levels of P and mineral components, which mobilize the metalloid to less bioavailable fractions. The multivariate (PCA and multiple regression) and Pearson's correlation analyzes demonstrate that the interaction of biochars with mining tailings is the key to understanding the reduced bioavailability of As. All studied biochars decreased the bioavailable concentrations of As, following the sequence palm kernel cake > Brazil nut shell > açaí seed in both tailings, reaching reductions of up to 13 mg kg^{-1} (underground mining tailings) and 17 mg kg^{-1} (cyanidation mining tailings). Consequently, the environmental risks decreased between 6 and 17% in the underground mining tailings and between 9 and 20% in the cyanidation mining

tailings. The incorporation of the bioavailable concentrations in risk assessments is an alternative for recommending the application of biochars in mining tailings contaminated by As, based on reliable indicators. Our results indicate that the tested biochars can contribute to the mitigation of the impacts caused by As, especially if applied considering the relief conditions and in association with techniques that improve efficiency. In addition, our findings may support new studies focused on the remediation of areas contaminated by As, including the use of new agro-industrial residues and application rates, aiming to reduce the risks to the ecosystem and human health.

ACKNOWLEDGEMENTS

The authors would like to thank the Coordination for the Improvement of Higher Education Personnel (CAPES) and the Brazilian National Council for Scientific and Technological Development (CNPq) (No. 425312/2018-6), for the financial support and the scholarships provided in the development of this study.

FIGURES

Fig. 1.

Concentrations of As in readily-soluble (F1), adsorbed (F2), amorphous and poorly-crystalline arsenates, oxides and hydroxosulfates of Fe (F3), well-crystalline arsenates, oxides, and hydroxosulfates of Fe (F4), and linked to sulfides/arsenides (F5) fractions, in underground mining tailings (A) and cyanidation mining tailings (B) after application of açaí seed (B1), Brazil nut shell (B2), and palm kernel cake (B3) biochars. Different letters indicate significant difference between treatments by the Tukey test ($p < 0.05$).

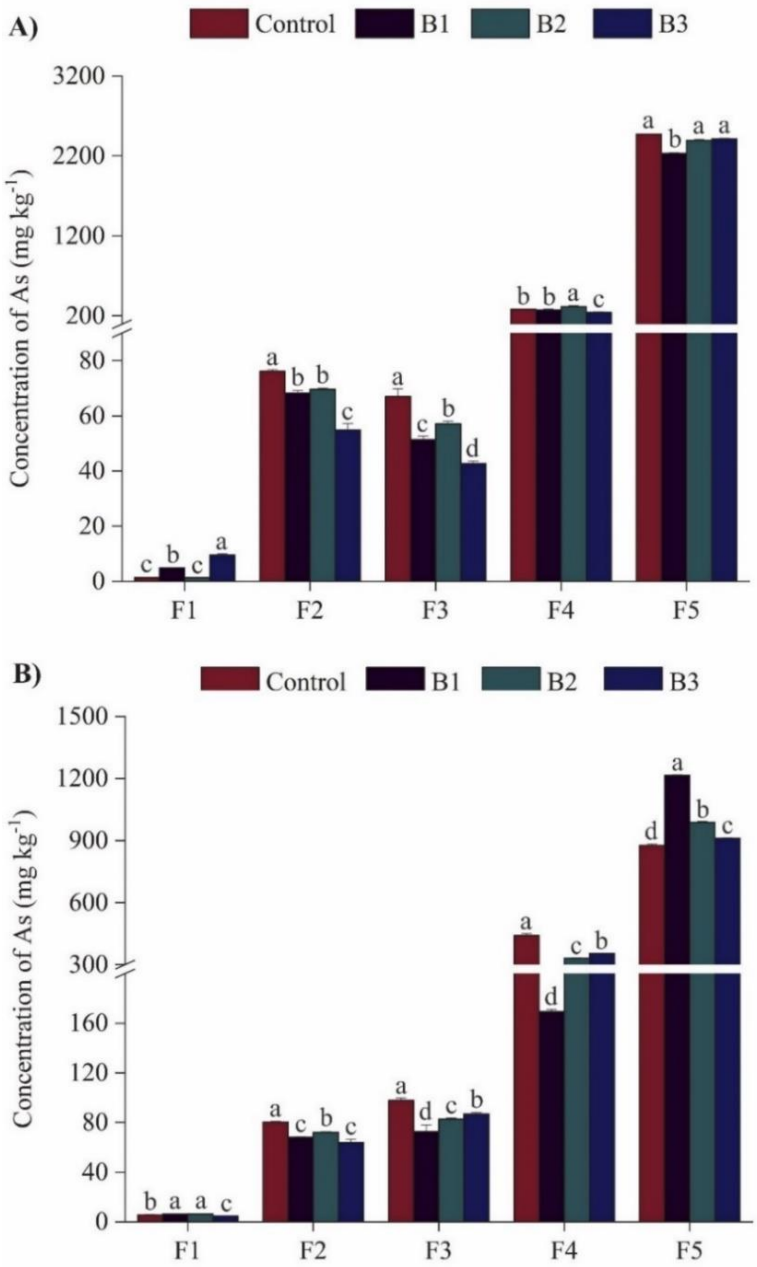

Fig. 2.

Principal component analysis between açaí seed (B1), Brazil nut shell (B2) and palm kernel cake (B3) biochars and fractions of As in gold mining tailings.

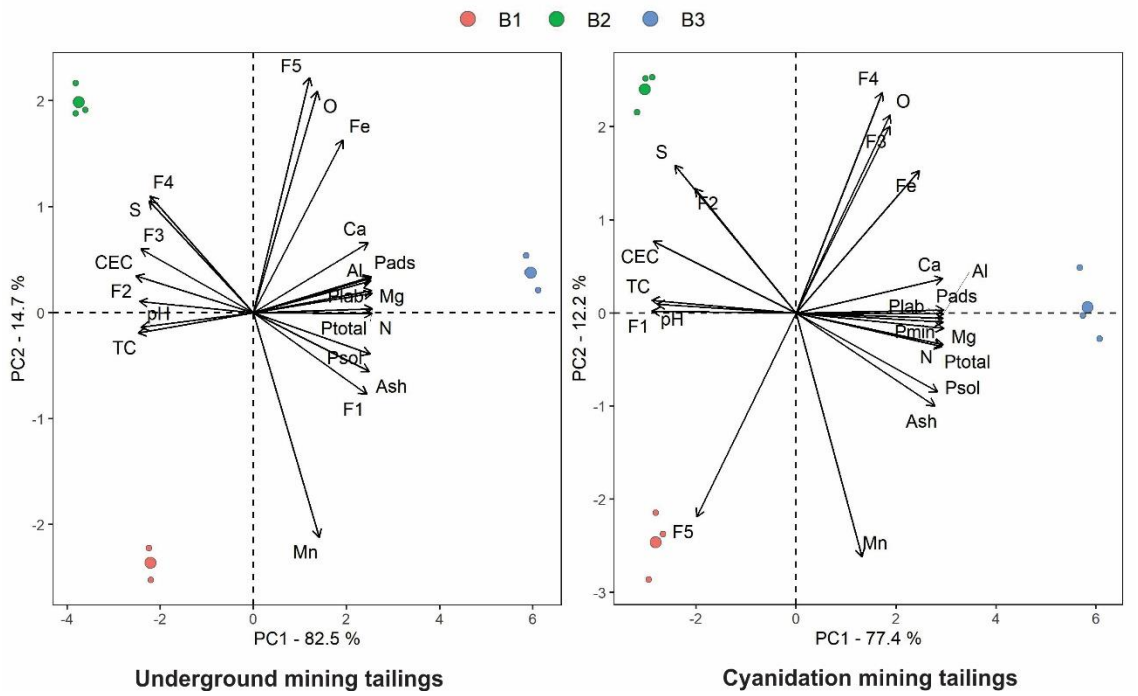

Fig. 3.

Potential ecological risk index ($PERI_m$) modified using bioavailable concentrations of As in gold mining tailings treated with açaí seed (B1), Brazil nut shell (B2) and palm kernel cake (B3) biochars. Different letters indicate significant difference between treatments by the Tukey test ($p < 0.05$).

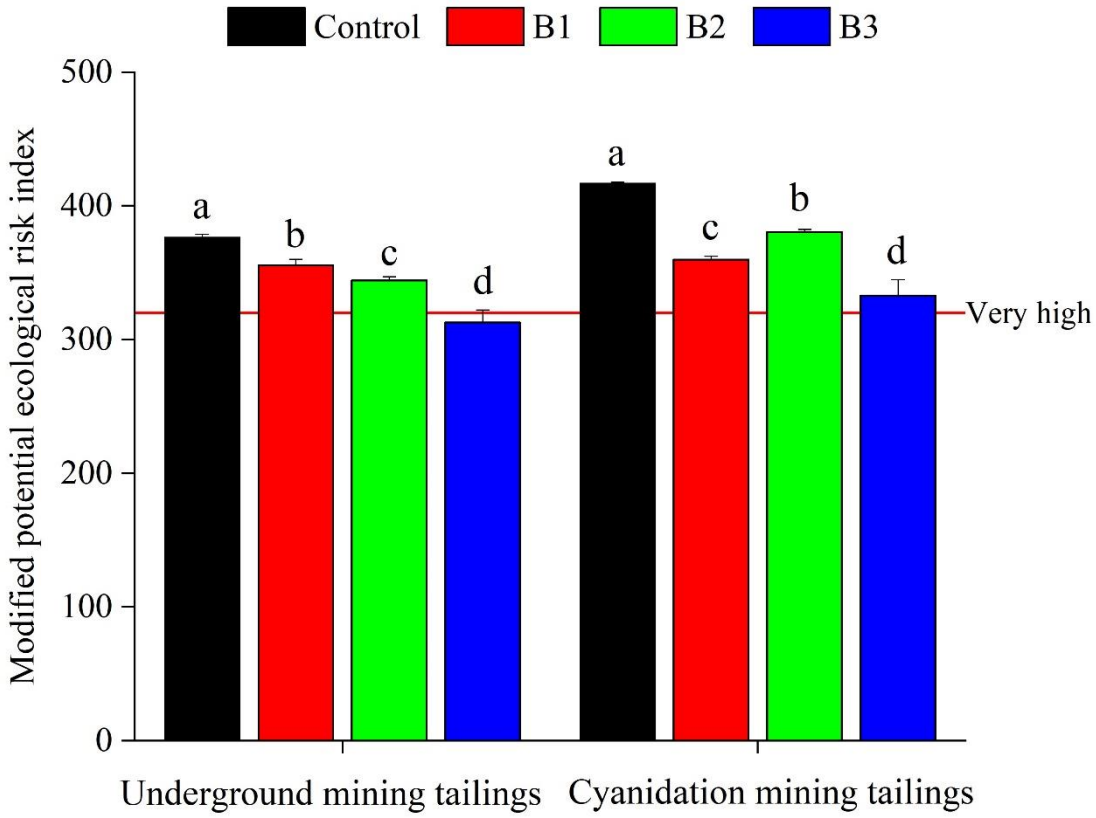

TABLES

Table 1.

Characterization of açaí seed (B1), Brazil nut shell (B2) and palm kernel cake (B3) biochars.

Property	Biochar		
	B1	B2	B3
pH (in water)	9.70 ± 0.49	9.90 ± 0.50	8.88 ± 0.44
Ash content (%)	4.80 ± 0.11	1.77 ± 0.04	10.19 ± 0.23
Point of zero charge	3.30 ± 0.02	6.75 ± 0.02	5.13 ± 0.02
Al (g kg^{-1})	0.11 ± 0.01	0.11 ± 0.01	0.66 ± 0.03
Ca (g kg^{-1})	1.06 ± 0.02	1.73 ± 0.04	6.3 ± 0.14
Fe (g kg^{-1})	1.01 ± 0.02	2.34 ± 0.02	3.19 ± 0.02
Mg (g kg^{-1})	8.44 ± 0.42	4.29 ± 0.21	51.00 ± 2.55
Mn (g kg^{-1})	0.46 ± 0.01	0.04 ± 0.00	0.428 ± 0.01
S (g kg^{-1})	0.23 ± 0.02	0.35 ± 0.02	0.12 ± 0.02
Soluble P (g kg^{-1})	1.25 ± 0.06	0.33 ± 0.02	3.27 ± 0.16
Labile P (g kg^{-1})	0.16 ± 0.00	0.03 ± 0.00	3.39 ± 0.08
Adsorbed P (g kg^{-1})	0.02 ± 0.02	0.01 ± 0.02	0.70 ± 0.02
Mineral-associated P (g kg^{-1})	0.36 ± 0.02	0.15 ± 0.01	3.05 ± 0.15
Total P (g kg^{-1})	2.03 ± 0.05	0.61 ± 0.01	10.06 ± 0.23
C (%)	79.2 ± 3.96	80.30 ± 4.02	67.22 ± 3.36
H (%)	1.70 ± 0.04	2.22 ± 0.05	1.99 ± 0.05
O (%)	11.60 ± 0.02	14.12 ± 0.02	15.00 ± 0.02
N (%)	1.86 ± 0.02	1.12 ± 0.02	5.60 ± 0.02

Table 2.

Elemental composition of mining wastes before application of biochars.

Element	Mining waste	
	Underground mining tailings	Cyanidation mining tailings
Fe (g kg^{-1})	109.00 ± 2.40	70.20 ± 1.54
Al (mg kg^{-1})	8400.00 ± 453.60	6500.00 ± 351.00
As (mg kg^{-1})	3000.00 ± 162.00	1600.00 ± 86.40
Ca (mg kg^{-1})	1800.00 ± 97.20	4300.00 ± 232.20
Co (mg kg^{-1})	51.00 ± 1.12	49.50 ± 1.09
Cu (mg kg^{-1})	215.00 ± 4.73	83.10 ± 1.83
K (mg kg^{-1})	800.00 ± 12.40	500.00 ± 16.50
Mg (mg kg^{-1})	1700.00 ± 91.80	3200.00 ± 172.80
Mn (mg kg^{-1})	1140.00 ± 61.56	789.00 ± 42.61
P (mg kg^{-1})	330.00 ± 10.89	284.00 ± 6.25
S (mg kg^{-1})	100.00 ± 2.20	200.00 ± 6.60
Zn (mg kg^{-1})	76.00 ± 1.67	48.00 ± 1.06

Table 3.

Elemental composition of mining wastes after application of açaí seed (B1), Brazil nut shell (B2) and palm kernel cake (B3) biochars.

Element	Underground mining tailings			Cyanidation mining tailings		
	B1	B2	B3	B1	B2	B3
Fe (g kg^{-1})	97.60 ± 2.24	100.50 ± 2.31	98.40 ± 2.26	72.10 ± 1.66	68.50 ± 1.58	69.80 ± 1.61
Al (mg kg^{-1})	7300.00 ± 379.60	6000.00 ± 312.00	6400.00 ± 332.80	6200.00 ± 322.40	5900.00 ± 306.80	5900.00 ± 306.80
Ca (mg kg^{-1})	1600.00 ± 83.20	1700.00 ± 88.40	1700.00 ± 76.35	4500.00 ± 234.00	4300.00 ± 223.60	4100.00 ± 213.20
Co (mg kg^{-1})	53.60 ± 1.23	53.90 ± 1.54	50.20 ± 1.15	43.50 ± 1.00	50.90 ± 1.17	48.00 ± 1.10
Cu (mg kg^{-1})	189.50 ± 4.36	198.50 ± 4.57	102.50 ± 2.36	88.10 ± 2.03	85.70 ± 1.97	70.50 ± 1.62
K (mg kg^{-1})	1000.00 ± 52.00	600.00 ± 21.34	900.00 ± 46.80	800.00 ± 41.60	600.00 ± 31.20	800.00 ± 41.60
Mg (mg kg^{-1})	1400.00 ± 72.80	1400.00 ± 68.40	1400.00 ± 72.80	3400.00 ± 176.80	3100.00 ± 161.20	2800.00 ± 145.60
Mn (mg kg^{-1})	1120.00 ± 58.24	1160.00 ± 60.32	1100.00 ± 57.20	800.00 ± 41.60	750.00 ± 39.00	742.00 ± 38.58
P (mg kg^{-1})	380.00 ± 13.51	330.00 ± 11.73	650.00 ± 33.80	360.00 ± 12.80	290.00 ± 10.31	680.00 ± 35.36
S (mg kg^{-1})	200.00 ± 7.11	200.00 ± 4.60	200.00 ± 5.54	500.00 ± 26.00	200.00 ± 4.12	200.00 ± 7.11
Zn (mg kg^{-1})	69.00 ± 1.59	72.00 ± 1.66	70.00 ± 1.61	50.00 ± 1.15	47.00 ± 1.08	50.00 ± 1.15

Table 4.

Property	Underground mining tailings				Cyanidation mining tailings			
	Control	B1	B2	B3	Control	B1	B2	B3
pH (in water)	7.07 ± 0.16	7.25 ± 0.27	7.19 ± 0.27	7.33 ± 0.18	8.33 ± 0.21	8.41 ± 0.19	8.27 ± 0.31	8.15 ± 0.28
CEC[a] ($cmol_c$ kg^{-1})	37.86 ± 0.95	129.60 ± 5.73	45.00 ± 1.77	47.12 ± 1.86	31.24 ± 0.78	50.77 ± 2.00	46.71 ± 1.84	44.41 ± 1.11
Soluble P (mg kg^{-1})	3.61 ± 0.09	17.44 ± 0.69	7.96 ± 0.24	90.17 ± 4.46	6.38 ± 0.19	16.57 ± 0.65	8.79 ± 0.27	80.02 ± 3.96
Labile P (mg kg^{-1})	12.93 ± 0.29	24.73 ± 0.88	13.10 ± 0.29	93.48 ± 3.72	17.69 ± 0.40	37.57 ± 1.33	22.87 ± 0.65	142.8 ± 5.68
Adsorbed P (mg kg^{-1})	64.90 ± 1.66	85.61 ± 3.06	50.80 ± 1.30	111.70 ± 3.89	55.38 ± 1.42	63.25 ± 1.62	62.42 ± 1.59	108.4 ± 3.88
Mineral P (mg kg^{-1})	6.09 ± 0.14	11.89 ± 0.27	7.75 ± 0.17	51.65 ± 2.46	19.14 ± 0.59	28.46 ± 1.36	18.52 ± 0.57	113.8 ± 5.42
Organic C (mg kg^{-1})	16.50 ± 0.39	42.50 ± 1.77	38.60 ± 1.61	46.40 ± 1.93	12.2 ± 0.29	41.3 ± 1.72	32.2 ± 1.02	38.5 ± 1.60
Inorganic C (mg kg^{-1})	4.60 ± 1.36	4.10 ± 1.21	4.30 ± 1.27	2.70 ± 0.06	20.1 ± 0.98	17.7 ± 0.86	21.1 ± 1.03	17.2 ± 0.84
Total C (mg kg^{-1})	21.10 ± 0.54	46.60 ± 2.31	42.90 ± 2.13	49.10 ± 2.44	32.3 ± 1.02	59 ± 2.93	53.3 ± 2.65	55.7 ± 2.77

Properties of mining wastes after application of açaí seed (B1), Brazil nut shell (B2) and palm kernel cake (B3) biochars.

[a]Cation exchange capacity.

SUPLEMENTARY MATERIAL

Fig. 1S.

Mineral processing and waste deposition in areas of underground (A and B) and cyanidation (C and D) gold mining in Cachoeira do Piriá, eastern Amazon.

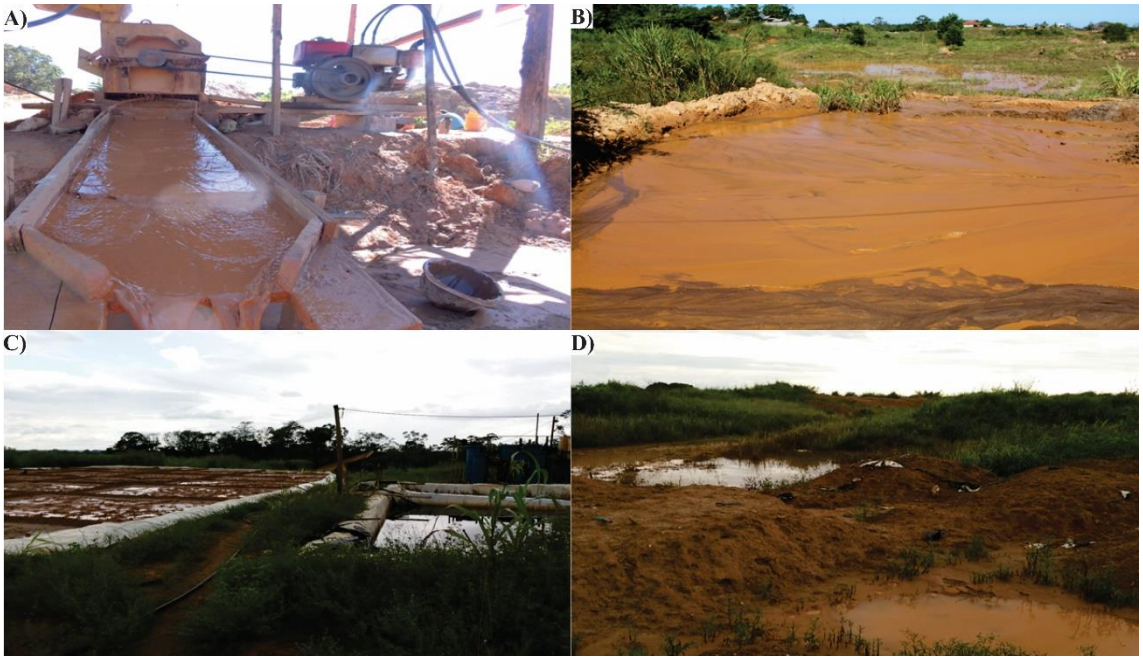

Fig. 2S.

Minerals containing As in gold mining tailings.

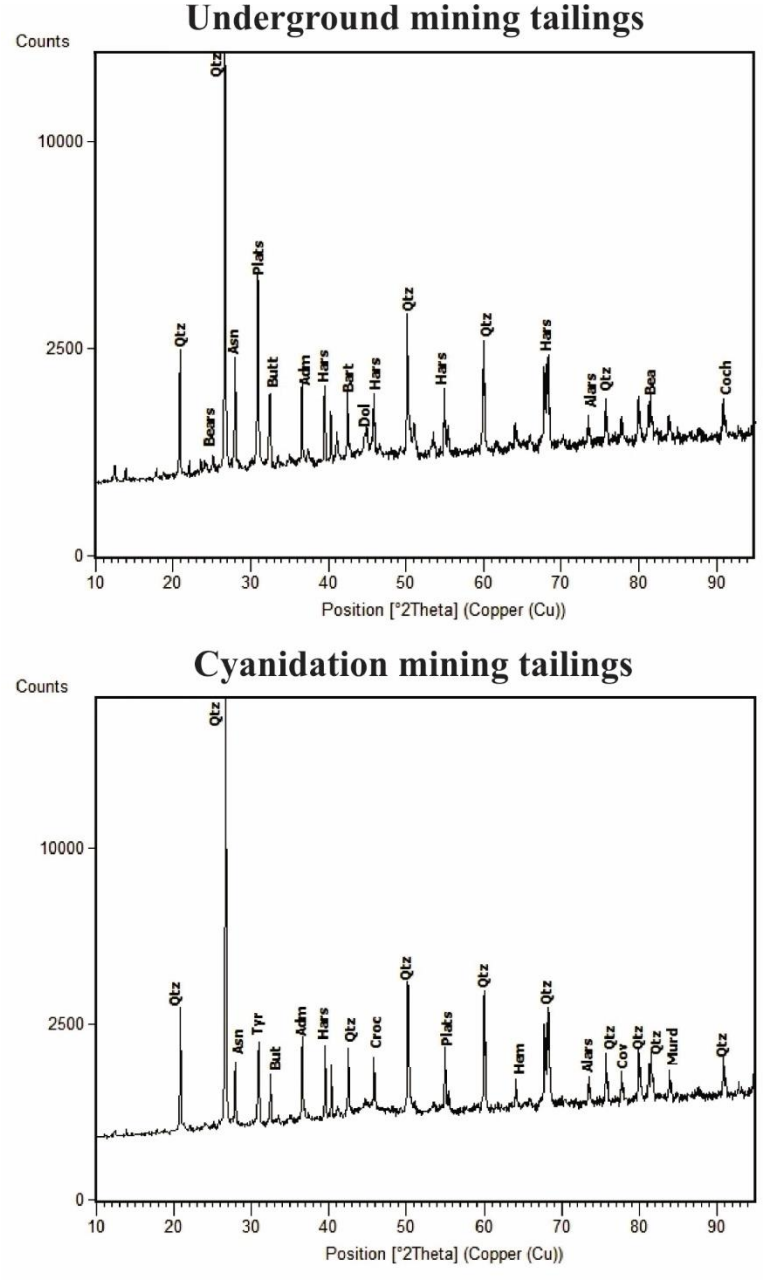

Underground mining tailing: Adm – adamite; Alars - alarsite; Asn **–** arsenolite; Bart – barite; Bears – bearsite; Butt – buttgenbachite; Coch – cochromite; Dol – dolomite; Hars – harstigite; Plats – platarsite; Qtz **–** quartz.

Cyanidation mining tailing: Adm – adamite; Alars – alarsite; Asn – arsenolite; Butt – buttgenbachite; Cov – covellite; Croc – crocoite; Hars – harstigite; Hem – hematite; Murd – murdochite; Plat – platarsite; Qtz – quartz; Tyr – tyrrellite.

Fig. 3S.

Multiple linear regression for predicting the bioavailability of As in tailings after the application of biochar.

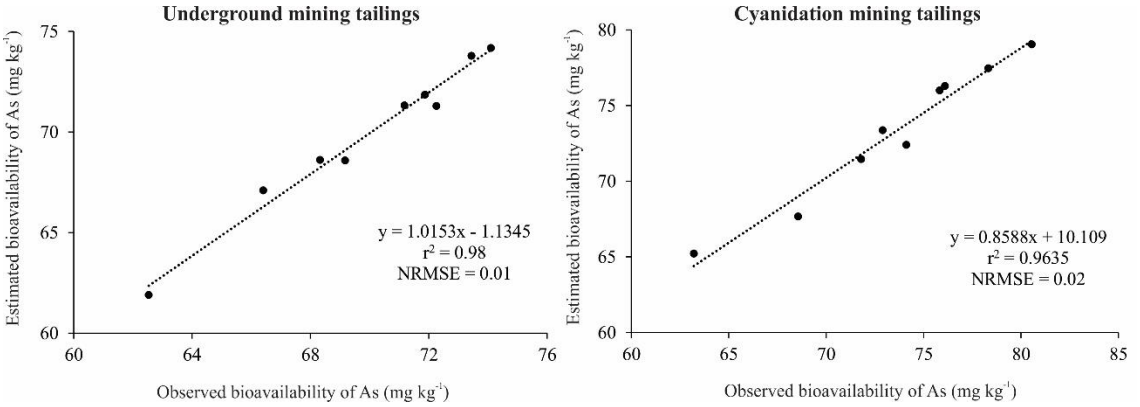

Fig. 4S.

Bioavailable concentrations of As in gold mining tailings (B) treated with açaí seed (B1), Brazil nut shell (B2) and palm kernel cake (B3) biochars. Different letters indicate significant difference between treatments by the Tukey test ($p < 0.05$).

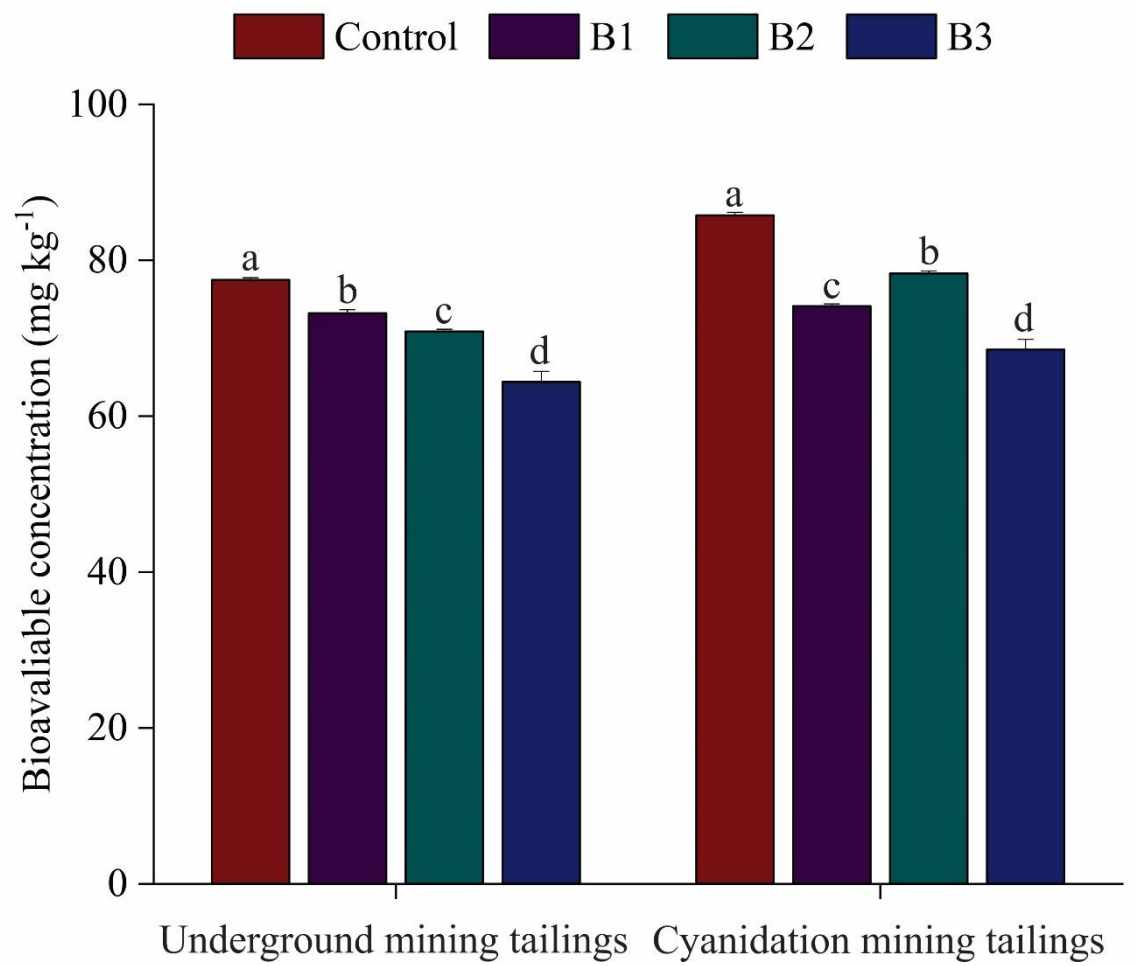

Table 1S.

Pearson's correlation coefficients between properties of tailings and concentrations of As in readily soluble (F1), adsorbed (F2), amorphous and poorly-crystalline arsenates, oxides and hydroxosulfates of Fe (F3), well-crystalline arsenates, oxides, and hydroxosulfates of Fe (F4), and sulfides and arsenides (F5) fractions in gold mining tailings after addition of açaí seed, Brazil nut shell, and palm kernel cake biochars.

Underground mining tailings																
Fractions	Ash	pH	CEC[a]	C	O	N	P_{sol}[b]	P_{lab}[c]	P_{ads}[d]	P_{min}[e]	P_{total}[f]	Fe	Ca	Al	Mn	Mg	S
F1	0.99*	-0.89*	-0.98*	-0.90*	0.27	0.95*	0.97*	0.90*	0.90*	0.93*	0.95*	0.52	0.84*	0.90*	0.77*	0.93*	-0.96*
F2	-0.93*	0.93*	0.94*	0.89*	-0.48	-0.96*	-0.91*	-0.91*	-0.94*	-0.96*	-0.94*	-0.65	-0.90*	-0.92*	-0.54	-0.94*	0.81*
F3	-0.97*	0.89*	0.96*	0.90*	-0.29	-0.95*	-0.95*	-0.90*	-0.91*	-0.93*	-0.94*	-0.55	-0.84*	-0.90*	-0.71*	-0.92*	0.88*
F4	-0.94*	0.79*	0.91*	0.77*	-0.14	-0.86*	-0.90*	-0.79*	-0.80*	-0.83*	-0.85*	-0.35	-0.72*	-0.79*	-0.82*	-0.83*	0.93*
F5	0.27	-0.47	-0.34	-0.50	0.95*	0.48	0.31	0.57	0.58	0.54	0.48	0.89*	0.67*	0.57	-0.47	0.53	-0.05
Cyanidation mining tailings																
Fractions	Ash	pH	CEC[a]	C	O	N	P_{sol}[b]	P_{lab}[c]	P_{ads}[d]	P_{min}[e]	P_{total}[f]	Fe	Ca	Al	Mn	Mg	S
F1	-0.92	0.95	0.95	0.96	-0.58*	-0.97	-0.92	-0.96	-0.98	-0.98	-0.97	-0.79*	-0.95*	-0.96	-0.45	-0.97	0.82
F2	-0.76	0.56	0.76	0.69	-0.21*	-0.69	-0.81	-0.72	-0.66	-0.65	-0.73	-0.42*	-0.65*	-0.70	-0.65	-0.70	0.78
F3	0.38	-0.62	-0.44	-0.60	0.81*	0.56	0.41	0.60	0.64	0.62	0.55	0.82*	0.69*	0.63	-0.27	0.60	-0.14
F4	0.27	-0.49	-0.35	-0.53	0.96*	0.47	0.33	0.57	0.58	0.54	0.48	0.92*	0.68*	0.58	-0.47	0.53	-0.05
F5	-0.38	0.61	0.46	0.62	-0.95*	-0.58	-0.43	-0.66	-0.68	-0.65	-0.58	-0.94*	-0.76*	-0.67	0.36	-0.63	0.16

*Statistically significant correlation ($p < 0.05$)

[a]Cation exchange capacity

[b]Soluble phosphorus

[c]Labile phosphorus

[d]Adsorbed phosphorus

[e]Mineral-linked phosphorus

[f]Total phosphorus

Table 2S.

Comparison between the models tested by analysis of variance.

Parameter	Analysis of variance		
	Biochars	Tailings	Biochars × Tailings
Residual degrees of freedom	8	12	3
Residual sum of squares	64.140	118.730	7.476
Degrees of freedom	-5	-4	
Sum of squares	-56.664	-54.591	
F	4.5476	5.4765	
p	0.12124	0.09696	

Table 3S.

Quality parameters of the models tested in the multiple linear regression.

Model quality parameters	Biochars	Tailings	Biochars × Tailings
Residual standard error	2.832	3.146	1.579
Degrees of freedom	8	12	3
Coefficient of determination (R^2)	0.8343	0.6932	0.9807
Adjusted coefficient of determination (R^2 adjusted)	0.6478	0.5653	0.8905
F	4.474 (9)	5.422 (5)	10.88 (14)
Akaike Information Criterion (AIC)	95.9	99	67.2
p	0.02316	0.007747	0.03673

Table 4S.

Multiple linear regression for estimating the bioavailability of As.

Equation	$BAC = 72.41 + 1.43*(F2)^a - 11.04*(ash)^b - 0.40*(CEC)^b + 15.37*(N)^b + 26.50*(P_{sol})^b - 211.73*(P_{ads})^b + 47*(P_{min})^b - 0.21*(P_{sol})^a - 0.25*(P_{lab})^a - 0.12*(P_{ads})^a - 0.05*(P)^a - 0.67*(OC)^a$
Coefficient of determination (R^2)	0.9807
Adjusted coefficient of determination (R^2 adjusted)	0.8905
Significance	0.03673
Normalized root mean-square error (NRMSE)	0.0013

[a]Mining tailing property; [b]Biochar property; F2 = adsorbed arsenic; CEC = cation exchange capacity; N = total nitrogen; P = total phosphorus; P_{sol} = soluble phosphorus; P_{lab} = labile phosphorus; P_{ads} = adsorbed phosphorus; P_{min} = mineral-linked phosphorus; OC = organic carbon.

REFERENCES

Adamo, P., Agrelli, D., Zampella, M., 2018. Chemical speciation to assess bioavailability, bioaccessibility and geochemical forms of potentially toxic metals (PTMs) in polluted soils, in: Environmental Geochemistry: Site Characterization, Data Analysis and Case Histories. Elsevier, pp. 153–194. https://doi.org/10.1016/B978-0-444-63763-5.00010-0

Adhikari, S., Gascó, G., Méndez, A., Surapaneni, A., Jegatheesan, V., Shah, K., Paz-Ferreiro, J., 2019. Influence of pyrolysis parameters on phosphorus fractions of biosolids derived biochar. Sci. Total Environ. 695, 133846. https://doi.org/10.1016/j.scitotenv.2019.133846

Agrafioti, E., Kalderis, D., Diamadopoulos, E., 2014. Ca and Fe modified biochars as adsorbents of arsenic and chromium in aqueous solutions. J. Environ. Manage. 146, 444–450. https://doi.org/10.1016/j.jenvman.2014.07.029

Alan, M., Kara, D., 2019. Assessment of sequential extraction methods for the prediction of bioavailability of elements in plants grown on agricultural soils near to boron mines in Turkey. Talanta 200, 41–50. https://doi.org/10.1016/j.talanta.2019.03.031

Amoakwah, E., Arthur, E., Frimpong, K.A., Parikh, S.J., Islam, R., 2020. Soil organic carbon storage and quality are impacted by corn cob biochar application on a tropical sandy loam. J. Soils Sediments 20, 1960–1969. https://doi.org/10.1007/s11368-019-02547-5

ATSDR, 2017. Substance Priority List | ATSDR, Agency for Toxic Substances and Disease Registry.

Bashir, S., Salam, A., Chhajro, M.A., Fu, Q., Khan, M.J., Zhu, J., Shaaban, M., Kubar, K.A., Ali, U., Hu, H., 2018. Comparative efficiency of rice husk-derived biochar (RHB) and steel slag (SS) on cadmium (Cd) mobility and its uptake by Chinese cabbage in highly contaminated soil. Int. J. Phytoremediation 20, 1221–1228. https://doi.org/10.1080/15226514.2018.1448364

Beesley, L., Inneh, O.S., Norton, G.J., Moreno-Jimenez, E., Pardo, T., Clemente, R., Dawson, J.J.C., 2014. Assessing the influence of compost and biochar amendments on the mobility and toxicity of metals and arsenic in a naturally contaminated mine soil. Environ. Pollut. 186, 195–202. https://doi.org/10.1016/j.envpol.2013.11.026

Beiyuan, J., Awad, Y.M., Beckers, F., Tsang, D.C.W., Ok, Y.S., Rinklebe, J., 2017. Mobility and phytoavailability of As and Pb in a contaminated soil using pine

sawdust biochar under systematic change of redox conditions. Chemosphere 178, 110–118. https://doi.org/10.1016/j.chemosphere.2017.03.022

Cao, C.T.N., Farrell, C., Kristiansen, P.E., Rayner, J.P., 2014. Biochar makes green roof substrates lighter and improves water supply to plants. Ecol. Eng. 71, 368–374. https://doi.org/10.1016/j.ecoleng.2014.06.017

Chen, X.-W., Wong, J.T.-F., Ng, C.W.-W., Wong, M.-H., 2016. Feasibility of biochar application on a landfill final cover—a review on balancing ecology and shallow slope stability. Environ. Sci. Pollut. Res. 23, 7111–7125. https://doi.org/10.1007/s11356-015-5520-5

Chen, X., He, H.-Z., Chen, G.-K., Li, H.-S., 2020. Effects of biochar and crop straws on the bioavailability of cadmium in contaminated soil. Sci. Rep. 10, 9528. https://doi.org/10.1038/s41598-020-65631-8

CONAMA, 2009. Resolução Nº 420. Conselho Nacional do Meio Ambiente, Brasília.

Derakhshan Nejad, Z., Rezania, S., Jung, M.C., Al-Ghamdi, A.A., Mustafa, A.E.-Z.M.A., Elshikh, M.S., 2021. Effects of fine fractions of soil organic, semi-organic, and inorganic amendments on the mitigation of heavy metal(loid)s leaching and bioavailability in a post-mining area. Chemosphere 271, 129538. https://doi.org/10.1016/j.chemosphere.2021.129538

Dias, Y.N., Souza, E.S., da Costa, H.S.C., Melo, L.C.A., Penido, E.S., do Amarante, C.B., Teixeira, O.M.M., Fernandes, A.R., 2019. Biochar produced from Amazonian agro-industrial wastes: properties and adsorbent potential of Cd2+ and Cu2+. Biochar 1, 389–400. https://doi.org/10.1007/s42773-019-00031-4

Ding, H., Ji, H., Tang, L., Zhang, A., Guo, X., Li, C., Gao, Y., Briki, M., 2016. Heavy metals in the gold mine soil of the upstream area of a metropolitan drinking water source. Environ. Sci. Pollut. Res. 23, 2831–2847. https://doi.org/10.1007/s11356-015-5479-2

Domingues, R.R., Trugilho, P.F., Silva, C.A., Melo, I.C.N.A. de, Melo, L.C.A., Magriotis, Z.M., Sánchez-Monedero, M.A., 2017. Properties of biochar derived from wood and high-nutrient biomasses with the aim of agronomic and environmental benefits. PLoS One 12, e0176884. https://doi.org/10.1371/journal.pone.0176884

Dong, H., Xun, Y., Feng, L., Yoneda, M., 2020. Nonlinear transformation and release of arsenic fractions in soil and its implication for site risk assessment. J. Clean. Prod.

262, 121304. https://doi.org/10.1016/j.jclepro.2020.121304

Dong, X., Singh, B.P., Li, G., Lin, Q., Zhao, X., 2019. Biochar increased field soil inorganic carbon content five years after application. Soil Tillage Res. 186, 36–41. https://doi.org/10.1016/j.still.2018.09.013

Drahota, P., Grösslová, Z., Kindlová, H., 2014. Selectivity assessment of an arsenic sequential extraction procedure for evaluating mobility in mine wastes. Anal. Chim. Acta 839, 34–43. https://doi.org/10.1016/j.aca.2014.06.022

Fernandes, A.R., Souza, E.S. de, de Souza Braz, A.M., Birani, S.M., Alleoni, L.R.F., 2018. Quality reference values and background concentrations of potentially toxic elements in soils from the Eastern Amazon, Brazil. J. Geochemical Explor. 190, 453–463. https://doi.org/10.1016/j.gexplo.2018.04.012

Gabarrón, M., Zornoza, R., Martínez-Martínez, S., Muñoz, V.A., Faz, Á., Acosta, J.A., 2019. Effect of land use and soil properties in the feasibility of two sequential extraction procedures for metals fractionation. Chemosphere 218, 266–272. https://doi.org/10.1016/j.chemosphere.2018.11.114

Gope, M., Masto, R.E., George, J., Hoque, R.R., Balachandran, S., 2017. Bioavailability and health risk of some potentially toxic elements (Cd, Cu, Pb and Zn) in street dust of Asansol, India. Ecotoxicol. Environ. Saf. 138, 231–241. https://doi.org/10.1016/j.ecoenv.2017.01.008

Hailegnaw, N.S., Mercl, F., Pračke, K., Száková, J., Tlustoš, P., 2019. Mutual relationships of biochar and soil pH, CEC, and exchangeable base cations in a model laboratory experiment. J. Soils Sediments 19, 2405–2416. https://doi.org/10.1007/s11368-019-02264-z

Hakanson, L., 1980. An ecological risk index for aquatic pollution control.a sedimentological approach. Water Res. https://doi.org/10.1016/0043-1354(80)90143-8

He, H., Qian, T.-T., Liu, W.-J., Jiang, H., Yu, H.-Q., 2014. Biological and chemical phosphorus solubilization from pyrolytical biochar in aqueous solution. Chemosphere 113, 175–181. https://doi.org/10.1016/j.chemosphere.2014.05.039

Hosseini, S.H., Liang, X., Niyungeko, C., Miaomiao, H., Li, F., Khan, S., Eltohamy, K.M., 2019. Effect of sheep manure-derived biochar on colloidal phosphorus release in soils from various land uses. Environ. Sci. Pollut. Res. 26, 36367–36379. https://doi.org/10.1007/s11356-019-06762-y

Huang, C., Wang, W., Yue, S., Adeel, M., Qiao, Y., 2020. Role of biochar and Eisenia fetida on metal bioavailability and biochar effects on earthworm fitness. Environ. Pollut. 263, 114586. https://doi.org/10.1016/j.envpol.2020.114586

Huang, J., Li, F., Zeng, G., Liu, W., Huang, X., Xiao, Z., Wu, H., Gu, Y., Li, X., He, X., He, Y., 2016. Integrating hierarchical bioavailability and population distribution into potential eco-risk assessment of heavy metals in road dust: A case study in Xiandao District, Changsha city, China. Sci. Total Environ. 541, 969–976. https://doi.org/10.1016/j.scitotenv.2015.09.139

Hussain, S., Sharma, V., Arya, V.M., Sharma, K.R., Rao, C.S., 2019. Total organic and inorganic carbon in soils under different land use/land cover systems in the foothill Himalayas. CATENA 182, 104104. https://doi.org/10.1016/j.catena.2019.104104

Jaishankar, M., Tseten, T., Anbalagan, N., Mathew, B.B., Beeregowda, K.N., 2014. Toxicity, mechanism and health effects of some heavy metals. Interdiscip. Toxicol. 7, 60–72. https://doi.org/10.2478/intox-2014-0009

Jayarathne, A., Egodawatta, P., Ayoko, G.A., Goonetilleke, A., 2018. Assessment of ecological and human health risks of metals in urban road dust based on geochemical fractionation and potential bioavailability. Sci. Total Environ. 635, 1609–1619. https://doi.org/10.1016/j.scitotenv.2018.04.098

Jia, X., Cao, Y., O'Connor, D., Zhu, J., Tsang, D.C.W., Zou, B., Hou, D., 2021. Mapping soil pollution by using drone image recognition and machine learning at an arsenic-contaminated agricultural field. Environ. Pollut. 270, 116281. https://doi.org/10.1016/j.envpol.2020.116281

Kim, H.-B., Kim, J.-G., Choi, J.-H., Kwon, E.E., Baek, K., 2019. Photo-induced redox coupling of dissolved organic matter and iron in biochars and soil system: Enhanced mobility of arsenic. Sci. Total Environ. 689, 1037–1043. https://doi.org/10.1016/j.scitotenv.2019.06.478

Kim, H.-B., Kim, J.-G., Kim, T., Alessi, D.S., Baek, K., 2020. Mobility of arsenic in soil amended with biochar derived from biomass with different lignin contents: Relationships between lignin content and dissolved organic matter leaching. Chem. Eng. J. 393, 124687. https://doi.org/10.1016/j.cej.2020.124687

Kim, H.-B., Kim, S.-H., Jeon, E.-K., Kim, D.-H., Tsang, D.C.W., Alessi, D.S., Kwon, E.E., Baek, K., 2018. Effect of dissolved organic carbon from sludge, Rice straw and spent coffee ground biochar on the mobility of arsenic in soil. Sci. Total Environ.

636, 1241–1248. https://doi.org/10.1016/j.scitotenv.2018.04.406

Koley, S., 2021. Future perspectives and mitigation strategies towards groundwater arsenic contamination in West Bengal, India. Environ. Qual. Manag. tqem.21784. https://doi.org/10.1002/tqem.21784

Kowalska, J.B., Mazurek, R., Gasiorek, M., Zaleski, T., 2018. Pollution indices as useful tools for the comprehensive evaluation of the degree of soil contamination - A review. Environ. Geochem. Health 40, 2395–2420. https://doi.org/10.1007/s10653-018-0106-z

Kuyucak, N., Akcil, A., 2013. Cyanide and removal options from effluents in gold mining and metallurgical processes. Miner. Eng. 50–51, 13–29. https://doi.org/10.1016/j.mineng.2013.05.027

Kyle, J.H., Breuer, P.L., Bunney, K.G., Pleysier, R., 2012. Hydrometallurgy review of trace toxic elements (Pb, Cd, Hg, As, Sb, Bi, Se, Te) and their deportment in gold processing. Hydrometallurgy 111–112, 10–21. https://doi.org/10.1016/j.hydromet.2011.09.005

Lehmann, J., Gaunt, J., Rondon, M., 2006. Bio-char Sequestration in Terrestrial Ecosystems – A Review. Mitig. Adapt. Strateg. Glob. Chang. 11, 403–427. https://doi.org/10.1007/s11027-005-9006-5

Lehmann, J., Rillig, M.C., Thies, J., Masiello, C.A., Hockaday, W.C., Crowley, D., 2011. Biochar effects on soil biota – A review. Soil Biol. Biochem. 43, 1812–1836. https://doi.org/10.1016/j.soilbio.2011.04.022

Li, J., Kosugi, T., Riya, S., Hashimoto, Y., Hou, H., Terada, A., Hosomi, M., 2017. Use of batch leaching tests to quantify arsenic release from excavated urban soils with relatively low levels of arsenic. J. Soils Sediments 17, 2136–2143. https://doi.org/10.1007/s11368-017-1669-5

Lima, M.W. de, Pereira, W.V. da S., Souza, E.S. de, Teixeira, R.A., Palheta, D. da C., Faial, K. do C.F., Costa, H.F., Fernandes, A.R., 2022. Bioaccumulation and human health risks of potentially toxic elements in fish species from the southeastern Carajás Mineral Province, Brazil. Environ. Res. 204, 112024. https://doi.org/10.1016/j.envres.2021.112024

Lin, L., Li, Z., Liu, X., Qiu, W., Song, Z., 2019. Effects of Fe-Mn modified biochar composite treatment on the properties of As-polluted paddy soil. Environ. Pollut. 244, 600–607. https://doi.org/10.1016/j.envpol.2018.10.011

Lin, L., Qiu, W., Wang, D., Huang, Q., Song, Z., Chau, H.W., 2017. Arsenic removal in aqueous solution by a novel Fe-Mn modified biochar composite: Characterization and mechanism. Ecotoxicol. Environ. Saf. 144, 514–521. https://doi.org/10.1016/j.ecoenv.2017.06.063

Lin, W., Wu, K., Lao, Z., Hu, W., Lin, B., Li, Y., Fan, H., Hu, J., 2019. Assessment of trace metal contamination and ecological risk in the forest ecosystem of dexing mining area in northeast Jiangxi Province, China. Ecotoxicol. Environ. Saf. 167, 76–82. https://doi.org/10.1016/j.ecoenv.2018.10.001

Liu, X., Wang, Y., Gui, C., Li, P., Zhang, J., Zhong, H., Wei, Y., 2016. Chemical forms and risk assessment of heavy metals in sludge-biochar produced by microwave-induced low temperature pyrolysis. RSC Adv. 6, 101960–101967. https://doi.org/10.1039/C6RA22511J

Lomaglio, T., Hattab-Hambli, N., Bret, A., Miard, F., Trupiano, D., Scippa, G.S., Motelica-Heino, M., Bourgerie, S., Morabito, D., 2017. Effect of biochar amendments on the mobility and (bio) availability of As, Sb and Pb in a contaminated mine technosol. J. Geochemical Explor. 182, 138–148. https://doi.org/10.1016/j.gexplo.2016.08.007

Luo, M., Lin, H., He, Y., Zhang, Y., 2020. The influence of corncob-based biochar on remediation of arsenic and cadmium in yellow soil and cinnamon soil. Sci. Total Environ. 717, 137014. https://doi.org/10.1016/j.scitotenv.2020.137014

Melo, L.C.A., Coscione, A.R., Abreu, C.A., Puga, A.P., Camargo, O.A., 2013. Influence of pyrolysis temperature on cadmium and zinc sorption capacity of sugar cane straw–derived biochar. BioResources 8, 4992–5004.

Mosher, G.Z., 2013. Technical report and resource estimate on the Cachoeira property, Pará state, Brazil. Vancouver.

Mujtaba Munir, M.A., Liu, G., Yousaf, B., Ali, M.U., Abbas, Q., Ullah, H., 2020. Synergistic effects of biochar and processed fly ash on bioavailability, transformation and accumulation of heavy metals by maize (Zea mays L.) in coal-mining contaminated soil. Chemosphere 240, 124845. https://doi.org/10.1016/j.chemosphere.2019.124845

Munera-Echeverri, J.L., Martinsen, V., Strand, L.T., Zivanovic, V., Cornelissen, G., Mulder, J., 2018. Cation exchange capacity of biochar: An urgent method modification. Sci. Total Environ. 642, 190–197.

https://doi.org/10.1016/j.scitotenv.2018.06.017

Murphy, J., Riley, J.P., 1962. A modified single solution method for the determination of phosphate in natural waters. Anal. Chim. Acta 27, 31–36. https://doi.org/10.1016/S0003-2670(00)88444-5

Nkinahamira, F., Suanon, F., Chi, Q., Li, Y., Feng, M., Huang, X., Yu, C.-P., Sun, Q., 2019. Occurrence, geochemical fractionation, and environmental risk assessment of major and trace elements in sewage sludge. J. Environ. Manage. 249, 109427. https://doi.org/10.1016/j.jenvman.2019.109427

O'Connor, D., Peng, T., Zhang, J., Tsang, D.C.W., Alessi, D.S., Shen, Z., Bolan, N.S., Hou, D., 2018. Biochar application for the remediation of heavy metal polluted land: A review of in situ field trials. Sci. Total Environ. 619–620, 815–826. https://doi.org/10.1016/j.scitotenv.2017.11.132

Ono, F.B., Guilherme, L.R.G., Penido, E.S., Carvalho, G.S., Hale, B., Toujaguez, R., Bundschuh, J., 2012. Arsenic bioaccessibility in a gold mining area: a health risk assessment for children. Environ. Geochem. Health 34, 457–465. https://doi.org/10.1007/s10653-011-9444-9

Panagopoulos, A., 2021a. Energetic, economic and environmental assessment of zero liquid discharge (ZLD) brackish water and seawater desalination systems. Energy Convers. Manag. 235, 113957. https://doi.org/10.1016/j.enconman.2021.113957

Panagopoulos, A., 2021b. Techno-economic assessment of minimal liquid discharge (MLD) treatment systems for saline wastewater (brine) management and treatment. Process Saf. Environ. Prot. 146, 656–669. https://doi.org/10.1016/j.psep.2020.12.007

Panagopoulos, A., 2021c. Study and evaluation of the characteristics of saline wastewater (brine) produced by desalination and industrial plants. Environ. Sci. Pollut. Res. https://doi.org/10.1007/s11356-021-17694-x

Pandit, N.R., Mulder, J., Hale, S.E., Martinsen, V., Schmidt, H.P., Cornelissen, G., 2018. Biochar improves maize growth by alleviation of nutrient stress in a moderately acidic low-input Nepalese soil. Sci. Total Environ. 625, 1380–1389. https://doi.org/10.1016/j.scitotenv.2018.01.022

Peijnenburg, W.J.G.M., 2020. Implementation of Bioavailability in Prospective and Retrospective Risk Assessment of Chemicals in Soils and Sediments. pp. 391–422. https://doi.org/10.1007/698_2020_516

Penido, E.S., Martins, G.C., Mendes, T.B.M., Melo, L.C.A., do Rosário Guimarães, I., Guilherme, L.R.G., 2019. Combining biochar and sewage sludge for immobilization of heavy metals in mining soils. Ecotoxicol. Environ. Saf. 172, 326–333. https://doi.org/10.1016/j.ecoenv.2019.01.110

Pereira, W.V. da S., Teixeira, R.A., Souza, E.S. de, Moraes, A.L.F. de, Campos, W.E.O., Amarante, C.B. do, Martins, G.C., Fernandes, A.R., 2020. Chemical fractionation and bioaccessibility of potentially toxic elements in area of artisanal gold mining in the Amazon. J. Environ. Manage. 267, 110644. https://doi.org/10.1016/j.jenvman.2020.110644

R Core Team, 2021. R: A language and environment for statistical computing.

Ray, I., Mridha, D., Roychowdhury, T., 2021. Waste derived amendments and their efficacy in mitigation of arsenic contamination in soil and soil–plant systems: A review. Environ. Technol. Innov. 24, 101976. https://doi.org/10.1016/j.eti.2021.101976

Richardson, A.E., Simpson, R.J., 2011. Soil Microorganisms Mediating Phosphorus Availability Update on Microbial Phosphorus. Plant Physiol. 156, 989–996. https://doi.org/10.1104/pp.111.175448

Rubinos, D.A., Iglesias, L., Díaz-Fierros, F., Barral, M.T., 2011. Interacting Effect of pH, Phosphate and Time on the Release of Arsenic from Polluted River Sediments (Anllóns River, Spain). Aquat. Geochemistry 17, 281–306. https://doi.org/10.1007/s10498-011-9135-2

Santos, R.N. do E.S., 2004. Investigação do passivo ambiental em Cachoeira do Piriá, NE do Pará: base para a gestão ambiental em áreas garimpadas na Amazônia. Universidade de São Paulo.

Shi, S., Zhang, Q., Lou, Y., Du, Z., Wang, Q., Hu, N., Wang, Y., Gunina, A., Song, J., 2021. Soil organic and inorganic carbon sequestration by consecutive biochar application: Results from a decade field experiment. Soil Use Manag. 37, 95–103. https://doi.org/10.1111/sum.12655

Silva Júnior, E.C., Martins, G.C., Wadt, L.H.O., Silva, K.E., Lima, R.M.B., Batista, K.D., Guedes, M.C., Oliveira Junior, R.C., Reis, A.R., Lopes, G., Menezes, M.D., Broadley, M.R., Young, S.D., Guilherme, L.R.G., 2019. Natural variation of arsenic fractions in soils of the Brazilian Amazon. Sci. Total Environ. 687, 1219–1231. https://doi.org/10.1016/j.scitotenv.2019.05.446

Singh, B., Arbestain, M.C., Lehmann, J., 2017. Biochar: A Guide to Analytical Methods. CRC Press.

Singh, N., Kumar, D., Sahu, A.P., 2007. Arsenic in the environment: Effects on human health and possible prevention. J. Environ. Biol. 28, 359–365.

Smith, E., Naidu, R., 2009. Chemistry of inorganic arsenic in soils: kinetics of arsenic adsorption–desorption. Environ. Geochem. Health 31, 49–59. https://doi.org/10.1007/s10653-008-9228-z

Souza, E.S., Dias, Y.N., Costa, H.S.C., Pinto, D.A., Oliveira, D.M., Souza Falção, N.P., Teixeira, R.A., Fernandes, A.R., 2019. Organic residues and biochar to immobilize potentially toxic elements in soil from a gold mine in the Amazon. Ecotoxicol. Environ. Saf. 169, 425–434. https://doi.org/10.1016/j.ecoenv.2018.11.032

Souza, E.S., Texeira, R.A., da Costa, H.S.C., Oliveira, F.J., Melo, L.C.A., do Carmo Freitas Faial, K., Fernandes, A.R., 2017. Assessment of risk to human health from simultaneous exposure to multiple contaminants in an artisanal gold mine in Serra Pelada, Pará, Brazil. Sci. Total Environ. 576, 683–695. https://doi.org/10.1016/j.scitotenv.2016.10.133

Souza Neto, H.F. de, Pereira, W.V. da S., Dias, Y.N., Souza, E.S. de, Teixeira, R.A., Lima, M.W. de, Ramos, S.J., Amarante, C.B. do, Fernandes, A.R., 2020. Environmental and human health risks of arsenic in gold mining areas in the eastern Amazon. Environ. Pollut. 265, 114969. https://doi.org/10.1016/j.envpol.2020.114969

Sun, J., Cui, L., Quan, G., Yan, J., Wang, H., Wu, L., 2020. Effects of biochar on heavy metals migration and fractions changes with different soil types in column experiments. BioResources 15, 4388–4406. https://doi.org/10.15376/biores.15.2.4388-4406

Tapia-Gatica, J., González-Miranda, I., Salgado, E., Bravo, M.A., Tessini, C., Dovletyarova, E.A., Paltseva, A.A., Neaman, A., 2020. Advanced determination of the spatial gradient of human health risk and ecological risk from exposure to As, Cu, Pb, and Zn in soils near the Ventanas Industrial Complex (Puchuncaví, Chile). Environ. Pollut. 258, 113488. https://doi.org/10.1016/j.envpol.2019.113488

Tian, X., Wang, D., Chai, G., Zhang, J., Zhao, X., 2021. Does biochar inhibit the bioavailability and bioaccumulation of As and Cd in co-contaminated soils? A meta-analysis. Sci. Total Environ. 762, 143117.

https://doi.org/10.1016/j.scitotenv.2020.143117

Uchimiya, M., Chang, S., Klasson, K.T., 2011. Screening biochars for heavy metal retention in soil: Role of oxygen functional groups. J. Hazard. Mater. 190, 432–441. https://doi.org/10.1016/j.jhazmat.2011.03.063

USEPA, 2007. METHOD 3051A: Microwave assisted acid digestion of sediments, sludges, soils, and oils. Test Methods Eval. Solid Waste.

Vodyanitskii, Y.N., 2006. Arsenic, lead, and zinc compounds in contaminated soils according to EXAFS spectroscopic data: A review. Eurasian Soil Sci. 39, 611–621. https://doi.org/10.1134/S1064229306060056

Wan, X., Li, C., Parikh, S.J., 2020. Simultaneous removal of arsenic, cadmium, and lead from soil by iron-modified magnetic biochar. Environ. Pollut. 261, 114157. https://doi.org/10.1016/j.envpol.2020.114157

Wang, J., Shi, L., Zhai, L., Zhang, H., Wang, S., Zou, J., Shen, Z., Lian, C., Chen, Y., 2021. Analysis of the long-term effectiveness of biochar immobilization remediation on heavy metal contaminated soil and the potential environmental factors weakening the remediation effect: A review. Ecotoxicol. Environ. Saf. 207, 111261. https://doi.org/10.1016/j.ecoenv.2020.111261

Wang, N., Xue, X.-M., Juhasz, A.L., Chang, Z.-Z., Li, H.-B., 2017. Biochar increases arsenic release from an anaerobic paddy soil due to enhanced microbial reduction of iron and arsenic. Environ. Pollut. 220, 514–522. https://doi.org/10.1016/j.envpol.2016.09.095

Wang, S., Gao, B., Zimmerman, A.R., Li, Y., Ma, L., Harris, W.G., Migliaccio, K.W., 2015. Removal of arsenic by magnetic biochar prepared from pinewood and natural hematite. Bioresour. Technol. 175, 391–395. https://doi.org/10.1016/j.biortech.2014.10.104

Wang, Yue. Wang, H.-S., Tang, C.-S., Gu, K., Shi, B., 2020b. Remediation of heavy-metal-contaminated soils by biochar: a review. Environ. Geotech. 1–14. https://doi.org/10.1680/jenge.18.00091

Wang, Yi-min, Wang, S., Wang, C., Zhang, Z., Zhang, J., Meng, M., Li, M., Uchimiya, M., Yuan, X., 2020a. Simultaneous Immobilization of Soil Cd(II) and As(V) by Fe-Modified Biochar. Int. J. Environ. Res. Public Health 17, 827. https://doi.org/10.3390/ijerph17030827

Waterlot, C., Pruvot, C., Bidar, G., Fritsch, C., De Vaufleury, A., Scheifler, R., Douay,

F., 2016. Prediction of Extractable Cd, Pb and Zn in Contaminated Woody Habitat Soils Using a Change Point Detection Method. Pedosphere 26, 282–298. https://doi.org/10.1016/S1002-0160(15)60043-1

Wierzbowska, J., Sienkiewicz, S., Żarczyński, P., Krzebietke, S., 2020. Environmental Application of Ash from Incinerated Biomass. Agronomy 10, 482. https://doi.org/10.3390/agronomy10040482

Williams, P.N., Zhang, H., Davison, W., Meharg, A.A., Hossain, M., Norton, G.J., Brammer, H., Islam, M.R., 2011. Organic Matter—Solid Phase Interactions Are Critical for Predicting Arsenic Release and Plant Uptake in Bangladesh Paddy Soils. Environ. Sci. Technol. 45, 6080–6087. https://doi.org/10.1021/es2003765

Wu, J., Li, Z., Huang, D., Liu, X., Tang, C., Parikh, S.J., Xu, J., 2020. A novel calcium-based magnetic biochar is effective in stabilization of arsenic and cadmium co-contamination in aerobic soils. J. Hazard. Mater. 387, 122010. https://doi.org/10.1016/j.jhazmat.2019.122010

Xiang, W., Zhang, X., Chen, J., Zou, W., He, F., Hu, X., Tsang, D.C.W., Ok, Y.S., Gao, B., 2020. Biochar technology in wastewater treatment: A critical review. Chemosphere 252, 126539. https://doi.org/10.1016/j.chemosphere.2020.126539

Xiao, R., Guo, D., Ali, A., Mi, S., Liu, T., Ren, C., Li, R., Zhang, Z., 2019. Accumulation, ecological-health risks assessment, and source apportionment of heavy metals in paddy soils: A case study in Hanzhong, Shaanxi, China. Environ. Pollut. 248, 349–357. https://doi.org/10.1016/j.envpol.2019.02.045

Xiao, Y., Liu, M., Chen, L., Ji, L., Zhao, Z., Wang, L., Wei, L., Zhang, Y., 2020. Growth and elemental uptake of Trifolium repens in response to biochar addition, arbuscular mycorrhizal fungi and phosphorus fertilizer applications in low-Cd-polluted soils. Environ. Pollut. 260, 113761. https://doi.org/10.1016/j.envpol.2019.113761

Xue, Q., Ran, Y., Tan, Y., Peacock, C.L., Du, H., 2019. Arsenite and arsenate binding to ferrihydrite organo-mineral coprecipitate: Implications for arsenic mobility and fate in natural environments. Chemosphere 224, 103–110. https://doi.org/10.1016/j.chemosphere.2019.02.118

Yin, D., Wang, X., Peng, B., Tan, C., Ma, L.Q., 2017. Effect of biochar and Fe-biochar on Cd and As mobility and transfer in soil-rice system. Chemosphere 186, 928–937. https://doi.org/10.1016/j.chemosphere.2017.07.126

Yin, N., Cui, Y., Zhang, Z., Wang, Z., Cai, X., Wang, J., 2015. Bioaccessibility and

dynamic dissolution of arsenic in contaminated soils from Hunan, China. J. Soils Sediments 15, 584–593. https://doi.org/10.1007/s11368-014-1022-1

Yin, Q., Liu, M., Li, Y., Li, H., Wen, Z., 2021. Computational study of phosphate adsorption on Mg/Ca modified biochar structure in aqueous solution. Chemosphere 269, 129374. https://doi.org/10.1016/j.chemosphere.2020.129374

Yu, Z., Qiu, W., Wang, F., Lei, M., Wang, D., Song, Z., 2017. Effects of manganese oxide-modified biochar composites on arsenic speciation and accumulation in an indica rice (Oryza sativa L.) cultivar. Chemosphere 168, 341–349. https://doi.org/10.1016/j.chemosphere.2016.10.069

Yu, Z., Zhou, L., Huang, Y., Song, Z., Qiu, W., 2015. Effects of a manganese oxide-modified biochar composite on adsorption of arsenic in red soil. J. Environ. Manage. 163, 155–162. https://doi.org/10.1016/j.jenvman.2015.08.020

Yuan, J.-H., Xu, R.-K., Zhang, H., 2011. The forms of alkalis in the biochar produced from crop residues at different temperatures. Bioresour. Technol. 102, 3488–3497. https://doi.org/10.1016/j.biortech.2010.11.018

Yuan, Y., An, Z., Zhang, R., Wei, X., Lai, B., 2021. Efficiencies and mechanisms of heavy metals adsorption on waste leather-derived high-nitrogen activated carbon. J. Clean. Prod. 293, 126215. https://doi.org/10.1016/j.jclepro.2021.126215

Zhang, P., Qin, C., Hong, X., Kang, G., Qin, M., Yang, D., Pang, B., Li, Y., He, J., Dick, R.P., 2018. Risk assessment and source analysis of soil heavy metal pollution from lower reaches of Yellow River irrigation in China. Sci. Total Environ. 633, 1136–1147. https://doi.org/10.1016/j.scitotenv.2018.03.228

Zhang, W., Tan, X., Gu, Y., Liu, Shaobo, Liu, Y., Hu, X., Li, J., Zhou, Y., Liu, Sijia, He, Y., 2020. Rice waste biochars produced at different pyrolysis temperatures for arsenic and cadmium abatement and detoxification in sediment. Chemosphere 250, 126268. https://doi.org/10.1016/j.chemosphere.2020.126268

Zheng, R.-L., Cai, C., Liang, J.-H., Huang, Q., Chen, Z., Huang, Y.-Z., Arp, H.P.H., Sun, G.-X., 2012. The effects of biochars from rice residue on the formation of iron plaque and the accumulation of Cd, Zn, Pb, As in rice (Oryza sativa L.) seedlings. Chemosphere 89, 856–862. https://doi.org/10.1016/j.chemosphere.2012.05.008

CAPITULO 2

BIOCHAR FOSFATADO AMENIZA EFEITOS TÓXICOS DE ARSÊNIO DE RESÍDUOS DE MINERAÇÃO ARTESANAL DE OURO

RESUMO

O enriquecimento do biochar com nutrientes pode aumentar a capacidade de absorção de íons metálicos, diminuindo a mobilidade e biodisponibilidade e aumentar a disponibilidade de nutrientes para as plantas, melhorando o crescimento. Avaliamos a influência do biochar enriquecido com fertilizantes fosfatados visando o aumento da capacidade de adsorção de elementos potencialmente tóxicos EPTs), principalmente As, e melhoria das características químicas de resíduo de mineração artesanal de ouro, tendo como planta de referência a *Lactuca sativa*. Para a produção dos biochars a biomassa foi enriquecida com superfosfato simples (SFS) e triplo (SFT), na proporção de 1:4, e produzidos na temperatura de 400°C e aplicados nas taxas de 0.5, 1.0 e 2.0% no resíduo de mineração. A após 1 ano de condicionamente foram cultivadas plantas de *Lactuca sativa* durante 70 dias. A adição dos biochars fosfatados melhoraram a fertilidade do resíduo de mineração, alteraram as formas de P, a solubilidade e a bioacessibilidade de As foram elevadas. Os biochars foram efetivos para diminuir a absorção de As pelo alface, melhorar o acumulo de biomassa e nutrientes, por consequência indicies vegetativos foram melhorados (BAS>BA>BAT). Os biochars foram efetivos em diminuir o risco não-carcinogênico para níveis aceitáveis em relação a crianças e adultos. As equações de regressão foram representativas para descrever o comportamento da absorção influenciada pelos biochars e como os nutrientes dos biochas são importantes na diminuição do estresse provocado pela acumulo de arsênio. O estudo demonstra a potencial do biochar enriquecido com P como condicionador de solo contaminado por

EPTs, diminuindo a disónibbilidade de As e aumentando a de P, e melhorando o crescimento de plantas de alface.

Palavras-chave: condicionador do solo, disponibilidade, bioacessibilidade, risco a saúde, elementos tíxicos

SUMMARY

Enrichment of biochar with nutrients can increase the absorption capacity of metal ions, decreasing mobility and bioavailability, and increase nutrient availability to plants, improving growth. We evaluated the influence of biochar enriched with phosphate fertilizers, aiming at increasing the adsorption capacity of potentially toxic elements (EPTs), mainly As, and improving the chemical characteristics of artisanal gold mining waste, using Lactuca sativa as a reference plant. For the production of biochars, the biomass was enriched with single (SFS) and triple (SFT) superphosphate, in a 1:4 ratio, and produced at a temperature of 400°C and applied at rates of 0.5, 1.0 and 2.0% in the residue of mining. After 1 year of conditioning, Lactuca sativa plants were cultivated for 70 days. The addition of phosphated biochars improved the fertility of the mining residue, altered the forms of P, the solubility and bioaccessibility of As were high. The biochars were effective to decrease the absorption of As by lettuce, improve the accumulation of biomass and nutrients, consequently vegetative indexes were improved (BAS>BA>BAT). The biochars were effective in decreasing the non-carcinogenic risk to acceptable levels in relation to children and adults. The regression equations were representative to describe the behavior of the absorption influenced by the biochars and how the nutrients of the biochas are important in the reduction of the stress caused by the accumulation of arsenic. The study demonstrates the potential of biochar enriched with P as a soil conditioner contaminated by EPTs, decreasing the availability of As and increasing that of P, and improving the growth of lettuce plants.

Keywords: soil conditioner, availability, bioaccessibility, health risk, toxic elements

1 INTRODUÇÃO

A atividade de mineração artesanal gera efeitos negativos nas regiões de exploração. Um dos principais problemas ambientais é a elevada quantidade de rejeitos que geralmente são depositados de maneira aleatória em grandes extensões, que na maioria dos casos estão expostos intemperisando e liberando elementos potencialmente tóxicos (EPTs) provocando a contaminação do ambiente (XIAO et al., 2019; YADAV et al., 2019; SOUZA et al., 2017; WONGSASULUK et al., 2021).

Dependo da riqueza mineral dos rejeitos, eles podem oferecer grande risco a saúde humana e ao ambiente, podendo provocar processos de bioacumulação e biomagnificação nos locais de deposição e em localidade próximas (NGOLE-JEME E FANTKE, 2017). Os EPTs estão propensos a absorção humana, principalmente na exploração artesanal, devido ao contato direto e manual na maioria dos processos realizados (COVRE et al., 2021; PERREIRA et al., 2020; NETO et al., 2020; SOUZA et al., 2017).

O arsênio (As) encontra-se no grupo dos EPTs sem funcionalidade biológica conhecida, por isso mínimas taxas de absorção podem gerar efeitos maléficos ao ser humano (ATSDR, 2019), devido sua semelhança química com o fósforo (P), atuando como substituto direto em todos os processos bioquímicos e fisiológicos relacionados ao P (KOFROŇOVÁ et al., 2018; SUN et al., 2020).

O risco relacionado aos EPT's deve-se aos problemas de saúde (carcinogênico e não-carcinogênico) ocasionados devido a ingestão acidental de solo ou de vegetais oriundos de locais contaminados (NETO et al., 2020; SOUZA et al., 2017; OLIVEIRA et al., 2017). Em áreas de exploração mineral, além da alta contaminação por EPT's, a deficiência de nutrientes como o P, tem sido amplamente observada e é um dos fatores negativos para processos de regeneração local (SALEEM et al., 2020).

Diante disso, várias estratégias modernas de remediação têm se concentrado progressivamente na mitigação, eliminação e controle dos níveis de EPT's no solo (MUHAMMAD et al., 2020). Dentre as alternativas se destacam o uso de biocarvão, produto originado a partir do processo de pirólise que consiste na conversão térmica da biomassa sob condições controladas de oxigênio com a carbonização do material de origem (ZHAO et al., 2014A; MEYER et al., 2012; LEHMANN & JOSEPH, 2009). Buscando melhorar a capacidade de revegetação de áreas degradadas, a adição do biochar enriquecido com nutrientes apresenta-se como uma alternativa prática para a otimização de suas características benéficas (YIN et al., 2017; ZHANG et al., 2020; ZHENG et al., 2020).

O enriquecimento do biocarvão com fertilizantes fosfatos além de melhorar características químicas, físicas e biológicas de solos empobrecidos, como os rejeitos da mineração, aumenta a disponibilidade de P e diminui a absorção de As pelas as plantas, devido a interação entre estes elementos, por ocorreram no solo na forma de oxiânions. Esse estudo avaliou: (1) a eficiência do biocarvão de resíduo de açaí enriquecido com fertilizantes fosfatado (BAT) na disponibilidade e absorção de P; (2) na biodisponibilidade/bioacessibilidade de As em rejeitos de área de mineração; (3) e a influência na absorção de As e crescimento de *Lactuca sativa* e no potencial risco a saúde humana.

2 MATERIAL E MÉTODOS

2.1 Amostragem do resíduo de mineração

As amostras de resíduo foram coletadas em áreas de mineração de ouro no município de Cachoeira do Piriá (01º 45' 35" S, 46º 32' 42" W) e devido a essa exploração os resíduos possuem elevadas concentrações de EPT's (Tabela S1). O município pertence

à microrregião Guamá, situada na mesorregião Nordeste paraense, Amazônia oriental, com extensão territorial de aproximadamente 2.419 km^2 (IBGE, 2020). As amostras foram coletadas da camada superficial das pilhas de rejeitos (0,0-0,2 m), secas ao ar, homogeneizadas, passadas em peneiras de 2 mm de abertura de malha e armazenadas em potes de polietileno até a realização das análises.

Tabela S1. Teores de EPT's no residuo de mineração de ouro

	As	**Ba**	**Co**	**Hg**	**Ni**	**Pb**	**Zn**	**Fe**	**Al**
	mg kg^{-1}							g kg^{-1}	
*RM	3260	70	58,6	0,99	454	34,2	112,05	125	7,1
[a] VRQ	1,4	14,3	-	0,26	1,4	4,8	7,2	7,1	5,9
[b] Prevenção	15	150	25	0,5	30	72	300	-	-
[b] Investigação	35	300	35	12	70	180	450	-	-

* resíduo de mineração; [a] valores de qualidade de referência do estado do Pará (FERNANDES et al., 2018); [b] Conama 2009.

2.2 Produção e caracterização dos biocarvões

Os resíduos da cadeia produtiva de açaí foram coletados em feiras urbanas da região metropolitana de Belém - PA. O material foi submetido à secagem durante 24 h em estufa a 60 ºC. Posteriormente, a biomassa de açaí foi triturada e adicionados os fertilizantes: superfosfato simples (SFS) e superfosfato triplo (SFT) na proporção 4:1 (biomassa: fosfato) (ZHAO et al., 2016). Os materiais (biomassa + fertilizantes) foram colocados em cadinhos de porcelana fechados (para garantir a baixa oxigenação) e submetido à pirólise a 400 °C, em forno tipo mufla, com taxa de aquecimento de 3.3 ºC/min (DIAS et al., 2019). A temperatura final de pirólise foi mantida por uma hora (pirólise lenta). Os biocarvões provenientes desse processo foram triturados e peneirados em peneira de malha de 1 mm. Os biocarvões foram identificados como: BA (biocarvão não enriquecido); BAT (biocarvão enriquecido com SFT) e BAS (biocarvão enriquecido com SFS).

O pH e a condutividade em água foram determinados pela razão de 1:10 (m:w) (Singh et al., 2017). O conteúdo de cinzas foi determinado via perda de massa (1 g) a 750 °C e o material volátil via perda de massa (1 g) a 950 °C (SINGH et al., 2017). A avaliação da capacidade de troca de cátions (CTC) e capacidade de troca de anions (CTA) foi realizada pelo método de saturação com nitrato de amônio, seguido da quantificação de NH_4 (CTC) e NO_3 (CTA) via colorimetria (SINGH et al., 2017; ITO, 2018). Os teores totais dos elementos foram determinados por digestão ácida em forno de micro-ondas (Mars Xpress 6, CEM Corporation), utilizando 500 mg do material e digeridos com ácido clorídrico (HCl) e nítrico (HNO_3) (água régia) e quantificado via ICP-MS.

2.3 Condução do experimento

O experimento foi conduzido em casa de vegetação (delineamento experimental em blocos casualizado) com dez tratamentos e cinco repetições, totalizando 50 unidades experimentais (1 kg). Foram avaliados um tratamento controle (T1), que foi composto apenas por resíduo de mineração (RM, enquanto que nos demais tratamentos foram adicionadas doses dos biocarvões, constando de 0.5, 1 e 2% do volume total do rejeito (Tabela S2). Os tratamentos foram incubados durante 1 ano, para garantir melhor interação dos biochars com os resíduos, com umidade mantida em 70% do volume total de poros. A espécie vegetal cultivada foi a alface (Lactuca Sativa), devido sua eficiência na absorção e acumulação de EPTs e por ser amplamente utilizada em testes de toxicidade e avaliações de risco à saúde humana (ABREU et al., 2014).

Tabela S2. Identificação dos tratamentos de acordo com os biocarvões e dosagens aplicadas.

Tratamentos	Identificação
Controle: resíduo de mineração (RM) (1 kg)	T1
RM (1 kg) + 0,5% de BA[1]	T2
RM (1 kg) + 1% de BA	T3
RM 1 kg) + 2% de BA	T4
RM (1 kg) + 0,5% de BAT[2]	T5
RM (1 kg) + 1% de BAT	T6
RM (1 kg) + 2% de BAT	T7
RM (1 kg) + 0,5% de BAS[3]	T8
RM (1 kg) + 1% de BAS	T9
RM (1 kg) + 2% de BAS	T10

[1]BA: biocarvão de biomassa de açaí sem enriquecimento; [2]BAT: biocarvão de biomassa de açaí enriquecido com SFT; [3]BAS: biocarvão de biomassa de açaí enriquecido com SFS.

2.4 Fertilidade do experimento

Análise de fertilidade do experimento foi realizada de acordo Teixeira et al., (2017). O pH em água (1:2,5), fósforo (P) e potássio (K+) extraídos por Mehlich 1, e determinado por colorimetria e fotometria de chama, respectivamente. A extração de cálcio (Ca^{2+}), magnésio (Mg^{2+}) e alumínio (Al^{+}) foi feita com KCl 1 mol L^{-1} e a determinação por titulometria. A determinação da acidez potencial (H+Al) foi feita com acetato de cálcio e a determinação por titulometria. A capacidade de troca de cátions (CTC) e capacidade de troca de anions (CTA) dos tratamentos foi realizada pelo método de troca compulsiva com solução de nitrato de amônio e posterior lavagem com KCl, seguido de quantificação de NH_4 (CTC) e NO_3 (CTA) via colorimetria (SINGH et al., 2017; ITO, 2018). O carbono orgânico (CO) e carbono inorgânico (CI) foram estimados pela perda de massa por combustão em forno de mufla nas temperaturas de 450 °C e 950 °C, respectivamente, e o carbono total (CT) através da somatória CO + CI (HUSSAIN et al., 2019).

2.5 Fracionamento de fósforo inorgânico

O fracionamento de P inorgânico foi realizado de acordo a metodologia de Qian & Jiang (2014), avaliando as seguintes frações de fósforo (P): P solúvel (Psol) extraído com

água ultrapura; P lábil (Plab) extraído com 0,5 mol de $NaHCO_3$; P adsorvido (Pads) extraído com 0,1 mol de NaOH; e P associado aos minerais (Pmin) extraído com 1 mol de HCl; o material sólido remanescente digerido pelo método EPA 3051A e considerado como P-residual. Todas as frações de P foram quantificadas via colorimetria (MURFEY & RILEY, 1960).

2.6 Nutrientes e arsênio na planta

Após 70 dias de experimento o material vegetal foi separado (raiz e folha), lavado com água destilada e seguido secagem em estufa a 50 °C até peso constante, para a avaliação da massa seca. Os teores de nutrientes e arsênio na planta (raiz e folha) foram obtidos por digestão ácida com HNO_3/H_2O_2 (SOUZA et al., 2017) em forno de micro-ondas (Mars Xpress 6, CEM Corporation) e o controle de qualidade das análises realizado com amostra do material de referência ERM-CD281 (rye grass), com branco de reagente em cada bateria de 16 amostras e avaliadas em triplicata. As concentrações foram obtidas por espectrometria de absorção atômica com chama (FAAS) (Thermo Scientific, modelo iCE3000) com gerador de hidretos para as leituras de As (Thermo Scientific, modelo VP100).

A melhoria das características vegetais após a adição dos biochars foi avaliada através dos índices: fator de bioconcentração (FB) (Equação 1), fator de translocação (FTr) (Equação 2) e o fator de tolerância (FTo) (Equação 1).

Equação 1: $Fator\ de\ bioconcentração\ (FB) = \left[\frac{Concentração\ (raiz\ ou\ PA)\ (mg\ kg^{-1})}{Concentração\ no\ rejeito\ \ (mg.kg^{-1})}\right]$

Equação 2: $Fator\ de\ translocação\ (FTr) = \left[\frac{Concentração\ na\ parte\ aérea\ (mg\ kg^{-1})}{Concentração\ na\ raíz\ (mg\ kg^{-1})}\right]$

Equação 3: $Fator\ de\ tolerancia\ (FTo) = \left[\frac{Biomassa\ Total-tratamentos(mg\ kg^{-1})}{Biomassa\ Total-controle\ (mg\ kg^{-1})}\right]$

2.7 Fracionamento e bioacessibilidade de arsênio

O fracionamento de arsênio (As) foi realizado com método proposto por Drahota et al., (2014): arsênio solúvel (F1), extraído com água ultrapura; arsênio adsorvidos (F2), extraído com mono-fosfato de amônio; arsênio ligado a minerais amorfos (F3), extraído com oxalato de amônio (em temperatura ambiente e no escuro); arsênio ligado a minerais cristalinos (F4), extraído com oxalato de amônio (80 °C); e arsênio residual (F5), extraídos com solução de KCl/ HCl/ HNO_3. A bioacessibilidade oral foi determinada pelo teste simples de extração de bioacessibilidade (SBET), simulando a absorção gastrointestinal humana, extraída com solução de glicina (0,4 mol L^{-1} e pH 1.5) (USEPA-1340, 2013), seguido de centrifugação, filtragem e posterior quantificação. O percentual bioacessivel foi avaliado através da equação 4:

Equação 4: $Bioac\ As\ (\%) = \left[\frac{SBET}{As-t}\right] * 100$

Onde: Bioac As (%): a bioacessibilidade de arsênio (%). SBET: a concentração bioacessivel (mg kg^{-1}) extraída com a solução de glicina. As-t: teor total de arsênio encontrado no resíduo de mineração (mg kg^{-1}).

Os teores em cada fração e as concentrações bioacessíveis de arsênio foram quantificadas por FAAS (Thermo Scientific, modelo série iCE 3000) com gerador de hidreto (Thermo Scientific, modelo VP100). Para garantia da qualidade, todas as extrações foram realizadas em triplicado.

2.8 Avaliação de risco para a saúde humana.

Os potenciais efeitos adversos para a saúde humana devido à exposição a EPTs de rejeitos de mineração de ouro no município de Cachoeira do Piriá foram avaliados utilizando o modelo de avaliação de risco desenvolvido pela USEPA (2001). Duas rotas de exposição foram avaliadas: (a) ingestão acidental de solo contaminado ($HQ_{ing\text{-}solo}$),

equação 5; (b) ingestão de vegetais oriundos de locais contaminado ($HQ_{ing\text{-}plant}$) equação 6. O risco exposição (HI) foi obtido usando a somatória dos quocientes de risco ($HQ_{ing\text{-}solo}$ e $HQ_{ing\text{-}plant}$) para crianças e adultos (LI et al., 2014).

Equação 5: $$HQ_{ing-solo} = \left[\frac{\mathrm{C}\, x\, \frac{ingR\ x\ EF\ x\ ED}{BW\ x\ AT}\, x\ CF}{Rfd-ing}\right] * \ Bioac\ As$$

Equação 6: $$HQ_{ing-plant} = \frac{C_{(plant)} x\, \frac{ingR\ x\ IR_{veg}\ x\ EF\ x\ ED}{BW\ x\ AT}\, x\ CF}{Rfd-ing}$$

Onde, C (mg kg^{-1}) = concentração total de As; Bioac As = percentual bioacessivel de As; C_{plant} = concentração de As na parte comestível do vegetal (mg kg^{-1}) (USEPA, 2011); ingR (mg d^{-1}) = taxa de ingestão do solo, 100 mg d^{-1} para adultos e 200 mg d^{-1} para crianças (USEPA, 2001); $IR_{vegetal}$: taxa de ingestão de plantas (kg d^{-1}), 200 mg para adultos e 100 mg para crianças (IBGE, 2020); EF (d y-1) = frequência de exposição, 279 dias (MOREIRA et al., 2018); ED = duração da exposição, 24 h para adultos e 4 h para crianças (MOREIRA et al., 2018); BW (kg) = peso corporal, 70 kg para adultos e 16 kg para crianças (MOREIRA et al., 2018); AT = tempo médio, sem efeitos carcinogênicos (DE x 365 d); CF = fator de conversão = 10^{-6} kg mg^{-1} (USEPA, 2001); Rfd = dose de referência, 0,0003 para As (mg kg d^{-1}) (USEPA, 2001); e SF = fator de inclinação, 1.51 (LU et al., 2014).

2.9 Análise estatística

Os resultados foram submetidos ao teste de normalidade de Shapiro-Wilk ($p < 0,05$). Diante da normalidade, foi realizada análise de variância (ANOVA) e as médias comparadas pelo teste de Tukey ($p < 0,05$). Uma análise de regressão linear múltipla foi realizada para gerar um modelo robusto para estimar o acúmulo de arsênio pela planta. As variáveis para modelagem foram selecionadas por meio do fator de inflação de variância (VIF), a equação da regressão linear múltipla foi obtida pelo método Stepwise,

eliminando-se as variáveis sem significância estatística para o modelo e com melhores valores de AIC (Akaike Information Criterion). A precisão e acurácia do modelo selecionado foram avaliadas por meio da significância do modelo (p-valor), coeficiente de determinação ajustado (R2 ajustado) e raiz quadrada média do erro normalizado (NRMSE) (WATERLOT et al., 2016). Todas as análises estatísticas foram realizadas usando R, versão 4.1.1 (R Core Team 2021).

3 RESULTADOS E DISCUSSÃO

3.1 Caracterização do biochar

A adição dos fertilizantes fosfatados proporcioram características distintas entre os biochars (Tabela 2). A adição dos fertilizantes fosfatados alteraram a quantidade de cargas e diminuiram os valores de pH dos biochars. A presença de oxihidroxidos metálicos (Fe e Al) são responsáveis pela formação do excesso de cargas aniônicas na superfície dos biochars (LAWRINENKO et al., 2017), esses elementos podem ser encontrados devido a origem das rochas fosfatadas que originam STS e SFT (CHEN & GRAEDEL, 2015; HUANG et al., 2019). Além disso, a utilização de ácidos no processo de produção dos fertilizantes fosfatados pode ter contribuido para a acidificação dos biocarvões enriquecidos com os fosfatos.

Tabela 2. Propriedades químicas dos biochars

Biochars	pH	Cinza	CTC[4]	CTA[5]	Al	Ca	Fe	K	Mg	Pt	P-F1	P-F2	P-F3	P-F4
			$cmol_c\ kg^{-1}$			$g\ kg^{-1}$					$mg\ kg^{-1}$			
BA[1]	6,70	3,60	13,84	11,14	0,10	1,10	0,10	8,10	1,00	2,91	0,93	0,14	0,06	1,23
BAT[2]	3,02	23,62	32,90	18,14	3,20	59,80	3,90	7,20	5,00	15,02	73,21	3,13	5,60	85,57
BAS[3]	4,25	15,77	26,71	14,27	0,90	88,10	3,50	7,80	1,40	10,05	22,25	1,20	0,13	51,18

[1]BA: biocarvão de biomassa de açaí sem enriquecimento; [2]BAT: biocarvão de biomassa de açaí enriquecido com SFT; [3]BAS: biocarvão de biomassa de açaí enriquecido com SFS; [4]CTC: capacidade de troca de cátions; [5]CTA: capacidade de troca de ânions.

As maiores quantidades de elementos químicos (Tabela 2), se deve ocorrência destes elementos nos fosfatos, principalmente Ca e P, super-fosfato-simples (21% de P e 16% de Ca) e triplo (46% de P e 12% de Ca). Normalmente biochars oriundos de resíduos vegetais são pobres em nutrientes, por isso faz-se necessário o enriquecimento com elementos que agreguem valor nutricional ao material carbonáceo (SEYEDSADR et al., 2022). O aumento no teor de cinzas dos biochars enriquecidos com fosfatos é devido ao aumento compostas inorgânicos, os quais não são degradados ou volatilizados durante o processo de pirolise, e por isso tendem a acumular na forma de óxidos/carbonatos/hidróxidos/fosfatos (DIAS et al., 2019). A quantidade de compostos inorgânicos encontrados nas cinzas dos biochars definiem o potencial como fontes de nutrientes (DEY & MAVI, 2022) para a melhoria da fertilidade.

3.2 Efeito dos biochars no resíduo de mineração

A adição dos biochars alteraram ($p<0.05$) todas as características químicas do resíduo de mineração (Tabela 3). O pH do resíduo foi mais alcalinizado pela adição de BA e BAS, enquanto que a maior dose de BAT (T7) proporcionou a acidificação do resíduo. Os biochars possuem valores de pH alcalinos oriundos de suas cinzas devido a pirolise de material orgânico, suas cinzas são ricas em carbonatos e hidróxidos as quais tendem a solubilização e alcalinizar o meio (FIDEL et al., 2017; SHETTY & PRAKASH, 2020), no entanto, a adição exógena de íons pode proteger compostos orgânico da carbonização completa, os quais durante o envelhecimento tendem a degradação, liberando compostos que acidificam o meio (WALI et al., 2020; PIASH et al., 2021). A maior quantidade de fósforo no BAT é o causador de sua maior acidez, devido as características mais acidas do SFT (ZHAO et al., 2016; LUSTOSA-FILHO et al., 2017).

Os valores de acidez (H+Al), diminuíram com a adição de BA e aumentaram com a adição de BAT e BAS, sendo proporcionais aos teores totais de Al dos biochar (BAT > BAS > BA) e aos teores trocáveis de Al (Tabela 2 e 2). Em condições de acidas pode ocorrer alta disponibilidade de Al, que em excesso no ambiente radicular pode provocar efeitos tóxicos, devido sua alta mobilidade e fácil absorção pelas raízes das plantas (DAI et al., 2017; SHETTY & PRAKASH, 2020; SHI et al., 2020). O biochar tem efeito de calagem, diminuindo a acidez devido a neutralização dos íons de Al através da reação com os carbonatos/hidróxidos disponibilizados pelos biochars (HALE et al., 2020), proporcionando uma melhoria da qualidade radicular.

Tabela 3. Propriedades químicas dos tratamentos.

TR	pH	CTC[11]	CTA[12]	H+Al[13]	Ca	Mg	Al	K	P	CO[14]	CI[15]	CT[16]
		$cmol_c\ dm^{-3}$							mg kg^{-1}			
T1[1]	6,46e	2,34i	2,17e	0,22d	0,94e	0,23b	0,11c	0,04c	17,67h	3,98g	5,32c	9,30g
T2[2]	6,99c	5,01h	2,17e	0,11e	1,08e	0,01d	0,11c	0,06c	16,09h	5,60f	3,96f	9,56g
T3[3]	7,17b	5,48g	2,18e	0,05f	0,84f	0,05d	0,11c	0,12b	18,37h	7,01d	4,79e	11,80e
T4[4]	7,34a	8,30c	2,38d	0,01f	0,83f	0,34a	0,11c	0,16b	34,26g	8,43b	4,56e	12,99c
T5[5]	6,99c	6,48f	2,32d	0,51c	1,12e	0,09c	0,11c	0,06c	110,50e	5,43f	5,25c	10,68f
T6[6]	6,46e	7072d	2,36d	0,81b	1,31d	0,10c	0,21b	0,09c	292,07b	6,87e	5,42c	12,29d
T7[7]	6,09f	9,77a	2,42c	1,85a	2,33b	0,20b	0,52a	0,26a	608,21a	8,65b	5,31c	13,96b
T8[8]	6,81c	7,06e	2,48c	0,26d	1,95c	0,05d	0,10c	0,04c	62,92f	6,14e	5,88a	12,02d
T9[9]	6,98c	8,06d	2,57b	0,54c	2,05c	0,20b	0,11c	0,04c	122,90d	7,14d	5,59b	12,73c
T10[10]	6,62d	8,53b	2,70a	0,81b	3,24a	0,20b	0,11c	0,09c	166,68c	9,88a	5,08d	14,96a

[1]T1: resíduo de mineração (RM); [2]T2: resíduo de mineração (RM) + 0.5% BA; [3]T3: resíduo de mineração (RM) + 1.0% BA; [4]T4: resíduo de mineração (RM) + 2.0% BA; [5]T5: resíduo de mineração (RM) + 0.5% BAT; [6]T6: resíduo de mineração (RM) + 1.0% BAT; [7]T7: resíduo de mineração (RM) + 2.0% BAT; [8]T8: resíduo de mineração (RM) + 0.5% BAS; [9]T9: resíduo de mineração (RM) + 1.0% BAS; [10]T10: resíduo de mineração (RM) + 2.0% BAS; [11]P-F1: fosforo solúvel; [12]P-F2: fosforo lábil; [13]P-F3: fosforo adsorvido; [14]P-F4: fosforo associado aos minerais. Letras diferentes indicam diferença significativa entre os tratamentos pelo teste de Tukey ($p < 0,05$).

Os nutrientes (Ca, Mg, K e P) foram alterados conforme o aumento das doses e proporcionais aos teores de cinzas dos biochars (Tabela 2 e 3). A adição dos fertilizantes (SFT e SFS) aos biochars foram fundamentais para a maior disponibilidade de P e Ca

para o resíduo de mineração, BAT e BAS respectivamente. Biomassas ricas em nutrientes geram biochars ricos em nutrientes os quais tendem a disponibiliza-los ao solo (LUSTOSA-FILHO et al., 2020), essa efetividade de disponibilidade de nutrientes depende diretamente das características da biomassa e da temperatura de pirolise (PURAKAYASTHA et al., 2019), sendo de fundamental importância a quantidade de cinzas formadas, pois essas fontes diretas de nutrientes ao solo (DOMINGUES et al., 2017; KORAI et al., 2021).

Os biochars aumentaram as cargas de CTC/CTA e os teores de CO do resíduo, proporcionais a quantidade aplicada (Tabela 3). O carbono não mineralizado pelo processo de pirolise (ZHAO et al., 2014) é responsável pelo aumento do carbono orgânico do solo, os resíduos orgânicos ainda presentes após a produção dos biochars tendem a solubilização tendem a aumentar o reservatório de carbono e nutrientes do solo (GUEDES et al., 2021; RAMOS et al., 2021). A elevação da quantidade de carbono orgânico tem reflexo no aumento das cargas do solo, os componentes orgânicos oriundos dos biochars são ricos em grupos funcionais orgânicos e quando oxidados aumentam a disponibilidade de sítios ativos para a adsorção de cátions e ânions (LAWRINENKO et al., 2016; HAILEGNAW et al., 2019; MASÍS-MELÉNDEZ et al., 2021).

3.3 Fracionamento de fósforo inorganico

A adição dos biochars alteraram as frações de fósforo no resíduo de mineração (Tabela 4). Ocorreu a diminuição ou estabilização dos teores de P após a adição de BA (T2 e T3) e nos tratamentos com os biochars enriquecidos os teores de P foram elevados em todas as frações. As maiores quantidades de P foram proporcionais a elevação das taxas e aos teores de P encontrados nos biochars (Tabela 2).

Tabela 4. Fracionamento químico de fosforo inorgânico do experimento.

TR	P-F1[11]	P-F2[12]	P-F3[13]	P-F4[14]
	mg.kg^{-1}			
T1[1]	6,72f	20,83g	63,79f	2,39f
T2[2]	1,47g	20,52g	68,36f	2,80f
T3[3]	4,08f	19,49g	68,73f	3,30f
T4[4]	10,02e	31,85f	94,32e	6,51e
T5[5]	25,88d	82,54d	149,49c	54,31c
T6[6]	129,72b	160,62b	211,30b	141,71b
T7[7]	307,93a	251,27a	345,22a	368,05a
T8[8]	8,53f	65,44e	105,41e	47,31d
T9[9]	29,88d	89,13d	133,01d	58,02c
T10[10]	70,55c	127,86c	153,20c	123,12b

[1]T1: resíduo de mineração (RM); [2]T2: resíduo de mineração (RM) + 0.5% BA; [3]T3: resíduo de mineração (RM) + 1.0% BA; [4]T4: resíduo de mineração (RM) + 2.0% BA; [5]T5: resíduo de mineração (RM) + 0.5% BAT; [6]T6: resíduo de mineração (RM) + 1.0% BAT; [7]T7: resíduo de mineração (RM) + 2.0% BAT; [8]T8: resíduo de mineração (RM) + 0.5% BAS; [9]T9: resíduo de mineração (RM) + 1.0% BAS; [10]T10: resíduo de mineração (RM) + 2.0% BAS; [11]P-F1: fosforo solúvel; [12]P-F2: fosforo lábil; [13]P-F3: fosforo adsorvido; [14]P-F4: fosforo associado aos minerais. Letras diferentes indicam diferença significativa entre os tratamentos pelo teste de Tukey ($p < 0,05$).

A adição dos biochars enriquecidos (BAS e BAT) foram eficientes em disponibilizar fósforo em formas de mais fácil absorção pelas plantas (Tabela 4), as formas solúvel/lábeis de P possuem maior mobilidade e absorção pelas raízes das plantas, além de maior possibilidade de adsorção pelos coloides/ minerais do solo (ZHANG et al., 2016; MAHMOUD et al., 2019). O incremento das frações adsorvido/mineral com a adição dos biochars é uma alternativa para a elevação do pool de P, sendo de grande importância para a liberação lenta (MATOSO et al., 2019; LI et al., 2020; YANG et al., 2021) suprindo a necessidade de fosforo em condições de estresse.

3.4 Fracionamento de arsênio

A adição dos biochars modificaram as frações de As no resíduo de mineração (Figura1). Todos os biochars aumentaram os teores da fração F1(As-solúvel) e diminuíram da fração F2 (As-adsorvido), essas frações mais moveis relacionam-se inversamente entre si e com todas as frações/disponibilidade de P, CO, CTC e pH (Tabela S2). As formas e a disponibilidade P tem ação na solubilidade de As devido as suas semelhança químicas e estruturais (BOORBOORI et al., 2021), as quais na condição de

excesso de P favorece a maior disponibilidade de As (LEE et al., 2015). As alterações de CO, CTC e pH tem efeito direto na mobilização de As no solo, favorecendo a solubilização de As devido a repulsão eletrostática proporcionada, devido ao aumento das cargas efetivas oriundas dos compostos orgânicos oriundos da adição dos biochars (BANDARA et al., 2019; KIM et al., 2018).

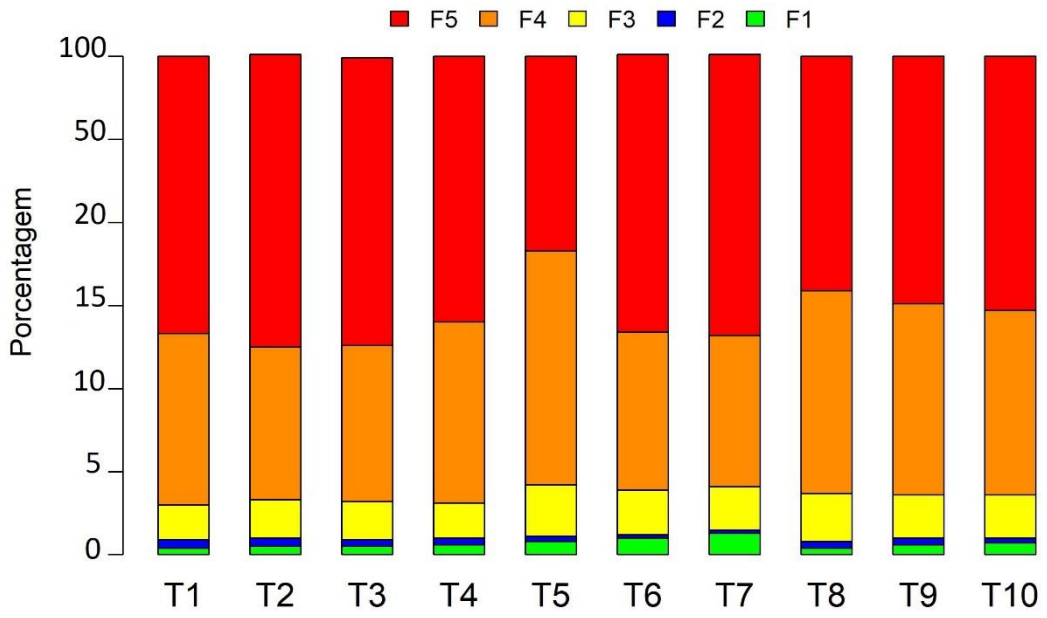

Figura 1. Fracionamento de arsênio do experimento.

[1]T1: resíduo de mineração (RM); [2]T2: resíduo de mineração (RM) + 0.5% BA; [3]T3: resíduo de mineração (RM) + 1.0% BA; [4]T4: resíduo de mineração (RM) + 2.0% BA; [5]T5: resíduo de mineração (RM) + 0.5% BAT; [6]T6: resíduo de mineração (RM) + 1.0% BAT; [7]T7: resíduo de mineração (RM) + 2.0% BAT; [8]T8: resíduo de mineração (RM) + 0.5% BAS; [9]T9: resíduo de mineração (RM) + 1.0% BAS; [10]T10: resíduo de mineração (RM) + 2.0% BAS; [11]F1: arsênio solúvel; [12]P-F2: arsênio adsorvido; [13]F3: arsênio associado aos minerais amorfos; [14]F4: arsênio associado aos minerais cristalinos; [15]F5: arsênio residual.

A adição dos biochars fosfatados (BAS e BAT) proporcionaram a diminuição da fração F5 (As-residual) e por consequência elevação dos teores de As nas frações F3/F4 (As-amorfo e As-cristalino) (Figura1). Ambas as frações obtiveram relação entre si e com F5, a fração F3 obteve relação com P-F2, P-F3, CI e CTA, e F4 apenas com P-F1 (Tabela S2). A maior estabilização de As nas frações F3/F4, acontece devido a adição dos biochars ricos em Ca/Al/Fe (Tabela 2) encontrados nas frações inorgânicas de carbono

do biochar, os quais podem auxiliar na formação de complexos insolúveis/estáveis de As (SIMON et al., 2015; ZHONG et al., 2020). A solubilização da As da fração mais estável ocorreu devido a adição em excesso de P, o qual favorece a troca iônica ou solubilização de As dos minerais do resíduo (BOORBOORI et al., 2021). Os teores de CO também tem importância significativa na solubilização de As devido a proporcional elevação das quantidades de compostos orgânicos de baixo peso molecular (AFTABTALAB et al., 2022), que tem papel importante na dissolução redutiva dos minerais contendo As presentes na fração residual (KIM et al., 2020).

Tabela S2: Correlação de Pearson entre as frações de arsênio e as características químicas dos tratamentos.

	As.F1	As.F2	As.F3	As.F4	As.F5
As.F2	-0,95**				
As.F3	0,32	-0,45*			
As.F4	-0,16	0,09	0,61**		
As.F5	-0,01	0,09	-0,74**	-0,98**	
P.F1	0,91**	-0,86**	0,17	-0,39*	0,23
P.F2	0,91**	-0,94**	0,41*	-0,17	0
P.F3	0,96**	-0,93**	0,36*	-0,18	0
P.F4	0,90**	-0,87**	0,27	-0,28	0,12
C.org	0,46*	-0,58**	-0,05	-0,16	0,11
C.ino	0,18	-0,28	0,47**	0,34	-0,39*
CTC	0,69**	-0,79**	0,33	0,05	-0,16
CTA	0,22	-0,45*	0,37*	0,32	-0,36
pH	-0,56**	0,54**	-0,18	0,33	-0,21
H.Al	0,28	-0,27	0,34	-0,2	0,04
Ca.cmolc.	0,3	-0,49	0,37	0,09	-0,16
Mg.cmolc.	0,16	-0,11	-0,46	0,03	0,04
Al.cmolc.	0,25	-0,24	0,07	-0,43	0,29
K.cmolc.	0,33	-0,30	-0,25	-0,45	0,37
P.mg.	0,93**	-0,89**	0,27	-0,3	0,13

**: p<0,01; *: p<0,05.

3.5 Interação Arsênio-Planta

A adição dos biochars alteraram significativamente os resultados, a biomassa foliar/radicular e os teores de nutrientes aumentaram conforme a aplicação de BA e BAS (Tabela 5 e Figura 2). O aumento da solubilidade de arsênio (Figura 1) não refletiu nos teores de arsênio absorvidos (Figura 2). Todos os índices referentes ao desenvolvimento

vegetativo da planta (*L. sativa*) melhoraram significativamente após a adição dos biochars (Tabela 6).

Tabela 5. Biomassa e nutrientes na raiz e folhas de *L. sativa*.

TR	Bio[11]	Ca	Mg	K	P	Fe	Bio[11]	Ca	Mg	K	P	Fe
	Folha (g/planta)						Raiz (g/planta)					
T1[1]	0,02 h	0,01 h	0,01 g	0,33 i	0,04 h	0,07 c	0,01 h	0,01 g	0,00 f	0,06 g	0,02 i	0,03 h
T2[2]	0,02 h	0,02 h	0,01 g	1,88 h	0,05 h	0,01 g	0,01 i	0,00 g	0,00 f	0,10 g	0,01 i	0,01 i
T3[3]	0,04 g	0,05 g	0,03 f	5,07 g	0,12 g	0,01 f	0,02 g	0,01 f	0,01 e	0,32 g	0,04 h	0,05 g
T4[4]	0,09 e	0,08 f	0,05 e	13,88 d	0,33 f	0,03 e	0,05 e	0,02 d	0,03 c	2,37 d	0,14 f	0,19 c
T5[5]	0,17 d	0,26 d	0,22 b	12,00 e	0,94 c	0,05 d	0,05 d	0,02 d	0,02 d	3,69 c	0,28 d	0,08 f
T6[6]	0,08 f	0,13 e	0,12 d	8,40 f	0,74 d	0,03 e	0,03 f	0,02 e	0,01 d	2,36 d	0,30 c	0,09 e
T7[7]	0,01 i	0,01 h	0,01 g	1,29 h	0,09 g	0,03 e	0,01 h	0,01 f	0,00 f	0,70 f	0,08 g	0,01 j
T8[8]	0,26 c	0,31 c	0,15 c	20,36 c	0,68 e	0,06 c	0,08 c	0,09 c	0,04 b	1,83 e	0,19 e	0,11 d
T9[9]	0,30 b	0,33 b	0,22 b	26,59 b	1,15 b	0,10 b	0,15 b	0,11 b	0,04 b	9,48 b	0,33 b	0,29 b
T10[10]	0,52 a	0,47 a	0,39 a	58,20 a	2,26 a	0,23 a	0,20 a	0,20 a	0,08 a	16,00 a	0,77 a	0,66 a

[1]T1: resíduo de mineração (RM); [2]T2: resíduo de mineração (RM) + 0.5% BA; [3]T3: resíduo de mineração (RM) + 1.0% BA; [4]T4: resíduo de mineração (RM) + 2.0% BA; [5]T5: resíduo de mineração (RM) + 0.5% BAT; [6]T6: resíduo de mineração (RM) + 1.0% BAT; [7]T7: resíduo de mineração (RM) + 2.0% BAT; [8]T8: resíduo de mineração (RM) + 0.5% BAS; [9]T9: resíduo de mineração (RM) + 1.0% BAS; [10]T10: resíduo de mineração (RM) + 2.0% BAS. Bio[11]: biomassa seca. Letras diferentes indicam diferença significativa entre os tratamentos pelo teste de Tukey ($p < 0,05$).

Os índices TF e BCF diminuíram com a adição dos biochars (com exceção aos tratamentos com BAT) e comprovando que a maior translocação ocorrida no tratamento sem biochar (T1) refletem nas maiores quantidades absorvida de As e por consequência o menor ganho de biomassa vegetal (Tabela 5). A maioria dos tratamentos com biochars obtiveram TI >1 sugerindo que a adição dos respectivos amenizantes melhoram a tolerância de *L. Sativa* ao excesso de As no resíduo de mineração, sendo a maior disponibilidade de nutrientes uma das explicações para esses resultados.

A diminuição da translocação raiz-folha tem efeito direto no alivio dos problemas fisiológicos relacionados ao acumulo de As nas folhas (GUSMAN et al., 2013; CORDON et al., 2018), a menor quantidade de elementos tóxicos nas folhas reflete em uma melhor capacidade fotossintética e tem como resposta um maior acumulo de nutrientes e biomassa (HAIDER et al., 2022). A maior absorção de nutrientes é de fundamental importância para a resistência ao estresse contra o As (LIU et al., 2018), refletindo

diretamente no melhor desenvolvimento vegetal (GHASSEMI-GOLEZANI & FARHANGI-ABRIZ, 2021).

Tabela 6. Índice de tolerância (TI), fator de translocação (TF), fator de bioconcentração (CF)

TR	TI	TF	CF-R[11]	CF-F[12]
T1[1]	-	1.95 a	0.49 c	0.96 a
T2[2]	0.80 i	0.35 d	0.75 b	0.27 c
T3[3]	1.86 g	0.30 d	0.82 a	0.10 e
T4[4]	4.35 e	0.07 g	0.32 e	0.05 f
T5[5]	7.05 d	0.24 e	0.39 d	0.09 e
T6[6]	3.60 f	0.45 c	0.32 e	0.14 d
T7[7]	0.86 h	0.85 b	0.73 b	0.62 b
T8[8]	10.61 c	0.25 e	0.35 e	0.09 e
T9[9]	14.34 b	0.22 e	0.34 e	0.08 e
T10[10]	22.17 a	0.17 f	0.73 b	0.12 d

[1]T1: resíduo de mineração (RM); [2]T2: resíduo de mineração (RM) + 0.5% BA; [3]T3: resíduo de mineração (RM) + 1.0% BA; [4]T4: resíduo de mineração (RM) + 2.0% BA; [5]T5: resíduo de mineração (RM) + 0.5% BAT; [6]T6: resíduo de mineração (RM) + 1.0% BAT; [7]T7: resíduo de mineração (RM) + 2.0% BAT; [8]T8: resíduo de mineração (RM) + 0.5% BAS; [9]T9: resíduo de mineração (RM) + 1.0% BAS; [10]T10: resíduo de mineração (RM) + 2.0% BAS; [11]CF-R: fator de bioconcentração radicular; [12]CF-F: fator de bioconcentração foliar. Letras diferentes indicam diferença significativa entre os tratamentos pelo teste de Tukey ($p < 0,05$).

Os nutrientes têm diferentes finalidades na melhoria do desenvolvimento vegetal e inibindo a absorção de As (BOORBOORI et al., 2021; KIM et al., 2021). O acumulo de P nas raízes ocorre devido a competição com o As pelos sítios de adsorção do solo ou absorção pelas raízes, devido ao efeito antoganista entre eles, a maior absorção de P auxilia inibição da absorção e posterior acumulo de As nas folhas (ZIA et al., 2017). A maior absorção de K é uma forma de melhoria de equilíbrio iônico, devido a absorção aniônica e a absorção em excesso auxilia no melhor desenvolvimento vegetal (LIU et al., 2018).

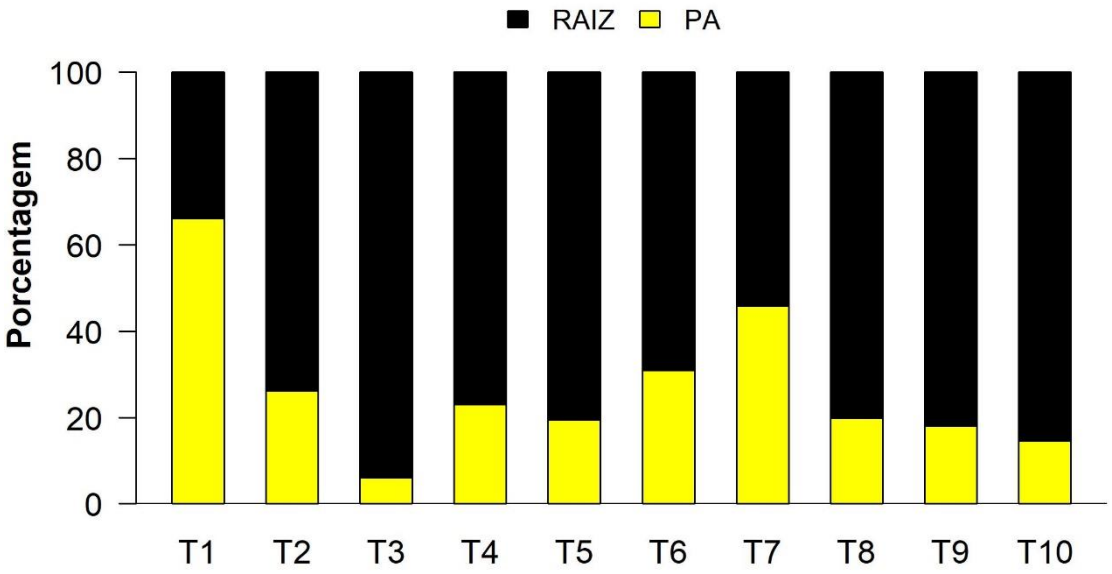

Figura 2. Porcentagem de arsênio na raiz e folhas de *L. sativa*, em relação ao total absorvido.

[1]T1: resíduo de mineração (RM); [2]T2: resíduo de mineração (RM) + 0.5% BA; [3]T3: resíduo de mineração (RM) + 1.0% BA; [4]T4: resíduo de mineração (RM) + 2.0% BA; [5]T5: resíduo de mineração (RM) + 0.5% BAT; [6]T6: resíduo de mineração (RM) + 1.0% BAT; [7]T7: resíduo de mineração (RM) + 2.0% BAT; [8]T8: resíduo de mineração (RM) + 0.5% BAS; [9]T9: resíduo de mineração (RM) + 1.0% BAS; [10]T10: resíduo de mineração (RM) + 2.0% BAS.

O acumulo de Ca e Mg, na raiz e folha, auxiliam na estabilização da integridade celular e na atividade fisiológica, melhorando o crescimento de plantas sobre estresse de As (RAFIQ et al., 2017; SINGH et al., 2020; SYU et al., 2020; GHASSEMI-GOLEZANI E FARHANGI-ABRIZ, 2021). O acumulo de Fe nas raízes da planta em efeito na quelação do As, funcionando como um mecanismo de defesa para a diminuição absorção ou sua translocação (ARCO-LAZARO et al., 2018).

3.6 Avaliação de risco para a saúde humana

A adição de todos os biochars obtiveram efeito na diminuição do risco (Figura 3a e b) proporcionado pelos elevados teores de As nos residuos de mineração. Para o risco não-carcinogênico todos os biochars, obtiveram exito em diminuir os valores de risco para criancas e adultos. Para o risco carcinogênico nenhum biochar conseguiu diminuir HI para niveis aceitaveis (USEPA, 2011), no entanto todos os biochars diminuiram

significativamente os valores de risco potencial. A atenuação do risco deve-se principalmente a diminuição da translocação de As para a parte comestivel do vegetal (Figura 2 e Tabela 6) e ao aumento do As ligado aos minerais amorfos e critalinos (menos biodisponiveis) (Figura 1).

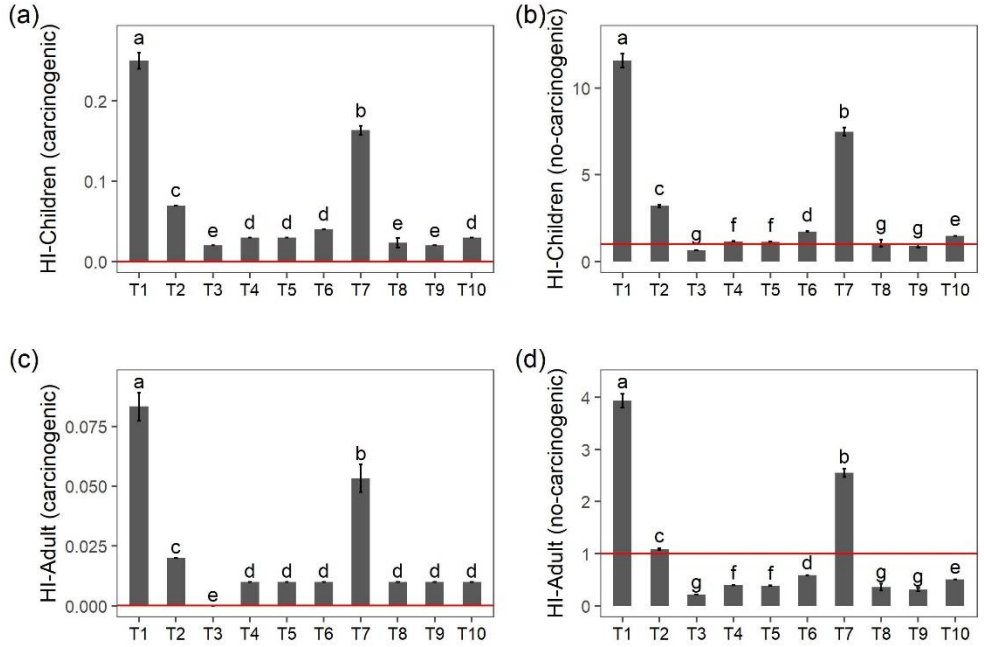

Figura 3. Índice de risco (HI) carcinogênico e não carcinogênico da ingestão acidental de solo e vegetal, oriundos de rejeitos de mineração de ouro.

[1]T1: resíduo de mineração (RM); [2]T2: resíduo de mineração (RM) + 0.5% BA; [3]T3: resíduo de mineração (RM) + 1.0% BA; [4]T4: resíduo de mineração (RM) + 2.0% BA; [5]T5: resíduo de mineração (RM) + 0.5% BAT; [6]T6: resíduo de mineração (RM) + 1.0% BAT; [7]T7: resíduo de mineração (RM) + 2.0% BAT; [8]T8: resíduo de mineração (RM) + 0.5% BAS; [9]T9: resíduo de mineração (RM) + 1.0% BAS; [10]T10: resíduo de mineração (RM) + 2.0% BAS. Letras diferentes indicam diferença significativa entre os tratamentos pelo teste de Tukey ($p < 0,05$).

Estudo realizado por SIMON et al (2015) propuseram a utilização amenizantes (calcário, material organico e oxido de ferro) para minimizar a mobilidade e biodisponibilidade de As, e concluiu que nenhum desses produtos conseguiu amenizar concentração de As na parte aérea vegetal e por isso seu uso não deve ser recomendado como condicionador de solo altamente poluídos. Em oposição a esses resultados, os biochars utilizados por Kim et al., (2021) em sua pesquisa elevaram a disponibilidade de As, mas não refletiram em uma maior translocação e justificam que essa baixa relação

ocorrem devido a provavel a melhoria da questão nutricional, relacionadas a adição dos biochars no solo. A diminuição dos valores do fator de transferência é de fundamental importância para a amenização dos possiveis maleficios saúde humana, relacionados ao consumo de vegetais comestiveis oriundos de áreas possivelmente contaminadas com As (OLIVEIRA et al., 2017).

3.7 Predição do acumulo de arsênio

A análise de regressão múltipla possibilitou a identificar quais as variáveis de solo e de planta que obtiveram maior influência na predição do acumulo de As (raiz e folhas) para cada biochar, gerando os modelos com melhores parâmetros estatísticos de validação (Tabela 7). Os modelos foram diferentes entre si, comprovando que o enriquecimento com fertilizantes fosfatados (SFS e SFT) tem reflexo distintos no acumulo de As na raiz (As-R) e folhas (As-F).

Tabela 7: Equações de regressões múltiplas referentes ao acumulo de arsênio (As) na folha (As-F) e na raiz (R-As), para os biochars.

EQUAÇÕES	p-value	NRMSE	R^2_{adj}
(a) As-F (BA)= $3.176*10^{-04}$ -6.5000*As.F1 -0.42640*As.F2 +2.8850*CO - 3.0340*Ca + 0.4323*P	2.23e-5	0.00185	0.916
(b) As-F (BAT)= $4.599*10^{-05}$ +0.6899*As.F5 +0.890*K -1.4190*P	3.77e-4	0.01275	0.914
(c) As-F (BAS)= $2.255*10^{-04}$ +1.07*As.F1 -0.2515*CO -1.29*Ca -1.479*Mg - 0.0484*P	2.20e-5	0.00040	0.903
(d) As-R (BA)= $-1.477e^{-10}$ +0.2157*Ca -0.7912*P.F2	9.46e-4	0.01386	0.908
(e) As-R (BAT)= $6.591*10^{-11}$ -0.3525*Al(soil) -0.2865*Ca +0.2925*Ca(soil) - 0.5222*Mg +0.6453*P.F1 -0.3063*P.F3 -0.05161*P.F4 -0.01515*pH	2.02e-6	0.00008	0.906
(f) As-R (BAS)= $-3.444*10^{-11}$ +0.9222*Ca(soil) +0.6485*K(soil) -0.58260*P.F4	1.54e-3	0.01403	0.918

Para os modelos relacionados ao BA, as características do resíduo (frações de arsênio e carbono orgânico) e da planta (Ca e P) influenciaram no arsênio foliar (equação

a), já arsênio radicular obteve relação com o cálcio e a fração F2 do fósforo do resíduo (equação d). A baixa quantidade de nutrientes encontrada no biochars sem enriquecimento proporciona uma maior absorção de arsênio (solúvel e adsorvido) os quais sua maior mobilidade tem efeito negativo no desenvolvimento vegetal (Tabela 5).

Nos modelos relacionados ao BAT, a fração F5 de arsênio do resíduo e da planta (K e P) influenciaram no arsênio foliar (equação b), e o arsênio radicular obteve relação com as características do resíduo (Al, Ca, pH e as frações de fósforo) e da planta (Ca, Mg) (equação e). As maiores quantidades de fosforo encontrado em BAT tem feito direto na maior translocação de arsênio (Tabela 6), menor acumulo de nutrientes e biomassa (Tabela 5). Devido as características semelhantes entre o fosfato e arsenato, em condições de elevadas quantidades do nutriente (fósforo) propicia a maior disponibilidade do arsênio, favorecendo a maior absorção

Os modelos relacionados ao BAS, as características do resíduo (fração F1 de arsênio e carbono orgânico) e da planta (Ca, Mg e P) influenciaram no As-F (equação c), e somente as características do resíduo (fração F4 de fosforo, Ca e K) no As-R (equação f). A quantidade de nutrientes (principalmente cálcio) e fosforo (Tabela 2) encontrada em BAS proporcionaram uma melhoria no acumulo de biomassa e nutrientes (Tabela 5), o que por consequência refletiu em menores valores de TF e maiores valores de TI (Tabela 6).

CONCLUSÃO

O uso de biochar enriquecido com fósforo é uma alternativa efetiva para a melhoria das características químicas de locais de deposição de resíduos contendo arsênio, oriundos de áreas de mineração artesanal, devido à baixa disponibilidade de nutrientes encontrada nessas áreas, o que prejudica o processo de recuperação. A adição

dos fertilizantes fosfatados melhoraram as características químicas dos biochars, as nutricionais do resíduo de mineração e por consequência o acumulo de biomassa/nutrientes. A adição dos nutrientes (principalmente cálcio e fosforo) após a adição do BAS conseguiu melhorar as características químicas dos resíduos e por consequência melhorando o desenvolvimento de Lactuca Sativa, amenizando os efeitos tóxicos do arsênio e diminuindo sua translocação. Esses resultados são promissores para a para indicação de uso do biochar fosfatado BAS em áreas degradadas contendo elevados teores de arsênio e em auxilio a nutrição de espécies fitorremediadoras.

REFERÊNCIAS

Abreu, m. M.; et al., Yield and uranium concentration in two lettuce (lactuca sativa l.) Varieties influenced by soil and irrigation water composition, and season growth. Journal of geochemical exploration, v. 142, p. 43-48, 2014.

Aftabtalab, A., Rinklebe, J., Shaheen, S. M., Niazi, N. K., Moreno-Jiménez, E., Schaller, J., & Knorr, K. H. (2022). Review on the interactions of arsenic, iron (oxy)(hydr)oxides, and dissolved organic matter in soils, sediments, and groundwater in a ternary system. Chemosphere, 286(July 2021). https://doi.org/10.1016/j.chemosphere.2021.131790

Arco-Lázaro, E., Pardo, T., Clemente, R., & Bernal, M. P. (2018). Arsenic adsorption and plant availability in an agricultural soil irrigated with As-rich water: Effects of Fe-rich amendments and organic and inorganic fertilisers. Journal of Environmental Management, 209, 262–272. https://doi.org/10.1016/j.jenvman.2017.12.042

Bandara, T., Chathurika, J. B. A. J., Franks, A., Xu, J., & Tang, C. (2021). Interactive effects of biochar type and pH on the bioavailability of As and Cd and microbial activities

in co-contaminated soils. Environmental Technology and Innovation, 23, 101767. https://doi.org/10.1016/j.eti.2021.101767

Bandara, T., Franks, A., Xu, J., Bolan, N., Wang, H., & Tang, C. (2020). Chemical and biological immobilization mechanisms of potentially toxic elements in biochar-amended soils. Critical Reviews in Environmental Science and Technology, 50(9), 903–978. https://doi.org/10.1080/10643389.2019.1642832

Boorboori, M. R., Gao, Y., Wang, H., & Fang, C. (2021). Usage of si, p, se, and ca decrease arsenic concentration/toxicity in rice, a review. Applied Sciences (Switzerland), 11(17). https://doi.org/10.3390/app11178090

Buschle, b. N. Et al., Cinética de liberação de chumbo de solos de área de mineração e metalurgia de metais pesados. Revista brasileira de ciência do solo, v. 34, n. 6, 2010.

Cantarella, h.; trivelin, p. C. O. Determinação de nitrogênio total em solo. (ed.). Análise química para avaliação da fertilidade de solos tropicais. Instituto agronômico de campinas, campinas, são paulo. 2001.

Chen, D., Liu, X., Bian, R., Cheng, K., Zhang, X., Zheng, J., Joseph, S., Crowley, D., Pan, G., & Li, L. (2018). Effects of biochar on availability and plant uptake of heavy metals – A meta-analysis. Journal of Environmental Management, 222(December 2017), 76–85. https://doi.org/10.1016/j.jenvman.2018.05.004

Chen, M., & Graedel, T. E. (2015). The potential for mining trace elements from phosphate rock. Journal of Cleaner Production, 91, 337–346. https://doi.org/10.1016/j.jclepro.2014.12.042

Chen, t. Et al., Adsorption of cadmium by biochar derived from municipal sewage sludge: impact factors and adsorption mechanism. Chemosphere, v. 134, p. 286-293, 2015.

Cordon, G., Iriel, A., Cirelli, A. F., & Lagorio, M. G. (2018). Arsenic effects on some photophysical parameters of Cichorium intybus under different radiation and water irrigation regimes. Chemosphere, 204, 398–404. https://doi.org/10.1016/j.chemosphere.2018.04.048

Coringa, j. E. S. Et al., Distribuição geoquímica e biodisponibilidade de metais traço em sedimentos no rio bento gomes, poconé-mt, brasil. Acta amazônica, v. 46, n. 2, p. 161-174, 2016.

Covre, W. P., Pereira, W. V. da S., Gonçalves, D. A. M., Teixeira, O. M. M., Amarante, C. B. do, & Fernandes, A. R. (2020). Phytoremediation potential of Khaya ivorensis and Cedrela fissilis in copper contaminated soil. Journal of Environmental Management, 268(January), 110733. https://doi.org/10.1016/j.jenvman.2020.110733

Covre, W. P., Ramos, S. J., Pereira, W. V. da S., Souza, E. S. de, Martins, G. C., Teixeira, O. M. M., Amarante, C. B. do, Dias, Y. N., & Fernandes, A. R. (2022). Impact of copper mining wastes in the Amazon: Properties and risks to environment and human health. Journal of Hazardous Materials, 421(April 2021), 126688. https://doi.org/10.1016/j.jhazmat.2021.126688

Cunha, a. M. B. Et al., Aspectos econômicos e sociais da atividade extrativa mineral: um olhar sobre os objetivos de desenvolvimento sustentável. Série estudos e documentos, 2019.

Dai, Y., Zheng, H., Jiang, Z., & Xing, B. (2020). Combined effects of biochar properties and soil conditions on plant growth: A meta-analysis. Science of the Total Environment, 713, 136635. https://doi.org/10.1016/j.scitotenv.2020.136635

Dey, D., & Mavi, M. S. (2022). Co-application of biochar with non-pyrolyzed organic material accelerates carbon accrual and nutrient availability in soil. Environmental Technology and Innovation, 25, 102128. https://doi.org/10.1016/j.eti.2021.102128

Dias, Y. N. Et al., Biochar produced from amazonian agro-industrial wastes: properties and adsorbent potential of Cd 2+ and Cu 2+. Biochar, p. 1-12, 2019.

Drahota, p. Et al., Selectivity assessment of an arsenic sequential extraction procedure for evaluating mobility in mine wastes. Analytica chimica acta, v. 839, p. 34-43, 2014.

Fidel, R. B., Laird, D. A., Thompson, M. L., & Lawrinenko, M. (2017). Characterization and quantification of biochar alkalinity. Chemosphere, 167, 367–373. https://doi.org/10.1016/j.chemosphere.2016.09.151

Fu, D. et al., Response of soil phosphorus fractions and fluxes to different vegetation restoration types in a subtropical mountain ecosystem. CATENA, v. 193, p. 104663, 2020.

Ghassemi-Golezani, K., & Farhangi-Abriz, S. (2021). Biochar-based metal oxide nanocomposites of magnesium and manganese improved root development and productivity of safflower (Carthamus tinctorius L.) under salt stress. Rhizosphere, 19(June). https://doi.org/10.1016/j.rhisph.2021.100416

Gusman, G. S., Oliveira, J. A., Farnese, F. S., & Cambraia, J. (2013). Arsenate and arsenite: The toxic effects on photosynthesis and growth of lettuce plants. Acta Physiologiae Plantarum, 35(4), 1201–1209. https://doi.org/10.1007/s11738-012-1159-8

Hailegnaw, N. S., Mercl, F., Pračke, K., Száková, J., & Tlustoš, P. (2019). Mutual relationships of biochar and soil pH, CEC, and exchangeable base cations in a model laboratory experiment. Journal of Soils and Sediments, 19(5), 2405–2416. https://doi.org/10.1007/s11368-019-02264-z

Hedley, M. J. et al., Changes in inorganic and organic soil phosphorus fractions induced by cultivation practices and by laboratory incubations 1. Soil Science Society of America Journal, v. 46, n. 5, p. 970-976, 1982.

Houba, V. J. G. et al., Soil and plant analysis, a series of syllabi part 5B: soil analysis procedures, other procedures. Department of Soil Science and Plant Nutrition, Agricultural University, Wageningen, The Netherlands, 1995.

Huang, Z., Cheng, C., Liu, Z., Zeng, H., Feng, B., Zhong, H., Luo, W., Hu, Y., Guo, Z., He, G., & Fu, W. (2019). Utilization of a new Gemini surfactant as the collector for the reverse froth flotation of phosphate ore in sustainable production of phosphate fertilizer. Journal of Cleaner Production, 221, 108–112. https://doi.org/10.1016/j.jclepro.2019.02.251

IBGE - INSTITUTO BRASILEIRO DE GEOGRAFIA E ESTATÍSTICA. Pesquisa de Orçamentos Familiares-2008-2009: aquisição alimentar domiciliar per capita, Brasil e grandes regiões. 2010.

IBGE. Instituto Brasileiro de Geografia e Estatística. Disponível em: <https://cidades.ibge.gov.br/brasil/pa/cachoeira-do-piria/panorama>. Acessado em: 08 de junho de 2020.

Jack, J. et al., Production of magnetic biochar from waste-derived fungal biomass for phosphorus removal and recovery. Journal of cleaner production, v. 224, p. 100-106, 2019.

Jan, A. T., Azam, M., Siddiqui, K., Ali, A., Choi, I., & Haq, Q. M. R. (2015). Heavy metals and human health: Mechanistic insight into toxicity and counter defense system of antioxidants. International Journal of Molecular Sciences, 16(12), 29592–29630. https://doi.org/10.3390/ijms161226183

Kim, H.-B., Kim, J.-G., Kim, T., Alessi, D. S., & Baek, K. (2020). Mobility of arsenic in soil amended with biochar derived from biomass with different lignin contents: Relationships between lignin content and dissolved organic matter leaching. Chemical Engineering Journal, 393, 124687. https://doi.org/10.1016/j.cej.2020.124687

Kim, H.-B., Kim, S.-H., Jeon, E.-K., Kim, D.-H., Tsang, D. C. W., Alessi, D. S., Kwon, E. E., & Baek, K. (2018). Effect of dissolved organic carbon from sludge, Rice straw and spent coffee ground biochar on the mobility of arsenic in soil. Science of The Total Environment, 636, 1241–1248. https://doi.org/10.1016/j.scitotenv.2018.04.406

Kim, M. S., Lee, S. H., & Kim, J. G. (2021). Evaluation of factors affecting arsenic uptake by Brassica juncea in alkali soil after biochar application using partial least squares path modeling (PLS-PM). Chemosphere, 275, 130095. https://doi.org/10.1016/j.chemosphere.2021.130095

Kofroňová, M., Mašková, P., & Lipavská, H. (2018). Two facets of world arsenic problem solution: crop poisoning restriction and enforcement of phytoremediation. Planta, 248(1), 19–35. https://doi.org/10.1007/s00425-018-2906-x

Kolo, M. T. et al., Assessment of health risk due to the exposure of heavy metals in soil around mega coal-fired cement factory in Nigeria. Results in Physics, v. 11, p. 755-762, 2018.

Korai, P. K., Sial, T. A., Pan, G., Abdelrahman, H., Sikdar, A., Kumbhar, F., Channa, S. A., Ali, E. F., Zhang, J., Rinklebe, J., & Shaheen, S. M. (2021). Wheat and maize-derived water-washed and unwashed biochar improved the nutrients phytoavailability and the grain and straw yield of rice and wheat: A field trial for sustainable management of paddy soils. Journal of Environmental Management, 297(June). https://doi.org/10.1016/j.jenvman.2021.113250

Lawrinenko, M., Jing, D., Banik, C., & Laird, D. A. (2017). Aluminum and iron biomass pretreatment impacts on biochar anion exchange capacity. Carbon, 118, 422–430. https://doi.org/10.1016/j.carbon.2017.03.056

Lawrinenko, M., Laird, D. A., Johnson, R. L., & Jing, D. (2016). Accelerated aging of biochars: Impact on anion exchange capacity. Carbon, 103, 217–227. https://doi.org/10.1016/j.carbon.2016.02.096

Lee, C. H., Wu, C. H., Syu, C. H., Jiang, P. Y., Huang, C. C., & Lee, D. Y. (2016). Effects of phosphorous application on arsenic toxicity to and uptake by rice seedlings in As-contaminated paddy soils. Geoderma, 270(2015), 60–67. https://doi.org/10.1016/j.geoderma.2016.01.003

Lehmann, j.; joseph, s.. Biochar for environmental management: an introduction. In: biochar for environmental management: science and technology, 2nd ed. Earth scan. 2009.

Lemanowicz, j. Et al., Activity of selected enzymes and phosphorus content in soils of former sulphur mines. Science of the total environment, v. 708, p. 134545, 2020.

Li, k-z et al., Improving the oxidation resistance of carbon/carbon composites at low temperature by controlling the grafting morphology of carbon nanotubes on carbon fibres. Corrosion science, v. 60, p. 314-317, 2012.

Li, Q., Zhong, H., & Cao, Y. (2020). Effects of the joint application of phosphate rock, ferric nitrate and plant ash on the immobility of As, Pb and Cd in soils. Journal of Environmental Management, 265(January), 110576. https://doi.org/10.1016/j.jenvman.2020.110576

Li, z. Et al., A review of soil heavy metal pollution from mines in china: pollution and health risk assessment. Science of the total environment, v. 468, p. 843-853, 2014.

Lichtenthaler, h. K. Chlorophylls and carotenoids: pigments of photosynthetic biomembranes. In: methods in enzymology. Academic press, 1987. P. 350-382.

Liu, X., Feng, H. Y., Fu, J. W., Chen, Y., Liu, Y., & Ma, L. Q. (2018). Arsenic-induced nutrient uptake in As-hyperaccumulator Pteris vittata and their potential role to enhance plant growth. Chemosphere, 198, 425–431. https://doi.org/10.1016/j.chemosphere.2018.01.077

Lustosa Filho, J. F., Penido, E. S., Castro, P. P., Silva, C. A., & Melo, L. C. A. (2017). Co-Pyrolysis of Poultry Litter and Phosphate and Magnesium Generates Alternative

Slow-Release Fertilizer Suitable for Tropical Soils. ACS Sustainable Chemistry and Engineering, 5(10), 9043–9052. https://doi.org/10.1021/acssuschemeng.7b01935

Mahmoud, E., Ibrahim, M., Abd El-Rahman, L., & Khader, A. (2019). Effects of Biochar and Phosphorus Fertilizers on Phosphorus Fractions, Wheat Yield and Microbial Biomass Carbon in Vertic Torrifluvents. Communications in Soil Science and Plant Analysis, 50(3), 362–372. https://doi.org/10.1080/00103624.2018.1563103

Masís-Meléndez, F., Segura-Chavarría, D., García-González, C. A., Quesada-Kimsey, J., & Villagra-Mendoza, K. (2020). Variability of physical and chemical properties of TLUD stove derived biochars. Applied Sciences (Switzerland), 10(2), 1–20. https://doi.org/10.3390/app10020507

Melo, l. C. A. Et al., Cadmium-and barium-toxicity effects on growth and antioxidant capacity of soybean (glycine max l.) Plants, grown in two soil types with different physicochemical properties. Journal of plant nutrition and soil science, v. 174, n. 5, p. 847-859, 2011.

Mendoza, c. J. Et al., Evaluation of the bioaccessible gastric and intestinal fractions of heavy metals in contaminated soils by means of a simple bioaccessibility extraction test. Chemosphere, v. 176, p. 81-88, 2017.

Meyer, s. Et al., Albedo impact on the suitability of biochar systems to mitigate global warming. Environmental science & technology, v. 46, n. 22, p. 12726-12734, 2012.

Midhat, l. Et al., Accumulation of heavy metals in metallophytes from three mining sites (southern centre morocco) and evaluation of their phytoremediation potential. Ecotoxicology and environmental safety, v. 169, p. 150-160, 2019.

Muhammad, n. Et al., Effect of biochars on bioaccumulation and human health risks of potentially toxic elements in wheat (triticum aestivum l.) Cultivated on industrially contaminated soil. Environmental pollution, p. 113887, 2020.

Murphy, j.; Riley, j. P. A modified single solution method for the determination of phosphate in natural waters. Analytica chimica acta, v. 27, p. 31-36, 1962.

Nahas, m. M. Et al., Especialização e diversificação produtiva: um modelo de painel espacial para a indústria extrativa mineral em minas gerais, 2000-2010. Nova economia, v. 29, n. 1, p. 7-40, 2019.

Ngole-Jeme, V. M., & Fantke, P. (2017). Ecological and human health risks associated with abandoned gold mine tailings contaminated soil. PLoS ONE, 12(2), 1–24. https://doi.org/10.1371/journal.pone.0172517

Oliveira, L. M., Suchismita, D., Gress, J., Rathinasabapathi, B., Chen, Y., & Ma, L. Q. (2017). Arsenic uptake by lettuce from As-contaminated soil remediated with Pteris vittata and organic amendment. Chemosphere, 176, 249–254. https://doi.org/10.1016/j.chemosphere.2017.02.124

Pan, H., Lu, X., & Lei, K. (2017). A comprehensive analysis of heavy metals in urban road dust of Xi'an, China: Contamination, source apportionment and spatial distribution. Science of the Total Environment, 609, 1361–1369. https://doi.org/10.1016/j.scitotenv.2017.08.004

Pereira, W. V. da S., Teixeira, R. A., Souza, E. S. de, Moraes, A. L. F. de, Campos, W. E. O., Amarante, C. B. do, Martins, G. C., & Fernandes, A. R. (2020). Chemical fractionation and bioaccessibility of potentially toxic elements in area of artisanal gold

mining in the Amazon. Journal of Environmental Management, 267(March), 110644. https://doi.org/10.1016/j.jenvman.2020.110644

Pérez-Romero, j. A. et al., Growth and photosynthetic limitation analysis of the Cd-accumulator Salicornia ramosissima under excessive cadmium concentrations and optimum salinity conditions. Plant Physiology and Biochemistry, v. 109, p. 103-113, 2016.

Piash, M. I., Iwabuchi, K., Itoh, T., & Uemura, K. (2021). Release of essential plant nutrients from manure- and wood-based biochars. Geoderma, 397(March), 115100. https://doi.org/10.1016/j.geoderma.2021.115100

Piash, M. I., Iwabuchi, K., Itoh, T., & Uemura, K. (2021). Release of essential plant nutrients from manure- and wood-based biochars. Geoderma, 397(March), 115100. https://doi.org/10.1016/j.geoderma.2021.115100

Puga, A. P., Abreu, C. A., Melo, L. C. A., & Beesley, L. (2015). Biochar application to a contaminated soil reduces the availability and plant uptake of zinc, lead and cadmium. Journal of Environmental Management, 159, 86–93. https://doi.org/10.1016/j.jenvman.2015.05.036

Purakayastha, T. J., Bera, T., Bhaduri, D., Sarkar, B., Mandal, S., Wade, P., Kumari, S., Biswas, S., Menon, M., Pathak, H., & Tsang, D. C. W. (2019). A review on biochar modulated soil condition improvements and nutrient dynamics concerning crop yields: Pathways to climate change mitigation and global food security. Chemosphere, 227, 345–365. https://doi.org/10.1016/j.chemosphere.2019.03.170

Qian, T-T.; JIANG, H.. Migration of phosphorus in sewage sludge during different thermal treatment processes. (2014). ACS Sustainable Chemistry & Engineering, v. 2, n. 6, p. 1411-1419.

Rafiq, M., Shahid, M., Abbas, G., Shamshad, S., Khalid, S., Niazi, N. K., & Dumat, C. (2017). Comparative effect of calcium and EDTA on arsenic uptake and physiological attributes of Pisum Sativum. International Journal of Phytoremediation, 19(7), 662–669. https://doi.org/10.1080/15226514.2016.1278426

Ramos, S.J., Pinto, D.A., Guedes, R.S., Dias, Y.N., Caldeira, C.F., Gastauer, M., Souza-Filho, P.W., Fernandes, A.R., (2021). Açaí biochar and compost affect the phosphorus sorption, nutrient availability, and growth of dioclea apurensis in iron mining soil. Minerals 11. https://doi.org/10.3390/min11070674

Rodríguez-Vila, A.et al., Assessing the influence of technosol and biochar amendments combined with Brassica juncea L. on the fractionation of Cu, Ni, Pb and Zn in a polluted mine soil. Journal of soils and sediments, v. 16, n. 2, p. 339-348, 2016.

Saleem, m. H. Et al., Influence of phosphorus on copper phytoextraction via modulating cellular organelles in two jute (corchorus capsularis l.) Varieties grown in a copper mining soil of hubei province, china. Chemosphere, v. 248, p. 126032, 2020.

Santos, d. R. Et al., Fatores que afetam a disponibilidade do fósforo e o manejo da adubação fosfatada em solos sob sistema plantio direto. Ciência rural, v. 38, n. 2, p. 576-586, 2008.

Sato, m. K. Et al., Biochar from acai agroindustry waste: study of pyrolysis conditions. Waste management, v. 96, p. 158-167, 2019.

Seyedsadr, S., Šípek, V., Jačka, L., Sněhota, M., Beesley, L., Pohořelý, M., Kovář, M., & Trakal, L. (2022). Biochar considerably increases the easily available water and nutrient content in low-organic soils amended with compost and manure. Chemosphere, 293(January). https://doi.org/10.1016/j.chemosphere.2022.133586

Shetty, R., & Prakash, N. B. (2020). Effect of different biochars on acid soil and growth parameters of rice plants under aluminium toxicity. Scientific Reports, 10(1), 1–10. https://doi.org/10.1038/s41598-020-69262-x

Shi, R. Y., Ni, N., Nkoh, J. N., Dong, Y., Zhao, W. R., Pan, X. Y., Li, J. Y., Xu, R. K., & Qian, W. (2020). Biochar retards Al toxicity to maize (Zea mays L.) during soil acidification: The effects and mechanisms. Science of the Total Environment, 719. https://doi.org/10.1016/j.scitotenv.2020.137448

Simón, M., González, V., de Haro, S., & García, I. (2015). Are soil amendments able to restore arsenic-contaminated alkaline soils? Journal of Soils and Sediments, 15(1), 117–125. https://doi.org/10.1007/s11368-014-0953-x

Singh, r. Et al., Multifaceted application of crop residue biochar as a tool for sustainable agriculture: an ecological perspective. Ecological engineering, v. 77, p. 324-347, 2015.

Neto, H. F. de, Pereira, W. V. da S., Dias, Y. N., Souza, E. S. de, Teixeira, R. A., Lima, M. W. de, Ramos, S. J., Amarante, C. B. do, & Fernandes, A. R. (2020). Environmental and human health risks of arsenic in gold mining areas in the eastern Amazon. Environmental Pollution, 265, 114969. https://doi.org/10.1016/j.envpol.2020.114969

Souza, e. S. Et al., Assessment of risk to human health from simultaneous exposure to multiple contaminants in an artisanal gold mine in serra pelada, pará, brazil. Science of the total environment, v. 576, p. 683-695, 2017.

Souza, e. S. Et al., Organic residues and biochar to immobilize potentially toxic elements in soil from a gold mine in the amazon. Ecotoxicology and environmental safety, v. 169, p. 425-434, 2019.

STAFF, E. P. A. Supplemental guidance for developing soil screening levels for superfund sites, peer review draft. Washington, DC: US Environmental Protection Agency Office of Solid Waste and Emergency Response, OSWER, v. 9355, p. 9354-9324, 2001.

Teixeira, P.C., Donagemma, G.K., Fontana, A., Teixeira, W.G. (Eds.). Manual de métodos de análise de solo, third ed. Embrapa Solos, Brasília. 2017.

USEPA - UNITED STATES ENVIRONMENTAL PROTECTION AGENCY. Method 3051 A: Micro-wave assisted acid digestion of sediments sludges, soils and oils. In: Sw-846: Test methods for evaluation solid waste physical and chemical methods. Washington, Office of Solid Waste, US. Environmental Protection Agency, p.1-20, 2007.

USEPA. Exposure Factors Handbook. National Center for Environmental Assessment Office of Research and Development, Edition. Washington, DC 20460, 2011.

USEPA. Method 1311: test methods for evaluating solid waste, physical/chemical methods. SW-846, 3rd ed.; US Environmental Pollution Agency: Washington, DC, 1992.

Vikrant, k. Et al., Engineered/designer biochar for the removal of phosphate in water and wastewater. Science of the total environment, v. 616, p. 1242-1260, 2018.

Vochozka, m. Et al., Biochar pricing hampers biochar farming. Clean technologies and environmental policy, v. 18, n. 4, p. 1225-1231, 2016.

Wali, F., Naveed, M., Bashir, M. A., Asif, M., Ahmad, Z., Alkahtani, J., Alwahibi, M. S., & Elshikh, M. S. (2020). Formulation of biochar-based phosphorus fertilizer and its impact on both soil properties and chickpea growth performance. Sustainability (Switzerland), 12(22), 1–20. https://doi.org/10.3390/su12229528

Weihrauch, c.; opp, c.. Ecologically relevant phosphorus pools in soils and their dynamics: the story so far. Geoderma, v. 325, p. 183-194, 2018.

Wongsasuluk, P., Tun, A. Z., Chotpantarat, S., & Siriwong, W. (2021). Related health risk assessment of exposure to arsenic and some heavy metals in gold mines in Banmauk Township, Myanmar. Scientific Reports, 11(1), 1–14. https://doi.org/10.1038/s41598-021-02171-9

Wu, W.-H. et al., Immobilization of trace metals by phosphates in contaminated soil near lead/zinc mine tailings evaluated by sequential extraction and TCLP. Journal of soils and sediments, v. 13, n. 8, p. 1386-1395, 2013.

Xiao, X. et al., Distribution and health risk assessment of potentially toxic elements in soils around coal industrial areas: A global meta-analysis. Science of The Total Environment, p. 135292, 2019.

Xue, l. Et al., Uptake of heavy metals by native herbaceous plants in an antimony mine (hunan, china). Clean–soil, air, water, v. 42, n. 1, p. 81-87, 2014.

Yadav, i. C. Et al., Spatial distribution, source analysis, and health risk assessment of heavy metals contamination in house dust and surface soil from four major cities of nepal. Chemosphere, v. 218, p. 1100-1113, 2019.

Yadav, k. K. Et al., Mechanistic understanding and holistic approach of phytoremediation: a review on application and future prospects. Ecological engineering, v. 120, p. 274-298, 2018.

Yan, P., Shen, C., Zou, Z., Fu, J., Li, X., Zhang, L., Zhang, L., Han, W., & Fan, L. (2021). Biochar stimulates tea growth by improving nutrients in acidic soil. Scientia Horticulturae, 283(March), 110078. https://doi.org/10.1016/j.scienta.2021.110078

Yang, J. E. et al., A simple spectrophotometric determination of nitrate in water, resin, and soil extracts. Soil Science Society of America Journal, v. 62, n. 4, p. 1108-1115, 1998.

Yang, L., Wu, Y., Wang, Y., An, W., Jin, J., Sun, K., & Wang, X. (2021). Effects of biochar addition on the abundance, speciation, availability, and leaching loss of soil phosphorus. Science of the Total Environment, 758, 143657. https://doi.org/10.1016/j.scitotenv.2020.143657

Yang, Y. et al., pH-dependence of pesticide adsorption by wheat-residue-derived black carbon. Langmuir, v. 20, n. 16, p. 6736-6741, 2004.

Yao, y. Et al., Engineered biochar reclaiming phosphate from aqueous solutions: mechanisms and potential application as a slow-release fertilizer. Environmental science & technology, v. 47, n. 15, p. 8700-8708, 2013.

Ye, s. Et al., The effects of activated biochar addition on remediation efficiency of co-composting with contaminated wetland soil. Resources, conservation and recycling, v. 140, p. 278-285, 2019.

Yuan, j.-h. Et al., The forms of alkalis in the biochar produced from crop residues at different temperatures. Bioresource technology, v. 102, n. 3, p. 3488-3497, 2011.

Zhang, H., Yuan, X., Xiong, T., Wang, H., & Jiang, L. (2020). Bioremediation of co-contaminated soil with heavy metals and pesticides: Influence factors, mechanisms and evaluation methods. Chemical Engineering Journal, 398(October 2019), 125657. https://doi.org/10.1016/j.cej.2020.125657

Zhang, y. Et al., Modest amendment of sewage sludge biochar to reduce the accumulation of cadmium into rice (oryza sativa l.): a field study. Environmental pollution, v. 216, p. 819-825, 2016.

Zhao, l. Et al., Copyrolysis of biomass with phosphate fertilizers to improve biochar carbon retention, slow nutrient release, and stabilize heavy metals in soil. Acs sustainable chemistry & engineering, v. 4, n. 3, p. 1630-1636, 2016.

Zhao, l. Et al., Phosphorus-assisted biomass thermal conversion: reducing carbon loss and improving biochar stability. Plos one, v. 9, n. 12, 2014a.

Zhao, l. Et al., Source identification and health risk assessment of metals in urban soils around the tanggu chemical industrial district, tianjin, china. Science of the total environment, v. 468, p. 654-662, 2014b.

Zheng, Q., Yang, L., Song, D., Zhang, S., Wu, H., Li, S., & Wang, X. (2020). High adsorption capacity of Mg–Al-modified biochar for phosphate and its potential for phosphate interception in soil. Chemosphere, 259, 127469. https://doi.org/10.1016/j.chemosphere.2020.127469

Zhong, D., Zhao, Z., Jiang, Y., Yang, X., Wang, L., Chen, J., Guan, C. Y., Zhang, Y., Tsang, D. C. W., & Crittenden, J. C. (2020). Contrasting abiotic As(III) immobilization by undissolved and dissolved fractions of biochar in Ca2+-rich groundwater under anoxic conditions. Water Research, 183, 116106. https://doi.org/10.1016/j.watres.2020.116106

Zia, Z., Bakhat, H. F., Saqib, Z. A., Shah, G. M., Fahad, S., Ashraf, M. R., Hammad, H. M., Naseem, W., & Shahid, M. (2017). Effect of water management and silicon on germination, growth, phosphorus and arsenic uptake in rice. Ecotoxicology and Environmental Safety, 144(February), 11–18. https://doi.org/10.1016/j.ecoenv.2017.06.004